

**SINTERING EFFECTS AND HYDROTHERMAL AGEING  
BEHAVIOUR OF YTTRIA-STABILISED ZIRCONIA WITH  
MnO<sub>2</sub> DOPING**

**TING CHEN HUNT**

**FACULTY OF ENGINEERING  
UNIVERSITY OF MALAYA  
KUALA LUMPUR**

**2018**

**SINTERING EFFECTS AND HYDROTHERMAL  
AGEING BEHAVIOUR OF YTTRIA-STABILISED  
ZIRCONIA WITH MnO<sub>2</sub> DOPING**

**TING CHEN HUNT**

**THESIS SUBMITTED IN FULFILMENT OF THE  
REQUIREMENTS FOR THE DEGREE OF DOCTOR OF  
PHILOSOPHY**

**FACULTY OF ENGINEERING  
UNIVERSITY OF MALAYA  
KUALA LUMPUR**

**2018**

\*(Please delete this part) Depending on the medium of thesis/dissertation, pick either the English or Bahasa Malaysia version and delete the other.

**UNIVERSITY OF MALAYA**

**ORIGINAL LITERARY WORK DECLARATION**

Name of Candidate: **TING CHEN HUNT**

Matric No: **KHA110072**

Name of Degree: **DOCTORATE OF PHILOSOPHY**

Title of Project Paper/Research Report/Dissertation/Thesis (“this Work”):

**SINTERING EFFECT AND HYDROTHERMAL AGEING BEHAVIOUR OF  
YTTRIA-STABILISED ZIRCONIA WITH MnO<sub>2</sub> DOPING**

Field of Study: **MANUFACTURING PROCESSES**

I do solemnly and sincerely declare that:

- (1) I am the sole author/writer of this Work;
- (2) This Work is original;
- (3) Any use of any work in which copyright exists was done by way of fair dealing and for permitted purposes and any excerpt or extract from, or reference to or reproduction of any copyright work has been disclosed expressly and sufficiently and the title of the Work and its authorship have been acknowledged in this Work;
- (4) I do not have any actual knowledge nor do I ought reasonably to know that the making of this work constitutes an infringement of any copyright work;
- (5) I hereby assign all and every rights in the copyright to this Work to the University of Malaya (“UM”), who henceforth shall be owner of the copyright in this Work and that any reproduction or use in any form or by any means whatsoever is prohibited without the written consent of UM having been first had and obtained;
- (6) I am fully aware that if in the course of making this Work I have infringed any copyright whether intentionally or otherwise, I may be subject to legal action or any other action as may be determined by UM.

Candidate’s Signature

Date:

Subscribed and solemnly declared before,

Witness’s Signature

Date:

Name:

Designation:

## ABSTRACT

YSZ ceramics has outstanding mechanical properties and has been used for many engineering applications. However, a major drawback of this ceramic is the undesirable ageing-induced tetragonal to monoclinic phase transformation resulting in properties deterioration when exposed to steam environment. In most cases for commercial YSZ powders, high sintering temperature or/and long holding time are required via the common pressureless sintering approach which leads to grain growth exceeding the critical size that triggered low temperature degradation consequently lead to structural failure. One possible approach to suppress the excessive grain growth of YSZ is conducting low temperature sintering by adding small amount of  $\text{MnO}_2$  as sintering aid. The present work investigate the influence of low temperature sintering, focusing on varying sintering holding times on the mechanical properties, microstructure and low temperature degradation behavior of undoped and  $\text{MnO}_2$  (0.5 & 1.0 wt%) doped YSZ ceramics were investigated. Green samples were sintered at temperatures ranging from 1100 to 1250 °C at varying holding times from 12 min to 480 min. The sintered bodies were characterized in terms of bulk density, fracture toughness, Vickers hardness, phase stability and microstructure evolution. Hydrothermal ageing tests up to 120 hr were conducted at 180 °C with pressure 10 bar in an autoclave. The amount of monoclinic  $\text{ZrO}_2$  on the aged surface was measured by X-ray diffraction (XRD). Another group of undoped YSZ samples were pressureless sintered at higher temperatures (1200 to 1500 °C) with standard heating rate 10 °C/min and holding time, 120 min were prepared for comparison purpose. Densification and mechanical properties of YSZ ceramics were improved even at low sintering temperature when doped with  $\text{MnO}_2$  additive. The results indicated the relative density of above 95 %, Vickers hardness of 14 GPa and fracture toughness of 5  $\text{MPam}^{1/2}$  were obtained when sintered at low sintering temperature of 1150 °C, holding time 480 min or 1250 °C, 12 min respectively for 1.0

wt% MnO<sub>2</sub>-doped YSZ ceramics. Grain growth at low sintering temperature was marginal and the average grain size of all samples ranged between 0.14 to 0.28 μm. The results indicated that the grain growth kinetics was influenced mainly by the sintering temperature and not by the sintering holding time. The low temperature degradation (LTD) experiment conducted in superheated steam for 120 hr indicated that all the undoped YSZ ceramics via standard heating profile and temperature < 1300 °C showed no the monoclinic phase which attributed to the lower grain size and homogeneous distribution of yttria in the tetragonal grains. However, small traces of monoclinic phase was formed in MnO<sub>2</sub>-doped YSZ ceramics even at low sintering temperature, 1200 & 1250 °C and the rate of transformation was increased with higher amount of dopant and longer sintering holding time beyond 120 min which could be attributed destabilising of tetragonal grain as the result of redistribution of yttria in the grain. Ageing mechanism was subsequently proposed to account for the LTD behaviour of the YSZ ceramics.

Keywords: YSZ ceramic; MnO<sub>2</sub>; Mechanical properties; Degradation; Grain size.

## ABSTRAK

Seramik YSZ mempunyai ciri-ciri mekanikal yang cemerlang dan telah digunakan untuk banyak aplikasi kejuruteraan. Walau bagaimanapun, kelemahan utama seramik ini adalah degradasi yang mencetuskan transformasi fasa tetragonal kepada monoklinik yang menyebabkan kemerosotan sifat apabila terdedah kepada persekitaran berwap. Kebanyakan serbuk YSZ komersil disinter dengan suhu tinggi atau/dan tempoh pegangan panjang melalui kaedah sinter konvensional tanpa tekanan dengan menghasilkan pertumbuhan grain melebihi saiz kritikal yang mencetuskan degradasi suhu rendah dan menyebabkan kegagalan struktur YSZ seramik. Satu kaedah yang berpotensi mengelakan pertumbuhan grain YSZ yang berlebihan adalah dengan melakukan sintering pada suhu rendah dengan penambahan sejumlah kecil  $\text{MnO}_2$  sebagai bantuan sintering. Kerja-kerja siasatan kesan sintering suhu rendah, terutamanya tempoh masa sintering terhadap sifat-sifat mekanikal, mikrostruktur dan kelakuan degradasi suhu rendah ke atas kedua-dua seramik YSZ (0, 0.5 dan 1.0 wt%  $\text{MnO}_2$ ) telah dilakukan. Sampel disinter pada suhu antara 1100 hingga 1250 °C pada waktu pegangan antara 12 min ke 480 min. Sampel yang telah sinter dinilai dari segi ketumpatan pukal, kekerasan Vickers, keliatan patah, kestabilan fasa dan evolusi mikrostruktur. Ujian penuaan hidrotermal sehingga 120 jam dilakukan pada suhu 180 °C dengan tekanan 10 bar dalam autoklaf. Jumlah  $\text{ZrO}_2$  monoklinik pada permukaan degradasi diukur dengan difraksi sinar-X (XRD). Satu kumpulan sampel YSZ disinter pada suhu yang lebih tinggi (1200 hingga 1500 °C) dengan masa memegang 120 min disediakan untuk tujuan perbandingan. Keputusan menunjukkan ketumpatan relatif melebihi 95%, kekerasan Vickers, 14 GPa dan keliatan patah, 5  $\text{MPam}^{1/2}$  diperolehi apabila disinter pada suhu yang lebih rendah 1150°C selama 480 min atau 1250 °C selama 12 min masing-masing atas YSZ ceramic yang mengandungi . dan tempoh masa yang lebih lama untuk sampel YSZ yang mengandungi 1.0 wt%  $\text{MnO}_2$ . Semua sampel

mempamerkan pertumbuhan grain yang minimum dengan purata saiz grain adalah di antara 0.14 hingga 0.28  $\mu\text{m}$ . Hasil kajian menunjukkan bahawa pertumbuhan kinetik grain dipengaruhi terutamanya oleh suhu sintering dan bukan masa pegangan sintering. Penambahan  $\text{MnO}_2$  didapati bermanfaat untuk meningkatkan kepadatan dan sifat mekanik YSZ terutama pada suhu sintering rendah dengan 1100  $^\circ\text{C}$  dan masa pegangan rendah dengan 12 minit. Kelakuan degradasi suhu rendah dilakukan dalam stim panas menunjukkan bahawa semua sampel tidak berubah kepada simetri monoklinik adalah berpunca daripada purata saiz grain kecil yang disinter pada suhu sintering yang agak rendah. Pertumbuhan grain apabila disinter pada suhu rendah adalah kecil dan purata saiz grain semua sampel adalah di antara 0.14 hingga 0.28  $\mu\text{m}$ . Keputusan menunjukkan bahawa kinetik pertumbuhan grain dipengaruhi terutamanya oleh suhu sintering dan bukan dengan masa pegangan sintering. Eksperimen degradasi suhu rendah yang dijalankan dalam stim panas selama 120 jam menunjukkan bahawa semua seramik YSZ tanpa kandungan  $\text{MnO}_2$  yang melalui profil sinter standard dan suhu  $<1300$   $^\circ\text{C}$  tidak menunjukkan sebarang fasa monoklinik yang disebabkan oleh saiz grain yang lebih rendah dan pengagihan yttria yang homogeneous dalam grain tetragonal. Walau bagaimanapun, monoklinik terbentuk dalam seramik  $\text{MnO}_2$ -YSZ walaupun disinter pada suhu rendah, iaitu 1200 & 1250  $^\circ\text{C}$  dan kadar transformasi meningkat dengan jumlah kandungan  $\text{MnO}_2$  yang lebih tinggi dan masa pegangan sintering yang melebihi 120 minit menyebabkan ketidakstabilan grain tetragonal berkemungkinan berpunca daripada pengagihan semula yttria dalam grain. Mekanisme degradasi kemudiannya dicadangkan untuk mengambil kira tingkah laku LTD yang berlaku ke atas seramik YSZ.

Kata-kata kunci: YSZ ceramik;  $\text{MnO}_2$ ; Sifat-sifat mekanikal; Degradasi; Size grain.

## ACKNOWLEDGEMENTS

I would like to convey my gratitude to the following individuals for their support  
in my research work:

- My project supervisor, Prof. Ir. Dr. Ramesh Singh, for allowing me to conduct my research work under his supervision together with his valuable advice, discussion, help and encouragement throughout this thesis.
- The Ministry of Higher Education of Malaysia (MOHE) for the financial support through the MyBrain15 scholarship.
- The research funding from Universiti Malaya (PG091-2015A) and Universiti Tunku Abdul Rahman (UTARRF/2014-C1/T10) for making this research possible.
- My research colleagues in Universiti Malaya, Ir. Dr. Tan Chou Yong, Dr. Kelvin Chew and Dr. Ali Niakan who gave their endless support in my experimental works.
- SIRIM Berhad for providing the support in this research, in particular Dr. Teng Wan Dung of Ceramics Technology Centre for providing the testing facilities and support in this work.
- Finally, I would like to thank my beloved family members for their constant support and encouragement throughout the whole duration of this research.



## TABLE OF CONTENTS

Abstract.....	iii
Abstrak.....	v
Acknowledgements.....	vii
Table of Contents.....	viii
List of Figures.....	xii
List of Tables.....	xvi
List of Symbols and Abbreviations.....	xvii
List of Appendices.....	xviii
<b>CHAPTER 1: GENERAL INTRODUCTION.....</b>	<b>1</b>
1.1 Research Background and Problem Statement.....	1
1.2 Research Objectives.....	3
1.3 Problem Statement.....	3
1.4 Structure of the Thesis.....	4
<b>CHAPTER 2: LITERATURE REVIEW.....</b>	<b>6</b>
2.1 Introduction to Zirconia Ceramics.....	6
2.1.1 Dispersion-Toughened Ceramics.....	8
2.1.2 Partially Stabilized Zirconia.....	8
2.1.3 Single Phase Polycrystalline t-ZrO <sub>2</sub> .....	10
2.2 Toughening Mechanism of Zirconia.....	10
2.3 Low Temperature Degradation (LTD).....	13
2.3.1 Ageing Mechanisms.....	15
2.4 Yttria-Tetragonal Zirconia Polycrystals (Y-TZP) Ceramics.....	21
2.4.1 Stabiliser Content.....	22

2.4.2	Yttria Distribution .....	23
2.4.3	Densification .....	25
2.4.4	Grain Size Effect .....	27
2.4.5	Influence of Additives .....	28
2.4.6	Sintering .....	32
2.4.6.1	Pressure Assisted Fast Sintering .....	39
2.4.6.2	Microwave Sintering .....	43
2.5	Summary .....	48
 <b>CHAPTER 3: METHODOLOGY .....</b>		<b>50</b>
3.1	Introduction.....	50
3.2	Powder Preparation.....	50
3.3	Green Body Preparation .....	53
3.4	Sintering.....	54
3.5	Grinding and Polishing .....	54
3.6	X-Ray Diffraction (XRD).....	54
3.7	Bulk Density Measurement .....	56
3.8	Young's Modulus Determination .....	57
3.9	Vickers Hardness Determination .....	59
3.10	Fracture Toughness Determination.....	61
3.11	Microstructure Examination .....	62
3.11.1	Scanning Electron Microscopy.....	62
3.11.2	Grain Size Measurement .....	63
3.12	Hydrothermal Ageing Experiment .....	66

<b>CHAPTER 4: RESULTS AND DISCUSSION .....</b>	<b>67</b>
4.1 Introduction.....	67
4.2 YSZ Powder Characteristic .....	67
4.3 Sintering Temperature Effect on Undoped YSZ Ceramic.....	68
4.3.1 Tetragonal Phase Retention.....	68
4.3.2 Density.....	69
4.3.3 Young's Modulus .....	70
4.3.4 Vickers Hardness.....	72
4.3.5 Fracture Toughness .....	74
4.3.6 Microstructural Evolution & Grain Size.....	76
4.4 Isothermal Sintering Effect at Low Sintering Temperature with MnO <sub>2</sub> Dopant ...	79
4.4.1 Tetragonal Phase Retention.....	79
4.4.2 Relative Density .....	81
4.4.3 Fracture Toughness .....	83
4.4.4 Vickers Hardness.....	86
4.4.5 Microstructure Evolution .....	89
4.5 Hydrothermal Behaviour .....	95
4.5.1 Sintering Temperature Effect of Undoped YSZ Ceramic.....	96
4.5.2 Hydrothermal Ageing Behaviour of Undoped and MnO <sub>2</sub> -doped YSZ Ceramic Isothermal Sintering at Low Temperature.....	102
4.5.3 Hydrothermal Ageing Mechanism .....	107
 <b>CHAPTER 5: CONCLUSION &amp; FURTHER WORK.....</b>	 <b>112</b>
5.1 Conclusions .....	112
5.2 Further Work .....	115
References.....	116

List of Publications and Papers Presented .....	131
Appendix A – Distilled Water Density.....	132
Appendix B – Instrumentations .....	133

University of Malaya

## LIST OF FIGURES

	Page
Figure 2.1: Stress-induced transformation toughening process (Butler, 1985). .....	11
Figure 2.2: Scheme of the ageing process occurring in a cross section, showing the transformation neighbor to neighbor. (a) Nucleation on a particular grain at the surface, leading to microcracking and stresses to the neighbours. (b) Growth of the transformed zone, leading to extensive microcracking and surface roughening. Transformed grains are gray. Red path represents the penetration of water due to microcracking around the transformed grains. (Chevalier, 2006). .....	15
Figure 2.3: The degradation process of Y-TZP by the OH <sup>-</sup> trigger mechanism (Yoshimura et al., 1987). .....	17
Figure 2.4: Reaction of water and Zr-O-Zr bonds at crack tip (Sato & Shimada, 1985). .....	18
Figure 2.5: Phase diagram for the Y <sub>2</sub> O <sub>3</sub> -ZrO <sub>2</sub> system (Scott, 1975). .....	21
Figure 2.6: Relation of Young's modulus versus bulk density of YSZ ceramic (Ramesh et al., 2008). .....	26
Figure 2.7: Relation of Hardness versus relative density of Y-TZP ceramics (Vasylykiv et al., 2003). .....	26
Figure 2.8: Relative density (a) and Vickers hardness (b) as a function of sintering temperature for different types of 3Y-TZP (Zhang et al., 2014). .....	30
Figure 2.9: Fracture toughness as a function of sintering temperature for different type of 3Y-TZP (Zhang et al., 2014). .....	30
Figure 2.10: Changes of relative density and average grain size with sintering temperature holding for 2 hr. (○), (□), (●), and (■) indicate 3Y, 3YS, 3YE, and 3YSE, respectively. .....	34
Figure 2.11: Various sintering profiles employed in the research (Sivakumar et al., 2011). .....	37
Figure 2.12: Spark Plasma Sintering Process (Chintapalli et al., 2010). .....	40

Figure 2.13: Microstructure of thermally etched samples observed from electron microscope: (a) SPS-65, (b)SPS-90, (c) SPS-120 and (d) SPS-800 (Chintapalli et al., 2010).....	42
Figure 2.14: FE-SEM micrographs of near full dense specimens sintered by PECS at 1400 °C/1min (a), MW at 1400 °C/10 min (b), and CS at 1400 °C/60 min (c) (Borrell et al., 2012).....	47
Figure 3.1: Optical Image of Polished Y-TZP Surface Containing the Vickers Impression. ....	59
Figure 3.2: Schematic Indentation Fracture Pattern of an Idealized Vickers Palmqvist Crack System.....	60
Figure 3.3: Schematic Indentation Fracture Pattern of an Idealized Vickers Palmqvist Crack System. (Khan et al., 2014).....	62
Figure 3.4: Sketch of Diagonal Line on SEM Micrograph.....	64
Figure 3.5: Schematic diagram of the score for several type of line interception. ....	65
Figure 4.1: SEM micrographs of agglomerates as-received YSZ powder.....	67
Figure 4.2: XRD plots of the undoped YSZ ceramics sintered at 1200 °C to 1500 °C revealing tetragonal (t) symmetry.....	68
Figure 4.3: Phase analysis of as-received YSZ ceramics sintered at 1200 °C to 1500 °C.....	69
Figure 4.4: The relationship of sintering temperatures and the relative density of the YSZ ceramics. ....	70
Figure 4.5: Young's modulus variation as a function of sintering temperature.....	71
Figure 4.6: The linear relationship of Young's modulus and bulk density of YSZ ceramics.....	72
Figure 4.7: Influence of sintering temperatures on the Vickers hardness of YSZ ceramic. ....	73
Figure 4.8: Changes of Vickers hardness and density in YSZ ceramic with sintering temperature.....	73
Figure 4.9: Variation of fracture toughness for YSZ ceramic sintered at various temperatures. ....	74

Figure 4.10: Variation of fracture toughness for YSZ ceramic sintered at various grain sizes. ....	75
Figure 4.11: Microstructure evolution of YSZ ceramics sintered at (a) 1200 °C, (b) 1250 °C, (c) 1300 °C, (d) 1350 °C, (e) 1400 °C, (f) 1450 °C and (g) 1500 °C. ....	77
Figure 4.12: Effect of sintering temperatures on the average grain size of the YSZ ceramics. ....	78
Figure 4.13: Effect of sintering temperatures on the density and grain size of the YSZ ceramics. ....	78
Figure 4.14: Cubic phase content of sintered undoped-YSZ ceramic. ....	80
Figure 4.15: Cubic phase content of sintered 0.5 wt.% MnO <sub>2</sub> doped-YSZ ceramic. ....	80
Figure 4.16: Cubic phase content of sintered 1.0 wt.% MnO <sub>2</sub> doped-YSZ ceramic. ....	81
Figure 4.17: Effect of sintering temperature and holding time on the relative density of MnO <sub>2</sub> doped (0, 0.5 & 1.0 wt%) YSZ ceramics. ....	83
Figure 4.18: Effect of sintering temperature and holding time on fracture toughness of MnO <sub>2</sub> (0, 0.5 & 1.0 wt%) doped 3Y-TZP. ....	85
Figure 4.19: The influence of grain size on the fracture toughness of YSZ ceramics for various sintering temperatures (a) 1100 °C, (b) 1150 °C, (c) 1200 °C & (d) 1250 °C. ....	86
Figure 4.20: Effect of sintering temperature and holding time on the Vickers hardness of MnO <sub>2</sub> doped (0, 0.5 & 1.0 wt%) YSZ ceramics. ....	87
Figure 4.21: Changes of Vickers hardness and density in undoped YSZ for various sintering temperatures (1100, 1150, 1200 and 1250°C). ....	88
Figure 4.22: Microstructure evolution of undoped YSZ ceramics sintered at 1100°C: (a) 12 min, (b) 480 min, 1150°C: (c) 12 min, (d) 480 min, 1200°C: (e) 12 min, (f) 480 min & 1250°C: (g) 12 min, (h) 480 min. (GS) Indicate grain size. ....	90
Figure 4.23: Microstructure evolution of 0.5 wt% MnO <sub>2</sub> -doped YSZ ceramics sintered at 1100°C: (a) 12 min, (b) 480 min, 1150°C: (c) 12 min, (d) 480 min, 1200°C: (e) 12 min, (f) 480 min & 1250°C: (g) 12 min, (h) 480 min. (GS) Indicate grain size. ....	91
Figure 4.24: Microstructure evolution of 1.0 wt% MnO <sub>2</sub> -doped YSZ ceramics sintered at 1100°C: (a) 12 min, (b) 480 min, 1150°C: (c) 12 min, (d)	

480 min, 1200°C: (e) 12 min, (f) 480 min & 1250°C: (g) 12 min, (h) 480 min. (GS) Indicate grain size. ....	92
Figure 4.25: Effect of sintering temperature and holding time on the average grain size of the MnO <sub>2</sub> doped (0, 0.5 & 1.0 wt%) YSZ ceramics. ....	93
Figure 4.26: Changes of grain size and density in undoped YSZ for various sintering temperatures (1100, 1150, 1200, 1250°C). ....	94
Figure 4.27: Changes of grain size and density in 0.5wt.% MnO doped YSZ for various sintering temperatures (1100, 1150, 1200, 1250°C). ....	94
Figure 4.28: Changes of grain size and density in 1.0wt.% MnO doped YSZ for various sintering temperatures (1100, 1150, 1200, 1250°C). ....	95
Figure 4.29: Low temperature degradation (LTD) on the monoclinic phase formation in YSZ ceramics when exposed to 120 hr superheated steam at various sintering temperatures. ....	97
Figure 4.30: Grain size dependence on the LTD induced monoclinic phase development in YSZ ceramics after exposure for 120 h in superheated steam. ....	100
Figure 4.31: Hydrothermal ageing on the monoclinic phase formation in 0.5 wt% MnO <sub>2</sub> doped YSZ ceramics when exposed to superheated steam sintered at 1250 °C. ....	103
Figure 4.32: Hydrothermal ageing on the monoclinic phase formation in 1.0 wt% MnO <sub>2</sub> doped YSZ ceramics when exposed to superheated steam sintered at 1200 and 1250 °C. ....	103
Figure 4.33: Grain size dependence on the LTD induced monoclinic phase development in YSZ ceramics sintered at 1250 °C for various holding time (12, 60, 120, 240 & 480 min) after exposure for 300 hr in superheated steam. ....	104
Figure 4.34: The relationship between the cubic phase content and average grain size on the (m) phase development for of the YSZ ceramic. ....	106
Figure 4.35: EDAX analysis at the grain interior of the 1.0 wt% MnO <sub>2</sub> -doped YSZ ceramic sintered at 1250 °C with holding time, 480 min. ....	107



## LIST OF TABLES

	Page
Table 2.1: Conditions and measured properties of the different specimens (Chintapalli et al., 2010).....	41
Table 2.2: Summary of sintering parameters and final grain size determined for all materials after conventional and microwave sintering (Presenda et al., 2015).....	45
Table 3.1: Starting powders compositions. ....	51
Table 3.2: Characteristic of the starting 3 mol% yttria-stabilized zirconia powder.....	52
Table 3.3: Characteristic of the doping MnO <sub>2</sub> powder. ....	52
Table 3.4: Samples labelling used in present study. ....	53
Table 4.1: The properties of YSZ samples sintered at various temperatures.....	101
Table 4.2: The properties of YSZ ceramics doped with MnO <sub>2</sub> , sintered at various sintering profiles.....	111

## LIST OF SYMBOLS AND ABBREVIATIONS

$\text{Al}_2\text{O}_3$	:	Aluminium oxide or Alumina
$\text{CuO}$	:	Copper oxide
c	:	Cubic phase
E	:	Young's modulus or modulus of elasticity
EDAX	:	Energy dispersive X-ray micro analysis
$\text{Fe}_2\text{O}_3$	:	Iron oxide
HIP	:	Hot Isostatic Press
$H_v$	:	Vickers hardness
$K_{Ic}$	:	Fracture toughness
LTD	:	Low Temperature Degradation
m	:	Monoclinic phase
$\text{MnO}_2$	:	Manganese oxide
$M_s$	:	The martensitic starting temperature of the t to m phase transformation on cooling
t	:	Tetragonal phase
$\rho$	:	Bulk density
SEM	:	Scanning Electron Microscope
$\text{SiO}_2$	:	Silicon oxide or Silica
XRD	:	X-ray diffraction
Y-TZP	:	Yttria-Tetragonal Zirconia Polycrystals
YSZ	:	Yttria Stabilised Zirconia
$\text{ZrO}_2$	:	Zirconium oxide or Zirconia
JCPDS- ICDD	:	Joint Committee of Powder Diffraction Standard International Center for Diffraction Data

## LIST OF APPENDICES

	Page
Appendix A: Distilled Water Density	132
Appendix B: Instrumentation	133

University of Malaya

## CHAPTER 1: GENERAL INTRODUCTION

### 1.1 Research Background and Problem Statement

Yttria-Tetragonal Zirconia Polycrystals (Y-TZP) ceramics are becoming popular in engineering applications due to combinations of attractive properties including superior strength ( $> 1000$  MPa) (Tong et al., 2016), high hardness and fracture toughness (Singh et al., 1996), high wear resistant (Valefi et al., 2012), good thermal properties, chemical stability and smooth appearance. These superior mechanical properties of Y-TZP can be attributed to a phenomenon known as transformation toughening (TT) (Garvie et al., 1975). This mechanism states that the stress of a propagating crack will be absorbed by the metastable tetragonal (t) grains in the vicinity and transformed to the monoclinic (m) symmetry with an accompanying volume expansion of 3 to 4%. The net effect is that higher level of stress would be required to maintain crack progression, thus explaining the high strength and toughness of the ceramic. The effectiveness of TT, however is controlled, in general by the amount of tetragonal phase retained and more specifically the stability of the (t) grains in the structure. The retention of the tetragonal structure to room temperature can be achieved by doping zirconia with yttria (2.5 to 3 mol%) (Cui et al., 2017). On the other hand, the stability of the tetragonal particles is dependent on several factors which include the yttria content and distribution, processing technique and the present or absent of sintering additives (Ramesh et al., 1999; Singh et al., 1996). In addition, the sintering conditions such as sintering techniques (e.g. hot pressing, HIPing, pressureless sintering and microwave sintering), soaking temperature, holding time and the ramp rates have a direct effect on the microstructure of the zirconia and this in turn will influence the mechanical properties of the zirconia. Chen and Brook (1989) suggested that the temperature has the greatest effect on the bulk density of the ceramic rather than the holding time or the ramp rates. Matsui et al. (1983) reported that sintering at  $1300^{\circ}\text{C}$

and 1500°C caused the density of the zirconia to increase with time but sintering beyond 1500°C was detrimental as the density was found to decrease with time. Lawson (1995) observed that although a high tetragonal phase retention (> 99%) could be retained in Y-TZPs sintered at 1250°C using a long holding time of 12 hours, the hardness of this ceramic was rather low (< 9 GPa). However these authors also reported that a two stage sintering (i.e. pre-sintering at 1250°C for up to 12 hours and then firing at 1450°C for 2 hours) resulted in enhanced densification, high tetragonal phase retention and good mechanical properties. However, one of the major problem with Y-TZP ceramic is the undesirable spontaneous transformation of tetragonal to monoclinic symmetry especially in the presence of water at temperatures ranging from 100 – 300°C (Cattani-Lorente et al., 2011; Keuper et al., 2014a). This phenomenon known as low-temperature degradation (LTD) or hydrothermal ageing spread from the surface into the body of the ceramic, causing compressive stresses induced by the volume expansion of the transformed monoclinic grains accompanied by crack formation and eventually results in fracture of the ceramic. The mechanism of LTD still remains a subject of intense debate, but the presence of water or hydroxyls has been identified as the catalyst in accelerating the ageing-induced tetragonal to monoclinic phase transformation. Different approaches have been experimented to enhance the ageing resistance of Y-TZP such as altering the content and distribution of the yttria stabilizer and decreasing the tetragonal grain size. Some of the approaches taken have resulted in either a compromise on the mechanical properties, the use of expensive chemicals and process equipment and can even be labour intensive. Therefore, enhancing the LTD resistance of YSZ ceramic is vital besides preserving the excellent mechanical properties, particularly the fracture toughness. Consequently, a new method to fabricate a YSZ ceramic that resistant to low temperature degradation (LTD) are developed where advanced ceramic product with good reliability and long life span could be produced.

Besides, various process parameters that governing the LTD mechanism YSZ ceramic are observed through current work.

## **1.2 Research Objectives**

The objectives of this project are:

1. To fabricate a solid YSZ ceramic body with enhanced LTD resistance when exposed to superheated steam at 10 bar and 180 °C without sacrificing the mechanical properties by pressureless sintering at low temperatures (below 1300 °C) and various holding times (12 to 480 min.).
2. To enhance densification and to control the grain growth of YSZ ceramic by using MnO<sub>2</sub> (0.5 and 1.0 wt%) as the sintering aid.
3. To determine the influence of MnO<sub>2</sub> on the densification, mechanical properties and LTD resistance of the sintered YSZ.
4. To determine the effect of grain size and yttria distribution on the ageing mechanism of YSZ ceramic.

## **1.3 Problem Statement**

1. Great potential of YSZ as structural material was hampered by Low Temperature Degradation (LTD) where surface initiated tetragonal to monoclinic phase transformation, accompanied by degradation of strength and/or fracture toughness during exposure to low temperature (<250 degree celsius) water or aqueous solutions. Accompany by micro and macro crack formation.
2. Different approaches sintering techniques (e.g. two step sintering, hot pressing, HIPing, Plasma sintering and microwave sintering) were developed to enhance the ageing resistance of YSZ. However these methods causes deteriorating mechanical properties and required high cost or even labour intensive.

3. Many studies on YSZ were focused either only on the mechanical properties or on the LTD behaviour. It is however important to preserve the excellent mechanical properties, especially the fracture toughness, when developing hydrothermally stable YSZ in humid environment at low temperature.
4. Sintering conditions of zirconia ceramics especially sintering temperature and holding time was found to be most substantial on the mechanical properties and ageing resistance on the sintered YSZ ceramic. Hence, understanding the sintering mechanism is vital for fabricating ceramic of an optimum grain size and phase composition that minimizes transformation and thus reduces degradation under hydrothermal environment without sacrificing the mechanical properties of YSZ ceramic.

#### **1.4 Structure of the Thesis**

The structure of this thesis is organized based on the outline described below:

Chapter 1 gives the overall background of current study, objectives of this work, problems statement and the structure of thesis.

In Chapter 2 reviews the mechanical properties especially on the transformation toughening mechanism that makes zirconia a superior in engineering materials for structural applications. Other toughening mechanisms are discussed according to the literature provided concerning the toughening of zirconia ceramics. In this chapter, all the factors that contribute to the sintering behavior of Y-TZP ceramics including stabilizer content, grain size effect, use of dopants and sintering technique. This chapter provides details on the sintering characteristic of Y-TZP which offers the ideas on enhancing the sintering process while improving mechanical properties and ageing resistance of the ceramics.

A details of the apparatus used and experimental procedures of the present work are described in Chapter 3, where the test samples are prepared before prior to all the testing.

The results and discussions are presented in Chapter 4. The influence of sintering temperature towards the densification and mechanical properties of YSZ are established at the initial section of this chapter. Subsequently the effects of low sintering temperatures at various holding periods on the properties of YSZ doped with different amount of MnO<sub>2</sub> are deliberated. In addition, the hydrothermal ageing mechanism that was consistent with the experimental results was proposed.

Conclusions of the research work and recommendations for further work are presented in Chapter 5.



## CHAPTER 2: LITERATURE REVIEW

### 2.1 Introduction to Zirconia Ceramics

Since the ancient times, Zircon has been known as precious stone. Zircon named after 'Zargon' (Arabic word for golden in colour). In 1789, zirconia (Zirconium dioxide) was discovered by Martin Heinrich Klaproth, a German chemist as the byproduct obtained after heating some gems. For quite some time, zirconia was used to gather with rare earth oxides as pigment for ceramics (Piconi & Maccauro, 1999). Relatively large quantity of  $ZrO_2$  exist naturally as baddeleyite (monoclinic zirconia) in Brazil and as zircon ( $ZrSiO_4$ ) sands in Australia and India. Pure zirconia is allotropy with the same chemical composition but different atomic arrangement. At room temperature and pressure, pure zirconia exists as monoclinic (m). However with an increase in the temperature, the material transforms to tetragonal (t) at  $1170^\circ C$  and to a cubic (c) above  $2370^\circ C$ . The tetragonal to monoclinic phase transformation occurs around  $950^\circ C$  on cooling in pure  $ZrO_2$  accompanied by a volume expansion of 4-5% and shear strain of 14-15%. Stresses by the expansion originate cracks and leads to extensive cracking in pure zirconia ceramics. Thus, at room temperature, pure zirconia can retain neither tetragonal nor cubic phase and is not suitable for structural application. It can only limit its application to refractory applications.

Zirconia has found its potential as engineering materials when attempt was made to retain the tetragonal, or even the cubic forms in metastable form at room temperature because the ceramic body remain intact with addition of other metal oxides to zirconia.

High wear resistant, excellent refractory and tough zirconia ceramics are used as engineering material to fabricate components operating in hostile environments, such as valves, port liners and extrusion dies for internal combustion engines, low corrosion, thermal shock resistant refractory liners and petrochemical valve parts (Saremi-

Yarahmadi et al., 2018). Zirconia based materials are used as cutting tools for Kevlar, magnetic tapes, cigarette filters (because of their reduced wear), knives and scissors used in paper industries, seals, thrust bearings, valve seats, valve guides for turbocharger rotors, pump parts, seal faces and milling media. Good ionic conductivity at high temperature condition makes zirconia ceramics as suitable material to fabricate solid electrolytes in fuel cells (Azim Jais et al., 2017) and oxygen sensors (Akasaka, 2016). Excellent chemical and corrosion resistance, dimensional stability, high mechanical strength and a Young's modulus equivalent to the stainless steel alloys was the main reason to be used as a ceramic biomaterial. Commercial application includes femoral ball heads for prostheses and dental restoratives (Camposilvan et al., 2015).

During occurrence of crack propagation around the affected grains, the metastable tetragonal grains transform into monoclinic structure with volume expansion which induces compressive stresses, eventually crack propagation was reduced or eliminated (Hannink et al., 2000a). The structural reinforcement by the phase transformation is also classified as phase transformation toughening (PTT). Thus far binary systems of zirconia with alloy and especially stabilizers (i.e. CaO, MgO, Y<sub>2</sub>O<sub>3</sub>, CeO<sub>2</sub>, Er<sub>2</sub>O<sub>3</sub>, Eu<sub>2</sub>O<sub>3</sub>, Gd<sub>2</sub>O<sub>3</sub>, Sc<sub>2</sub>O<sub>3</sub>, La<sub>2</sub>O<sub>3</sub>, and Yb<sub>2</sub>O<sub>3</sub>) (Lughi & Sergio, 2010) are available. Owing to its strength which resembles steel (Garvie et al., 1975), scientists began to put interest in using zirconia ceramic as a biomaterial. Various studies have been conducted on biomedical application of zirconia from the late sixties. The use of zirconia as ball heads material alternative to alumina (due to brittleness) for Total Hip Replacement (THR) was then commercially introduced. In addition, most work done was for biomaterials purposes are CaO (Fassina et al., 1992), MgO, Y<sub>2</sub>O<sub>3</sub> and CeO<sub>2</sub>. Generally, there are three classes of Zirconia ceramics. Two out of the three are with minimum two-phase materials with t- ZrO<sub>2</sub> as the minor phase (dispersed and precipitated respectively) and another one is solely tetragonal single-phase zirconia.

### 2.1.1 Dispersion-Toughened Ceramics

This material is characterized by the dispersion of 5-30 % t-  $ZrO_2$  or unstabilised zirconia in a ceramic matrix such as alumina (Shin et al., 1990). The common dispersion-toughened materials are  $ZrO_2$  – toughened mullite (ZTM) and the most commercially developed system  $ZrO_2$  – toughened alumina (ZTA). The stability of the t phase in  $ZrO_2$  at room temperature is mainly controlled by particle size, particle morphology and location instead of the use of stabilizer. ZTA for instant experiences t-m phase transformation when the particles are above critical size upon cooling to room temperature. The observation of particle size effects that influence the martensitic start ( $M_s$ ) temperature has implied that the particle size effect is likely besides other factors such as effects of surface strain energy and chemical free energy driving forces (Denry & Kelly, 2008; Heuer et al., 1982). Commercially available of a dispersion-toughened ceramics consist of 30% glass and 70% polycrystalline ceramic with  $Al_2O_3$  :  $ZrO_2$  in a vol.% ratio of approximately 70:30.

### 2.1.2 Partially Stabilized Zirconia

Partially stabilised zirconia (PSZ) comprised of coarse grain microstructure with t- $ZrO_2$  precipitates embedded in c- $ZrO_2$  grains (Hannink et al., 2000b; Rühle & Evans, 1989). Fine lenticular precipitates of tetragonal phase are formed in the cubic zirconia matrix by heat treating in the two-phase (c + t) field at temperature  $\sim 1600$  °C. The two-phase  $ZrO_2$  system, partially stabilized zirconia (PSZ) is formed with low solubility stabilizers (such as MgO and CaO) in concentrations lower than that required for full c- $ZrO_2$  stabilization and precipitated systems with tetragonal or monoclinic precipitates inside the cubic matrix as the minor phase and these precipitates were formed at grain boundaries and in the cubic matrix grains (Subbarao, 1981). Garvie and Nicholson

Garvie and Nicholson (1972) revealed that the mechanical strength of PSZ ceramic was enhanced by homogeneous distribution of fine monoclinic phase inside the cubic matrix. Then Garvie et al. (1975) successfully turned zirconia into engineering material by developing metastable tetragonal precipitates in the cubic matrix with addition of 8% mol of MgO to ZrO<sub>2</sub> which further improve mechanical strength and toughness of the material. The increase in toughness as the result of tetragonal (t) to monoclinic (m) transformation of zirconia particle that will be discussed in latter section. Precipitates are fully coherent with the cubic lattice where a lenticular morphology is formed with about 200 nm diameter and 75 nm thicknesses. Ageing process was performed by solution annealing in the cubic solid solution single-phase field (approximately >1850 °C). Next, precipitates are nucleated and grown at lower temperatures (approximately >1100 °C) within the two-phase solid solution comprises of tetragonal and cubic phase field. Ageing optimization (time-temperature-transformation) involves both precipitate size and phase stability. Metastability will not be achieved if tetragonal precipitates are small in size but large precipitates leads to spontaneous t to m transformation that causes twinning and microcracking. Magnesia partially stabilized zirconia (Mg-PSZ) was the first zirconia introduced in orthopedics, but was abandoned due to modest strength and fracture toughness. There are a few factors to this which are elaborated in the following paragraphs.

Sintered Mg-PSZ is characterized by residual porosity which is common in ceramics with grain size around 30 - 40 µm and the wear rate of UHMWPE sockets that are couple with zirconia ball heads was intensified. In terms of technical aspect, Mg-PSZ requires high sintering temperature 1800°C as compare to 1400 °C; implying the need for special furnace as well as stringent control during the cooling process at 1100 °C as the formation of t-phase occurs (Piconi & Maccauro, 1999). Followed by the formation of enstatite (MgSiO<sub>3</sub>) and forsterite (Mg<sub>2</sub>SiO<sub>4</sub>) as the impurities (SiO<sub>2</sub> and

$\text{Al}_2\text{O}_3$ ) originated from the wear of milling media during the powder processing drain out much Mg and causing t-phase losses its stability in the wet condition. Therefore the use of such additives in tetragonal zirconia polycrystals is not encouraged especially as ceramic biomaterials (Leach, 1987). The issue of impurities contains in Mg-PSZ have raised the concern to bioceramics manufacturer to focus on alternative materials. Therefore yttria was introduced in the zirconia matrix as the stabilizer to formed PSZ.

### **2.1.3 Single Phase Polycrystalline t-ZrO<sub>2</sub>**

Single-phase ZrO<sub>2</sub> system, tetragonal zirconia polycrystal (TZP) is obtained when a solid solution forms at high temperature and is retained upon cooling with the high solubility of the stabilizer (Y<sub>2</sub>O<sub>3</sub> and CeO<sub>2</sub>). PSZ ceramics could be produced with addition of yttria but it has been used as the main stabilizer for TZP ceramics for structural ceramic and production of solid-electrolyte material. Yttria-Tetragonal Zirconia Polycrystal (Y-TZP) is better in term of mechanical properties and chemical inertness as well as the ease of manufacturing as compared to the preparation of PSZ ceramic which requires proper control.

## **2.2 Toughening Mechanism of Zirconia**

Zirconia ceramics have high toughness as compared to the other engineering ceramics mainly due to the nature of the phase transformation zirconia particles. The toughening mechanisms involved are stress-induced transformation toughening, microcracking toughening and surface toughening.

Stress-induced transformation toughening is the main mechanism in which TZP ceramics gain substantial improvement in toughness and flexural strength. The

metastable tetragonal particles will undergo t to m transformation when stresses are exerted on them (Chevalier et al., 1996). Tensile stresses were generated as the result of crack extension at the crack tip on the surface of the YSZ ceramic. The grains experience phase transformation t to m when the intensity of the stress at the crack tip overcomes the matrix constraint of the tetragonal grains ahead of the crack front. The volume expansion (3 – 5%) characteristic of the t – m transformation creates a compressive stress which acts in opposition to the stress field that promotes the propagation of the crack. This leads to the enhancement in toughness and strength. Figure 2.1 depicted the schematic representation of this phenomenon.

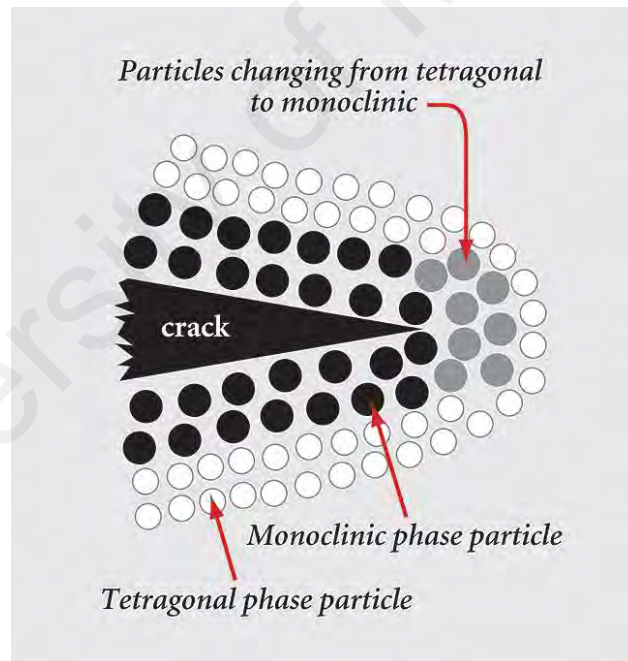


Figure 2.1: Stress-induced transformation toughening process (Butler, 1985).

The stress-induced microcrack in zirconia contributes to toughness enhancement as the result of energy dissipation and it is an irreversible deformation phenomenon (Evans & Heuer, 1980). The microcracks are formed due to volume expansion during

cooling from the sintering temperature where a restricted number of  $ZrO_2$  particles experience the t to m transformation. Interaction between the propagating crack and these microcracks leads to deflection and blunting of the crack, which enhance the toughness of the ceramic structure. The effectiveness of the microcrack toughening mechanism is dependent on the size of t- $ZrO_2$  particles in which it must be large enough to allow phase transformation but small enough to cause limited microcracking formation. Furthermore, the strength is dependent on the size of the microcracks and its effect on the inherent flaws and grain sizes. The microcracks formed can pose adverse effects on other properties such as elastic modulus, coefficient of thermal expansion and thermal conductivity.

The surface toughening is of significance when tensile stress is applied on the free surface of a ceramic. This toughening mechanism can be formed by altering (grinding, polishing or ageing transformation) the tetragonal grains in the surface layer (thickness of 10 to 100  $\mu m$ ) to induce t to m phase transformation while tetragonal grains in the bulk are remained in the tetragonal form. The surface toughening is found to improve the strength of zirconia-based ceramics as the compressive surface stresses are able to seal surface flaws yet subjected to the roughness of the grinded surface. It was found that surface ground with finer grit was stronger than the one with coarser grit as the later grinding condition resulted in more residual stress and thicker layer on the free surface. Furthermore, ceramics with grinded surface were relatively less strength than those that were polished or lapped (Curtis et al., 2006). On the contrary, the strength of zirconia ceramic was found to increase with the roughness of the grinding media due to higher compressive stress generated by higher content of transformed monoclinic grain at the surface (Gupta, 1980). The surface toughening was also found to be beneficial in improving degradation resistance of Y-TZP ceramics when exposed in the superheated steam (Deville et al., 2006). However the process of inducing the

stress on the free surface of zirconia ceramics required proper preparation to achieve the desirable strength enhancement or it may damage the ceramics' structural integrity.

### **2.3 Low Temperature Degradation (LTD)**

Zirconia based materials is one of the ceramics materials that have properties close to steel with excellent mechanical properties such as bending strength and high fracture toughness ( $>12 \text{ MPam}^{1/2}$ ) owing to the transformation toughening (tetragonal to monoclinic phase transformation) around propagating crack tips. However due to the metastable of the tetragonal, transformation to monoclinic phase accompanied by property degradation is the major setback of the material for the wide range of engineering application as well as biomaterials. Consequently, this t - m transition can be both beneficial and detrimental to the properties and the lifetime of the ceramic (Keuper et al., 2014b).

Recently, zirconia ceramics have regained popularity among biomedical application specifically dental implantology with approximately 25 million dental implants inserted worldwide every year and the number escalates to more than 12% per year. As result of excellent biocompatibility, low thermal conductivity, high flexural strength coupled with an excellent "white esthetic", zirconia ceramics are used as the material for implant abutment and also tooth supported restorations (single crowns, fixed dental prostheses or telescopic crowns), albeit all these dental restorations are exposed in the oral cavity that will promote degradation. Some works have shown that spontaneous transformation of tetragonal to monoclinic is apparent in a humid environment at temperature range from 20 – 300 °C (Cattani-Lorente et al., 2011). For example, aqueous saliva, temperature changes, acidification during food intake and cyclic loading during chewing which leads to degradation and eventually deteriorating



of mechanical strength. The issue of degradation is yet to be fully resolved even though it is not a major concern for the time being. However there is no guarantee on the long term survival of zirconia implant abutments and other zirconia based restorations remains puzzle.

The drawback of the highly potential in advanced materials of TZP is the occurrence of the low temperature degradation (LTD) which was found by Kobayashi et al. (1981), subsequently many literatures have reported on the similar event on the rapid deterioration of mechanical properties whereby LTD initiates at the surface of polycrystalline zirconia and then progresses towards the bulk of the material. During LTD progresses in the humid environment at considerably low temperatures (150 – 400 °C), phase transformation from metastable tetragonal phase to the more stable monoclinic phase was occurred in grains at the ceramic surface. As described in Figure 2.2, phase transformation t – m begins in isolated grains on the surface and followed by a volume increase (4%) which stress was building up on the neighboring grains and then leads to microcracking. Cracking path allows water to penetrate into the bulk sample and giving way for further growth on the adjacent grains. The continuous transformation of t to m grains leads to severe microcracking, grain pullout and followed by surface roughening, which eventually deteriorate in mechanical strength. Further than hydrothermal degradation of 3Y-TZP, factors that cause low temperature degradation such as grain size, the stabiliser content and residual stresses was discussed in literature.

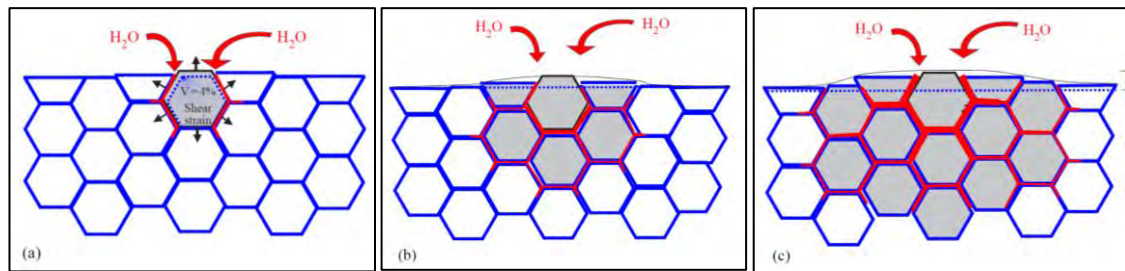


Figure 2.2: Scheme of the ageing process occurring in a cross section, showing the transformation neighbor to neighbor. (a) Nucleation on a particular grain at the surface, leading to microcracking and stresses to the neighbours. (b) Growth of the transformed zone, leading to extensive microcracking and surface roughening. Transformed grains are gray. Red path represents the penetration of water due to microcracking around the transformed grains. (Chevalier, 2006).

### 2.3.1 Ageing Mechanisms

In Lange et al. (1986)'s work on 6.6 mol% of Y-TZP ageing at 250 °C in the tube furnace with humid environment and discovered regular traces of yttrium rich crystallites which found to be  $\alpha$ -Y(OH)<sub>3</sub> next to the transformed monoclinic grains. Their hypothesis stated that the formation of Y(OH)<sub>3</sub> was attributed to the continuous drawing of Yttrium from the grain surface in the presence of water and thus destabilizing small volume element where monoclinic nucleus grow (Lange et al., 1986). The spontaneous growth of monoclinic grains will occur once it attained a critical size without any further Yttrium diffusion from the tetragonal grains in which it was growing. Similar observation was found by (Winnubst, 1988) and he suggested the tetragonal to monoclinic transformation will occurred when a critical grain size and composition are reached.

Ageing induce transformation was described in two different explanations which are mechanical and chemical degradation mechanisms. For the mechanical degradation

mechanism, stress corrosion cracking of the amorphous intergranular glassy phase or of the tetragonal grains has been considered. On the other hand, chemical degradation mechanism claims that the water is believed to form  $\text{OH}^-$  by the chemisorption at the surface of Y-TZP grains, or form  $\text{Y}(\text{OH})$  which is leading to the depletion of yttrium. Sato and Shimada (1985) proposed that the water reacted primarily with Zr-O-Zr bonds on the ceramic surface instead of the stabilizing oxide. Yoshimura et al. (1987) investigated the function of water molecule on degradation in Y-TZPs and proposed that degradation was attributed to the  $\text{OH}^-$  ion according to the anion diffusion mechanism as described below and shown schematically in Figure 2.3.

- Step 1: Chemical adsorption of  $\text{H}_2\text{O}$  at the surface.
- Step 2: The formation of Zr-OH and/or Y-OH bond at the surface, at which points stressed sites are created.
- Step 3: The accumulation of strain by the migration of  $\text{OH}^-$  ions at the surface and in the lattice, to prepare nucleating defects.
- Step 4: The nucleation of monoclinic phase in the tetragonal grains: then the tetragonal-monoclinic transformation yields micro and macro-cracking.

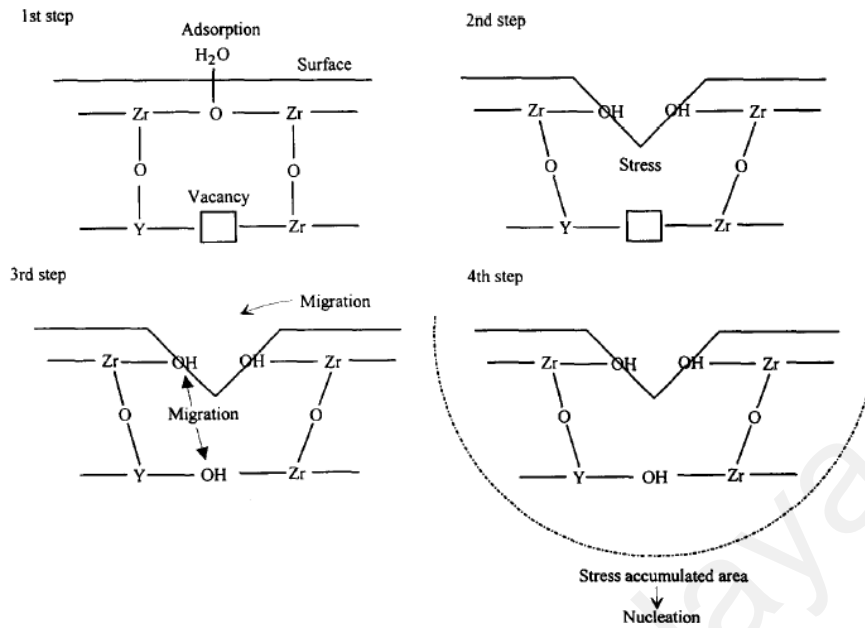


Figure 2.3: The degradation process of Y-TZP by the  $OH^-$  trigger mechanism (Yoshimura et al., 1987).

Based on the IR spectroscopy and confirmed by Raman spectroscopy, the inclusion of  $-OH$  ion in the crystal lattice on transformed monoclinic grains during ageing and exclusion of the  $-OH$  ion accompanied by decreasing lattice parameter after the degraded sample was heated at high temperatures. Yoshimura et al. (1987) measured about 60% of oxygen vacancies were consist of  $-OH$  ions due to more charge and similar ion size which allow  $-OH$  ions to travel faster than  $O^{2-}$  ions. Yoshimura et al. (1987) disproved with Lange's hypothesis by mentioning that at low temperature and in short period of time, yttrium diffusion as the result of  $Y(OH)_3$  formation is unlikely. The activation energy for t-m formation remained constant irrespective of high temperature and high water pressure which further proposes that it is controlled by  $-OH$  diffusion. According to the energy barrier of t-m transformation, once the critical value of strains energy is achieved, spontaneous nucleation of monoclinic occurred and it becomes autocatalytic.

The development of Zr-OH at the surface and formation of OH<sup>-</sup> leading to the release of strain which is to stabilize the t-ZrO<sub>2</sub> grains in the matrix was also proposed by Sato *et al.* (Figure 2.4). The degradation happened when the strain was released and developed on the pre-existing crack which will lead to the phase transformation.

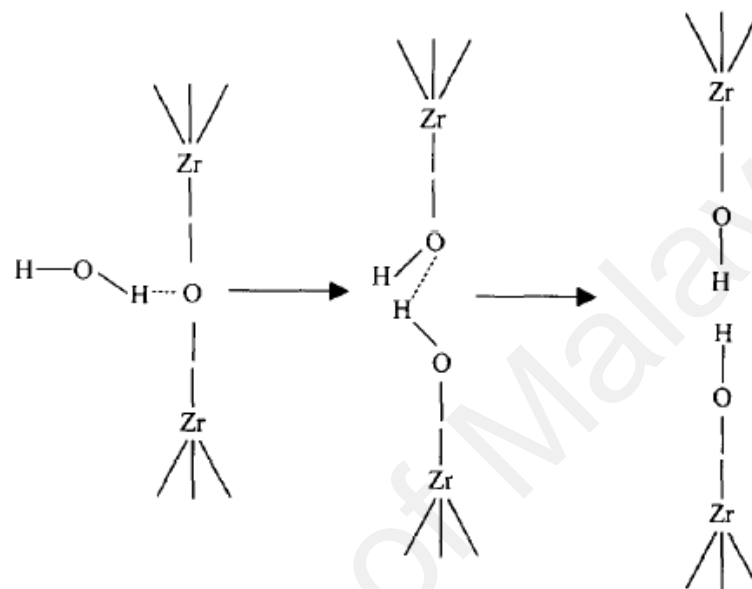


Figure 2.4: Reaction of water and Zr-O-Zr bonds at crack tip (Sato & Shimada, 1985).

(Swab, 1991) claimed the small portion of tetragonal grain surface of the test samples transformed to monoclinic structure when sufficient amount of yttria was depleted by the water vapour that occurs at the interface between water and grain surface. The monoclinic nucleus will grow as water continues to draw yttria from the grain until a critical size was achieved. Above critical size, the growth of monoclinic nucleus is spontaneous without the need of any diffusion of yttria from the grain to transform the tetragonal grain to monoclinic completely. However, only sufficient monoclinic grain size will create microcracks that will expose the sub layer of tetragonal grains for further diffusion of yttria. Therefore, long range diffusion of yttria

to the ceramic surface is necessary if the monoclinic grain is smaller than the critical grain size for t to m transformation.

A number of experimental observations have shown oxygen vacancies mechanism plays a vital role in stabilization of  $ZrO_2$ . (Kim, 1990) alloyed 3Y-TZP with  $Ta_2O_5$  and  $Nb_2O_5$  and annealed (100-265C) in air, dry air, and vacuum to further explore the function of moisture in the low temperature degradation (LTD). Based on the observation, he suggested that the accumulation of residual stress on the specimen surface due to the diffusion of oxygen vacancies from the sample surface into the interior where distortion of the Zr-O bonds on the surface took place, which enhanced the t-m transformation as well as the reaction between Zr-O-Zr bond and  $H_2O$  (Kim, 1997). Kim (1997) extended research work implied that the LTD in Y-TZP is governed by thermally activated oxygen vacancy diffusion instead of water (Kim et al., 1998).

Hernandez et al. (1991) suggested formation of oxyhydroxide  $YO(OH)$  from the reaction between OH and  $Y_2O_3$  did enhance the transformation of t-m. Nevertheless none of the above mentioned mechanisms are able to relate to the grain size effect. Chevalier et al. propose that  $O_2^-$  originating from the dissociation of water, and not OH<sup>-</sup>, is responsible for the filling of oxygen vacancies which is believed to be one of the causes of destabilization and, hence, of LTD and for the long diffusional path.

Research has shown that internal stresses have certain effects on the LTD of Y-TZP (Schmauder & Schubert, 1986) where by shear and tensile stresses are destabilizing but not for the compressive stresses. The transformation was mainly triggered by the largest stress component which is the shear stress attributed to the anisotropy of the thermal expansion and the stresses increase upon cooling. (Schmauder & Schubert, 1986) suggested stress corrosion caused by the water vapour to destabilised the grains on the surface. Formation of  $Y(OH)_3$  on the surface grains

causing stress-corrosion at the location where Yttrium depleted as monoclinic nucleated and grew along with anisotropy stresses during thermal expansion. The water vapour propagates auto catalytically into the grains at the sublayer through microcracks as the result of volume expansion of transformation grains. Matsui et al. (1986) reported that the area subjected to tension showed nearly 100% of tetragonal grains of an aged 3Y-TZP sample transformed into monoclinic grains as compared to the area subjected to compression stresses with lower rate of transformation.

Three basic mechanisms are proposed based on the several view points on degradation of zirconia based materials by the researchers which are corrosion mechanism, destabilization mechanism and stress induced transformation (Lawson, 1995).

For corrosion mechanism, the Zr-OH bonds were formed as the result from the interaction of zirconia with the presence of water. The stress was building up at these bonds as OH<sup>-</sup> ions in the lattice occupying the oxygen vacancies. Micro and macro-cracks were formed as the result of the nucleation of the monoclinic phase. Second, the destabilization mechanism, the Y(OH)<sub>3</sub> or Y(O)OH were formed based on the interaction of OH<sup>-</sup> ions with the stabilizer, yttria resulting in depleting of yttrium followed by the destabilization of t-ZrO<sub>2</sub> and formation of m-ZrO<sub>2</sub>. The stress induced transformation mechanism occurred as the consequence of the stresses which contributed by thermal expansion anisotropy and becomes intensify when cooling down from the high sintering temperature. The stress caused by water vapour acting on ceramic grains on the material surface has been referred to as thermal expansion anisotropic stress. An accompanying phenomenon is the formation of Y(OH)<sub>3</sub> as the consequence of water diffusion through the material. Due to volume changes, the transformed grains cause microcracks and the material becomes degraded.

## 2.4 Yttria-Tetragonal Zirconia Polycrystals (Y-TZP) Ceramics

3mol % Yttria Tetragonal Zirconia Polycrystalline (3Y-TZP) having 3 mol%  $Y_2O_3$  content, are characterised by ~100% tetragonal structure with minute of cubic phase at temperature 1400 °C to 1500 °C as depicted in Figure 2.5. The Y-TZP had high flexural strength which is about 900 to 1200 MPa and the fracture toughness is about 9 to 10 MPam<sup>1/2</sup> (Vidotti et al., 2013). The Young's modulus of Y-TZP is about 210 GPa (Sevilla et al., 2010) and excellent wear properties (Basu et al., 2004). 3Y-TZP is widely used in engineering application, such as cutting tool, watch casing, abrasive tools due to its high fracture toughness (Masaki, 1986a). It is extremely commonly used in dental implantation due to its great bio-compatibility to a human body (Malkondu et al., 2016). Such material will not any adverse effect on the human body even in prolonged implanted with living cells (Picconi & Maccauro, 1999). The strength and fracture toughness of Y-TZP is very much dependent on the starting powder and sintering parameters. However, all designers are aware that the usage of 3Y-TZP suffers from low temperature degradation (Lawson, 1995).

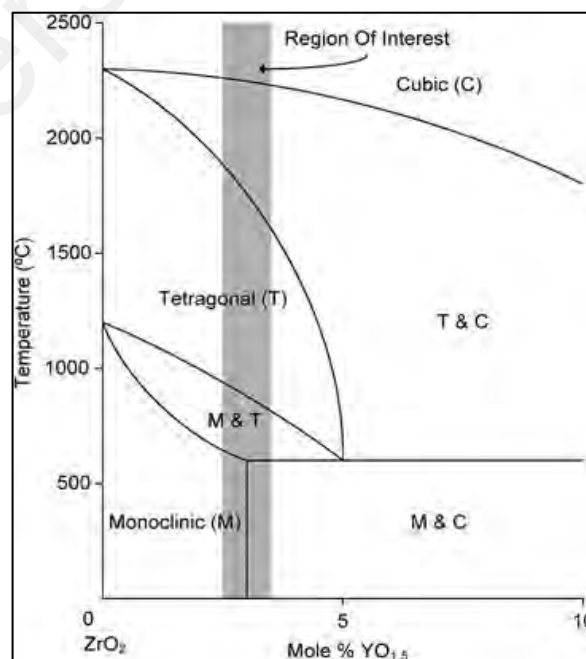


Figure 2.5: Phase diagram for the  $Y_2O_3$ - $ZrO_2$  system (Scott, 1975)



Several known factors have direct influence on the degradation of the 3Y-TZP ceramics such as amount and distribution of stabilizer (Eichler et al., 2007; Suresh et al., 2003), grain morphology and presence of secondary phases. It has been reported that Y-TZP ceramics with close to full densification, equiaxed fine grains, homogeneous distribution with higher content of yttria and surface treatment results in better hydrothermal ageing resistance as well as enhanced mechanical properties (Chevalier, 2006; Lughì & Sergo, 2010). It is well known that the room-temperature phase stability, strength and toughness of Y-TZP ceramics also depend strongly on a critical grain size ( $<0.8 \mu\text{m}$ ) (Bravo-Leon et al., 2002; Lange, 1982). For instance, the Y-TZP shows enhancement of strength with reduced grain size (Eichler et al., 2007). In contrast, the fracture toughness reaches its maximum at larger grain size where the tetragonal grains undergo spontaneous tetragonal to monoclinic transformation at room temperature. It was found that the critical grain size depends on the yttria content (Eichler et al., 2007; Suresh et al., 2003). The most common zirconia ceramic, 3 mol% yttria stabilize zirconia exhibits wide range of critical grain size ( $1 \sim 6 \mu\text{m}$ ) as the result of the different processing methods (Lange, 1986; Ruiz & Readey, 1996). The critical grain size of the ceramic has to be reduced to  $\sim 0.25 \mu\text{m}$  for better hydrothermal ageing resistance when exposed to humid atmosphere (Durán et al., 1996).

#### **2.4.1 Stabiliser Content**

The property of the Y-TZP ceramic is mainly affected by the type and content of the stabilizer. In the aspect of chemical free energy, Schubert and Petzow (1986) suggested that residual stresses and undercooling effect (2Y-TZP -  $660 \text{ }^\circ\text{C}$ ; 3Y-TZP -  $360 \text{ }^\circ\text{C}$ ) reduce with increasing yttria content. The work of (Matsui et al., 1986) showed that the stability of Y-TZP with certain average grain size was subject to critical yttria content,

$X_{cr}$ . For instance, TZP ceramic with average grain size of 0.3  $\mu\text{m}$  has the  $X_{cr}$  ranged between 4 and 5 wt.%. However when the yttria content is less than  $X_{cr}$ , the t – m phase transformation driving force is greater as the ceramic was cooled down from sintering temperature. Hence, microcracking occurred as the result of spontaneous thermally induced tetragonal transformation.

Matsui et al. (1986) related the strength of Y-TZP to yttria content and found that maximum strength of 980 MPa was achieved with 2.5 mol% of  $\text{Y}_2\text{O}_3$ . Below 2.5 mol%, lower strength was observed as the consequences of spontaneous phase change t – m in the  $\text{ZrO}_2$  structure during cooling from sintering temperature. Similarly, strength of the Y-TZP ceramic decline as the  $\text{Y}_2\text{O}_3$  content  $> 2.5$  mol%. Most literatures reported that fracture toughness of Y-TZP decreases with increasing yttria content. It was found that the strength reduction was attributed to the increase stability of Y-TZP and experimental result showed that more stabilized c-phase was formed at the expense of metastable t-phase which leads to noticeably loss in the fracture toughness and strength. TZP samples prepared by (Sakuma et al., 1985) with yttria content ranged 1 to 3 mol% sintered by both conventional sintering and arc melting showed that toughness peaked at about 2 mol%  $\text{Y}_2\text{O}_3$ . Identical fracture toughness trend was also observed by other researchers although differs in fracture toughness,  $K_{Ic}$  value which can be attributed to variation in microstructure which rely on the starting powder and subsequent processing conditions.

#### **2.4.2 Yttria Distribution**

Distribution of the stabilizer is another factor affecting the stability of the tetragonal grain and fracture toughness of Y-TZP ceramics (Lei et al., 1997; Singh et al., 1996). Y-TZP powder made of co-precipitated method and yttria coated  $\text{ZrO}_2$

display different fracture toughness behaviour with microstructure evolution. It was found that co-precipitated Y-TZP exhibits homogeneous distribution of yttria in the grains to prevent micro and macro cracking attributable to the martensitic transformation. Fracture toughness of the co-precipitated 2.5 mol% Y-TZP ceramics enhanced with increasing grain size (e.g. mean grain size from 0.38 to 0.98, fracture toughness from 5 to 10.2 MPam<sup>1/2</sup> respectively) (Singh et al., 1996). The fracture toughness of the co-precipitated Y-TZPs are improved by high temperature sintering or long period of post sintering annealing at high temperature in order to enlarge the t-ZrO<sub>2</sub> grain. Conversely, refinement of tetragonal grains leads to K<sub>Ic</sub> enhancement of coated Y-TZP above a critical value which was due to the heterogeneous distribution of stabiliser in the tetragonal grains leading to transformation enhancement of the grain core (e.g. mean grain size from 0.24 to 1.08, fracture toughness from 12.2 to 6.7 MPam<sup>1/2</sup> respectively).

Another method to modify the microstructure and toughness Y-TZP ceramic by mixing the two zirconia powders of different yttria content (0 and 3 mol%) has been reported (Basu et al., 2004). After sintering for 1 h at 1450 °C, average grain size of 2Y-TZP by mixed powders (referred as TM2) and co-precipitated 3Y-TZP were 0.3 µm and 0.5 µm respectively. In terms of toughness, the TM2 produced high toughness, 10 MPam<sup>1/2</sup> as compared to co-precipitated 3Y-TZP with only 2.5 MPam<sup>1/2</sup>. A co-precipitated powder Y-TZP ceramic with mean grain size (0.5 µm) similar to TM2 but reported a lower K<sub>Ic</sub> (6 MPam<sup>1/2</sup>). It is well established for co-precipitated powder-based Y-TZP, the enhancement of transformation toughening is related to the grain size dependence of martensitic transformation start temperature  $M_s$ . However the TM2 contradict this theory in predicting the  $M_s$ . On the other hand, the coated Y-TZP achieved high fracture toughness of 9 MPam<sup>1/2</sup> at average t grain size of 0.19 µm, whereas the co-precipitated Y-TZP grains are highly stable at the equivalent average

grain size (Basu, 2005). It can be concluded that the Y-TZP processed from mixing of 3Y-TZP and undoped zirconia showed different toughening behavior from Y-TZP prepared by coated or co-precipitated powder.

### **2.4.3 Densification**

It has been reported that Y-TZP ceramics with close to full densification results in better phase stability and enhanced mechanical properties (Chevalier, 2006; Lughì & Sergo, 2010). Generally all the structural ceramics are required to achieve close to theoretical density in order to obtain high strength that may be weakened by crack initiation attributed to defect such as porosity. The strength of the Y-TZP ceramics depends heavily on the retention of the tetragonal phase which is relying on the density achieved during sintering. Higher density of ceramic body induces greater constraint among the grains but void or porosity leads to low elastic modulus and introduces free surface that reduces the strain energy for t to m phase transformation during cooling from sintering.

There is a correlation between the bulk density and mechanical properties such as Young's modulus and Vickers hardness. According to Ramesh et al. (2008), the modulus of elasticity has a linear relationship with the bulk density of the sintered Y-TZP ceramic as depicted in Figure 2.6.

It was reported that the Vickers hardness is influenced by the density of the Y-TZP ceramics. For example, Figure 2.7 showed that the hardness of YSZ ceramic was enhanced with density to its peak and then decreased.

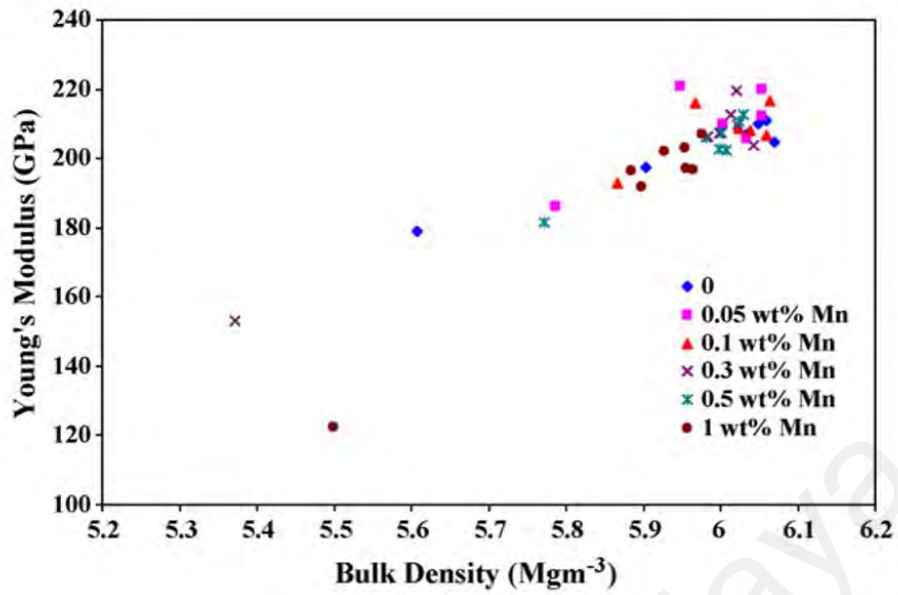


Figure 2.6: Relation of Young's modulus versus bulk density of YSZ ceramic (Ramesh et al., 2008).

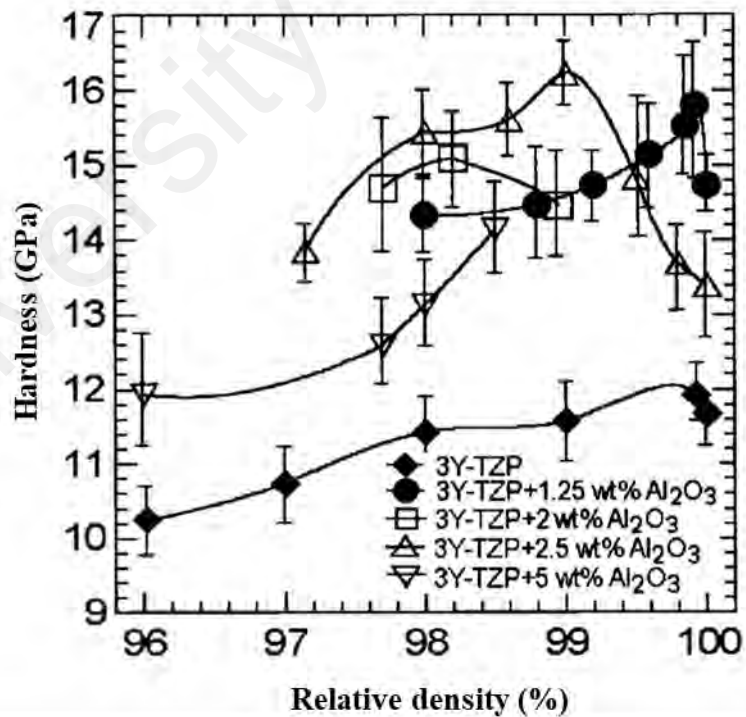


Figure 2.7: Relation of Hardness versus relative density of Y-TZP ceramics (Vasylykiv et al., 2003).

#### 2.4.4 Grain Size Effect

It is well known that the room-temperature phase stability, strength and toughness of Y-TZP ceramics also depend strongly on a critical grain size. Gupta et al. (1977) discovered the sintered samples of  $ZrO_2$  comprise ~ 98% equiaxed of fine grain (<0.5  $\mu m$ ) with small amount of  $Y_2O_3$  stabilizer (Gupta et al., 1977) and sintered to 96 – 99.5% of theoretical density (Matsui et al., 2003a). Gupta et al. (1978) successively revealed that below a critical grain size of 0.3  $\mu m$ , the ceramic showed the highest toughness and strengths at 6 – 9  $MPam^{1/2}$ , 700 MPa respectively. This critical grain size phenomenon of TZP ceramics of strength/toughness mechanism has gone beyond the common flaw-related grain size for polycrystalline ceramics.

Grain size is a predominant factor that controls the  $M_s$  temperature and the ease of t – m transformation. The t grains are getting less stable as the service temperature is close to  $M_s$  temperature and reciprocally enhancing the toughness. However, ceramics with same level of dopants shows signs of toughness reduction when the grains is smaller than the critical size (Bravo-Leon et al., 2002).

This critical grain size effect is governed by the type of dopant and its concentration which determining the degree of tetragonality and the thermal expansion anisotropy of the unit cells. The zirconia ceramics appeared to be less stable with higher tetragonality as the result of an increased  $M_s$  temperature (Kim, 1990). On the other hand, residual strains in t grains are influenced by the anisotropic thermal expansion. In the presence of crack-tip strain energy, the nucleation stress threshold for t – m is lowered as residual stresses increased (Becher & Swain, 1992).

#### 2.4.5 Influence of Additives

It has been established that the starting particles, the powder composition (stabilizer content and distribution), sintering parameters and the addition of sintering additives or metal oxides are among the main variables that controlled the sintering behavior and the phase stability of Y-TZP ceramics. Ageing resistance can be enhanced by increasing Ytria content, using other stabilizer such as CeO<sub>2</sub> (Kwon & Jung, 2017) and preparing alumina-zirconia composites with trade-off in terms of strength or esthetic appearance. A popular method to enhance densification at low sintering temperature meanwhile suppress the grain growth of the 3Y-TZP ceramic is by doping a minute of sintering additives (Lawson, 1995). Several studies have shown that addition of ions, e.g. Al<sup>3+</sup> (Ross et al., 2001), Fe<sup>3+</sup>, Pr<sup>3+</sup>, La<sup>3+</sup> (Zhang, Vanmeensel, Batuk, et al., 2015) and Si<sup>3+</sup> (Samodurova et al., 2015) or even co-doping Al<sup>3+</sup> Bi<sup>3+</sup> (Shah et al., 2008) and Al<sup>3+</sup> La<sup>3+</sup> (Nogiwa-Valdez et al., 2013b) are able to achieve a balance between ageing resistance, improving the properties and esthetic appearance of the ceramics.

Guo and Xiao (2012) successfully produce high relative densities (>95 %) of 3Y-TZP sintered at 1150 °C when doped up to 2 mol% of Fe<sub>2</sub>O<sub>3</sub> with an average grain size of < 0.20 μm. On the other hand, Ramesh et al. (2013) Flegler et al. (2014) discovered that high densification of 8Y-TZP could be achieved at lower sintering temperature with MnO<sub>2</sub> dopant. However, certain additive such as graphene oxide (GO) has shown poor LTD resistance in 3Y-TZP although there is improvement in sintering properties (Ramesh et al., 2016).

Additives such as titanium oxide (TiO<sub>2</sub>), iron (III) oxide (Fe<sub>2</sub>O<sub>3</sub>) and aluminium oxide (Al<sub>2</sub>O<sub>3</sub>) (Zhang, Vanmeensel, Inokoshi, et al., 2015) are common additives that has seen success in inhibiting the t to m transformation, increasing LTD resistance (Masaki, 1986b). Wu et al. (2013) reported that addition of 0.25 wt% Al<sub>2</sub>O<sub>3</sub> could

effectively retard the aging of 3Y-TZP. With the same amount of  $\text{Al}_2\text{O}_3$ , (Zhang et al., 2014) was able to increase the densification and hardness of 3Y-TZP while addition of 0.5wt.%  $\text{Al}_2\text{O}_3$  is effective to reduce the LTD on 3Y-TZP (Chevalier & Gremillard, 2009).

Zhang et al. (2014) studied the addition of 0.25wt.%  $\text{Al}_2\text{O}_3$  to both  $\text{Y}_2\text{O}_3$  stabiliser coated and co-precipitated type of 3Y-TZP powders. The ceramics were pressureless sintered in air for 2 and 4 h at 1350 – 1550 °C. The relative density and hardness of the 3Y-TZP increased with the grain size when sintered up to 1450 °C and experiencing deterioration above 1500 °C while fracture toughness showed opposite relationship as depicted in Figure 2.8 & 2.9. Samples added with  $\text{Al}_2\text{O}_3$  showed enhanced relative density and hardness at sintering temperature <1450 °C compared to the one without dopant. In terms of LTD, samples sintered at temperature above 1450 °C will have a higher degradation rate as compared to samples sintered below 1450°C. Yttria-coated powder with  $\text{Al}_2\text{O}_3$  exhibited good ageing resistance without compromising on fracture toughness among other 3Y-TZP samples. The results also showed that the increase in the sintering temperature and holding time significantly increased the LTD of the ceramics. This is due to the enlargement of the t grain, increasing of cubic phase and overall yttria stabilizer content in the remnant of tetragonal grains was decreased. The yttria coated zirconia ceramics doped with  $\text{Al}_2\text{O}_3$  had a better ageing resistance without compromising on the fracture toughness as the result of the segregation of  $\text{Al}^{3+}$  and the non-homogeneous distribution of  $\text{Y}^{3+}$  at the grain boundary. Other dopants that segregated at the grain boundary were found to affect the ageing kinetic of 3Y-TZP ceramics were reported (Chevalier, 2006; Chevalier et al., 2009) where some of these dopants ( $\text{Al}^{3+}$ ,  $\text{La}^{3+}$ ,  $\text{Cu}^{2+}$ ,  $\text{Mg}^{2+}$  and  $\text{Ge}^{4+}$ ) are effective in enhance the ageing resistance of the ceramic (Guo, 2003, 2004; Matsui et al., 2014; Nogiwa-Valdez et al., 2013a). Recent studies have reported the size of cation dopant



segregating at the grain boundary as a contributing factor to determine the degradation rate of the zirconia. Larger trivalent cations was found enhancing the ageing resistance of the ceramics without sacrificing the mechanical properties (Zhang et al., 2016).

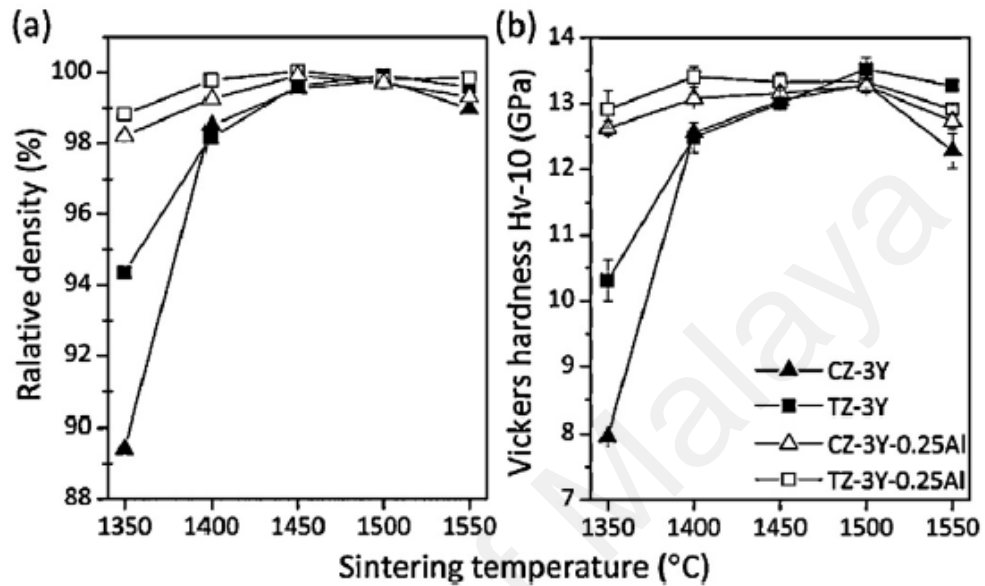


Figure 2.8: Relative density (a) and Vickers hardness (b) as a function of sintering temperature for different types of 3Y-TZP (Zhang et al., 2014).

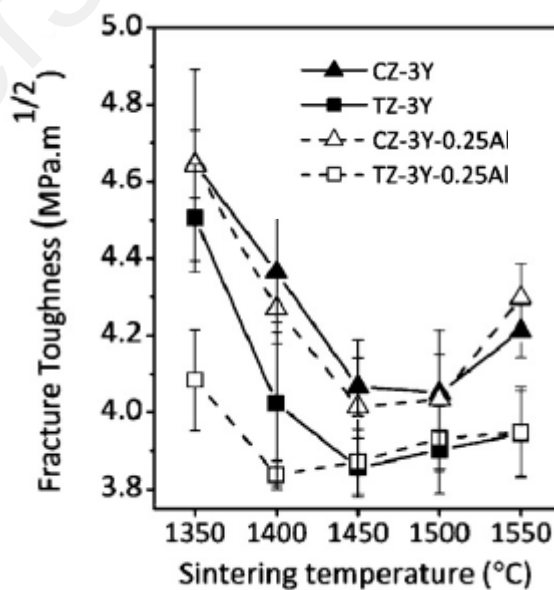
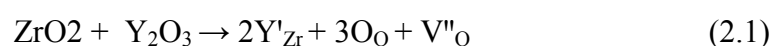


Figure 2.9: Fracture toughness as a function of sintering temperature for different type of 3Y-TZP (Zhang et al., 2014).

3Y-TZP that were doped with alumina was found to have larger grain size compared to pure 3Y-TZP that were sintered at the same temperature, however the one that was doped with alumina exhibit better ageing resistance than the one that was not doped. This implies that the LTD resistance is not associated to grain size reduction as it contradicts the theory that smaller grain size leads to better LTD resistance. The ageing resistance was not due to the dopant but the cation of the additive, in this case, Al<sup>3+</sup>. Other cations include Si<sup>4+</sup>, or any other cations with an oxidation number of either +3 and +4, such as iron, Fe<sup>3+</sup> which was mentioned (Zhang et al., 2016). Oxides of these cations are chosen as they are well known in stabilizing the tetragonal structure of 3Y-TZP (Li, Chen, & Penner, 1994).

Trivalent cations, such as Al<sup>3+</sup> or Fe<sup>3+</sup> was found to have been separate at the charge layer of the grain boundary, thus the grain boundary was strengthened with extra oxygen vacancies and thus improving LTD resistance since LTD was induced due to depletion of oxygen vacancies. More trivalent cations would further increase the LTD resistance (Zhang et al., 2016). Moreover, these cations can bind the oxygen vacancies and form a defect cluster, slowing down the diffusion of water through the oxygen vacancies. This greatly hinder and disrupt the annihilation of oxygen and thus further stopping the degradation (Sakib Khan et al., 1998). It was also reported that cations such as Al<sup>3+</sup> increases the activation energy of hydrothermal aging process, up to an energy required of 106 kJ/mol (Zhang, Inokoshi, et al., 2015).

The involvement of oxygen vacancies in the hydrothermal ageing in Y-TZP is the most prevailing mechanism emphasizing the role of oxygen vacancies annihilation. Oxygen vacancies were produced in the ZrO<sub>2</sub> lattice when zirconia was stabilized with yttria to maintain local charge neutrality based on the following reaction:



The product of oxygen vacancy was claimed to be responsible for the degradation of 3Y-TZP (Lepistö & Mantyla, 1989). The role of oxygen vacancies in the yttria-stabilised zirconia lattice to the stability of the tetragonal (t) and cubic (c) phase of the zirconia has been reported widely (Bartolomé et al., 2004; Fabris et al., 2002; Li, Chen, & Penner-Hahn, 1994).

#### **2.4.6 Sintering**

Sintering is a firing process, or a heating process in which a powder compact is being transformed into a dense body upon heating (Barsoum, 2002). It is almost impossible to fabricate the ceramics into desired shape with metal casting approach as the melting point of ceramic is extremely high and requires sophisticated equipment which is not economically viable. Hence, the most popular approach is powder metallurgy where by the ceramic powder is compacted as a green body and then consolidated to form a net shape product by sintering at temperatures around 60 - 80 % of its melting temperature.

Sintering is a thermal process in which powder is transformed into a dense material without pores and it is one of the most important processes in fabricating ceramics product. Various sintering methodologies with diverse mechanisms are currently available and the suitable sintering procedure is vital for the superior performance of zirconia bodies. The most common commercial available sintering technique is Conventional sintering methods (pressureless sintering, hot pressing, sinter forging, hot isostatic pressing, etc.) and these methods are normally operate in high temperatures to achieve close to full densification as ceramic materials generally exhibit low thermal conductivity.

In conventional heating, heat is generated by means of electrical resistance and heat flows to the object by radiation and convection where the material's surface is first heated followed by the heat moving inward by conduction, creating a temperature gradient from the surface to the inside that leads to significant differential sintering. For structural ceramics application, high densification of 3Y-TZP ceramic is one of the top requirements in the fabrication process. Therefore conventional heating with resistance heating method required high sintering temperature, low heating rate and long holding time. However high temperature will always result in large grain growth due to Ostwald ripening and make it extremely difficult to obtain dense materials especially with nanometric and submicrometric grain sizes (Anselmi-Tamburini et al., 2006). Zirconia ceramics with large grains are found affecting the mechanical properties and utmost issue concerning LTD of 3Y-TZP ceramic. Furthermore the requirement of slow heating rate with high temperature in 3Y-TZP ceramic is definitely leading to significant thermal energy losses (Yadoji et al., 2003). Therefore the alternative approach such as non-conventional sintering techniques (microwave and spark plasma sintering) is of great interest as high densification of 3Y-TZP ceramic could be achieved at a relatively low temperature.

The sintering conditions such as sintering techniques (e.g. hot pressing, HIPing, pressureless sintering and microwave sintering) and sintering profile (e.g. soaking temperature, holding time and the ramp rates) have direct effect on the microstructure of the zirconia and this in turn will influence the mechanical properties (Hallmann, Ulmer, et al., 2012) as well as the ageing resistance (Wei & Gremillard, 2018) of the YSZ ceramic. Among the parameters, sintering temperature has the highest impact on the properties of Y-TZP ceramics. Yang et al. (2005) reported that the final density of the Y-TZP ceramic was mainly influenced by the sintering temperature. Figure 2.10 depicted the relative density and average grain size of 3Y-TZP ceramics were increased

with sintering temperature and further enhanced with addition of  $\text{Al}_2\text{O}_3$  additive (Matsui et al., 2007) and also conclude that the higher specific surface area of the starting powder enhancing the densification with increasing sintering temperature.

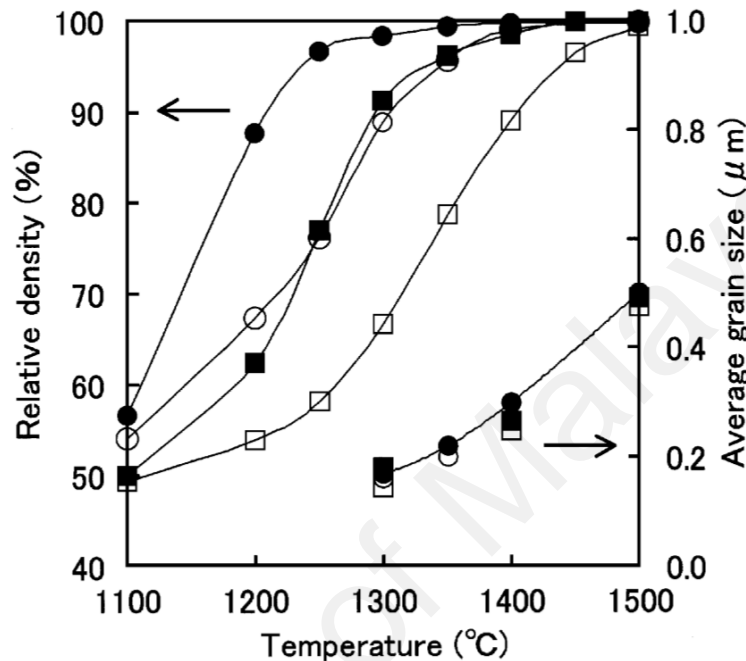


Figure 2.10: Changes of relative density and average grain size with sintering temperature holding for 2 hr. (○), (□), (●), and (■) indicate 3Y, 3YS, 3YE, and 3YSE, respectively.

In most cases for commercial Y-TZP powders, sintering temperature at 1400 – 1500 °C and holding time 2 – 4 hr are required via the common pressureless sintering approach (Kanellopoulos & Gill, 2002; Yu et al., 2007). Significant grain growth followed by decreased in the bulk density was observed with higher sintering temperature and elongated holding time (Chevalier et al., 2004; Inokoshi et al., 2014; Lange, 2008; Ruiz & Readey, 1996; Trunec, 2008). Furthermore, higher sintering temperatures render the formation of large cubic grains that depleting the stabilizer from the adjacent tetragonal grains (Matsui et al., 2003b; Matsui et al., 2008; Matsui et al.,

2009). Eventually the tetragonal grains become unstable and susceptible to hydrothermal degradation (Chevalier et al., 2004; Denry & Kelly, 2008; Feder & Anglada, 2005; Ruiz & Readey, 1996; Scott, 1975).

Some studies reviewed that the sintering profile (e.g. temperature, heating and cooling rates, and holding time) is directly affecting the microstructure and properties of the ceramic (Chevalier, 2006; Ebeid et al., 2014; Maca & Simonikova, 2005) especially the conventional pressureless sintering where a fine grain microstructure with enhanced densification was achieved by selecting appropriate sintering profile (Lange & Kellett\*, 1989).

The effects of elevated sintering temperature on the densification, properties and microstructure of yttria-stabilised zirconia (YSZ) have been investigated by many workers (Stawarczyk et al., 2013). Stawarczyk et al. (2013) performed sintering at temperature range from 1300 to 1700 °C with 120 min holding time on the commercial Y-TZP ceramic and found that highest flexural strength was observed on ceramics sintered between 1400 and 1550 °C while the grain size showed enlargement with higher sintering temperature (>1300 °C) followed by formation of pores in the zirconia microstructure when sintered above 1600 °C.

Long sintering holding/dwelling time which is found to enhance the grain growth, consequently leads to micropores formation and resulting poor mechanical properties in the Y-TZP ceramics (Tekeli & Erdogan, 2002). It was observed that shorter holding times resulted in better ageing resistant although the Y-TZP ceramics sintered with longer period showed slight improvement in terms of densification and mechanical properties when Kanellopoulos and Gill (2002) studied the effects co-precipitated Y-TZP doped with 0.05wt.% of CuO sintered at 1300 - 1325 °C and time varying from 12 to 240 min. They concluded both zirconia samples (undoped and

doped) displayed excellent ageing resistance as less than 1 % monoclinic phase content was detected after 3000 h of hydrothermal ageing (180 °C) when sintered at respective profiles (1300 °C; 120 min and 1315 °C; 12 min). This has been reported in other studies the hydrothermal ageing resistance of Y-TZP ceramic depends highly on grain sizes of the microstructure of this material that is sensitive also towards the sintering time (Hjerpe et al., 2009; Kosmac̆ et al., 2000; Sato & Shimada, 1985).

(Kim et al., 2013), having examined various conventional sintering (CS) holding times (20, 120, 600, 2400 min) at 1450 and 1500 °C, and near 10 °C/min on the dental 3Y-TZP ceramics, have reported the mean grain size increases with sintering holding time ranging from 415 to 1512 nm without much affecting the densities (6.06 – 6.07 g/cm<sup>3</sup>) of the samples. The zirconia samples sintered at higher rate, 50 °C/min with microwave sintering yielded smaller average grain size (347 nm) as compared to the CS at the similar sintering profile (temperature and holding time). The light translucency increased with decreasing average grain size as the result of shorter holding time. It is apparent that sintering for long period is detrimental to the mechanical properties of Y-TZP ceramics and must be avoided although enhancement taking place in densification of the ceramic. Therefore short sintering holding time is desired without sacrificing the properties of the Y-TZP ceramics.

Sivakumar et al. (2011) evaluated the properties and ageing resistance of 3Y-TZP sintered with four different heating profiles at 1400 °C as shown in Figure 2.11. It was found out that Sample 4 has the highest hardness (13.8 GPa) among all the other samples within the range of 12.1 to 12.4 GPa but the fracture toughness (~7 MPam<sup>1/2</sup>) and Young's modulus (~195 GPa) was not affected by the sintering profiles. All samples except sample 4 do not reveal to have any monoclinic content (100% in tetragonal phase) after 50 hours of hydrothermal aging at 180 °C. Sample 4 is very

susceptible to low temperature degradation, since majority of the tetragonal content had undergone monoclinic transformation, whereas sample 1, 2 and 3 are very resistant to degradation. From the finding, it is concluded that to improve LTD resistant, a short dwell time of single stage sintering or two stages sintering in the sintering process is preferable.

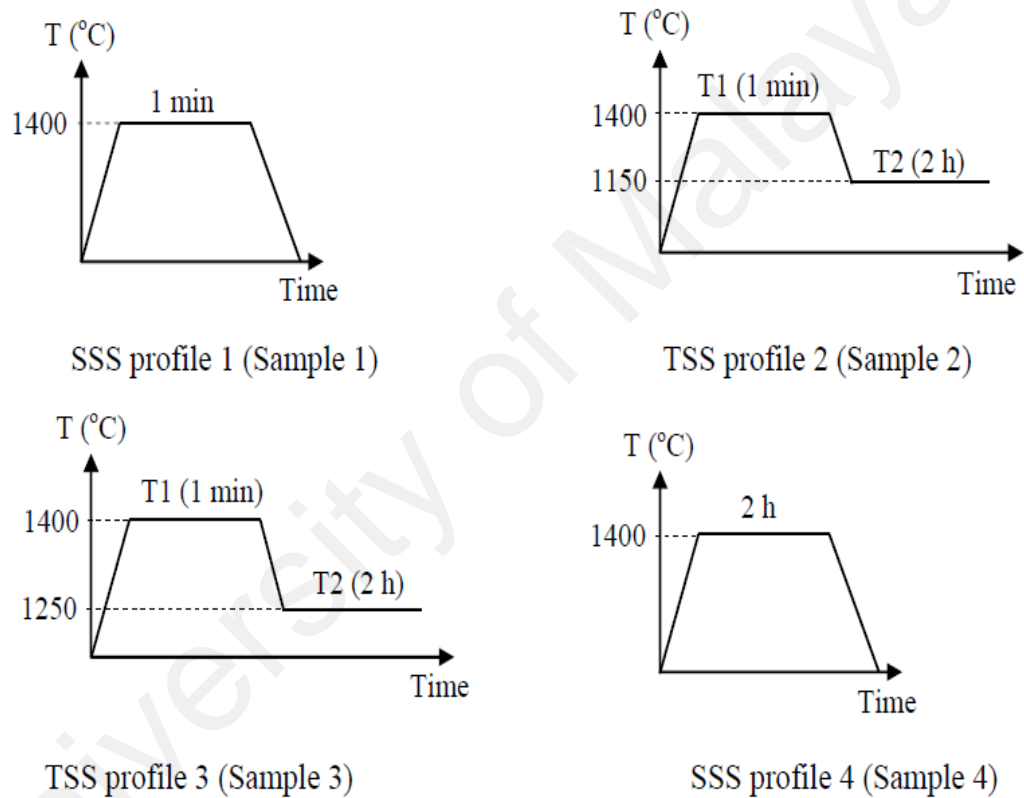


Figure 2.11: Various sintering profiles employed in the research (Sivakumar et al., 2011).

For instance two-step sintering (TSS) has been investigated as a viable option to achieve high density without inducing grain growth in the final stage of sintering. This method has managed to produced nanostructured yttrium oxide ceramic (Chen & Wang,



2000a). In addition, TSS has also been applied successfully in the sintering of silicon carbide (Lee et al., 2003), barium titanate (Polotai et al., 2005), Ni-Cu-Zn ferrite (Wang, Deng, et al., 2006), alumina (Maca et al., 2008), titania (Mazaheri, Zahedi, et al., 2008) and zirconia (Lourenço et al., 2011). In TSS, sintering temperature in the first and second steps plays an important role in controlling the grain growth and final density of the sintered body (Wang, Chen, et al., 2006).

Two step sintering has been developed by Chen and Wang (2000a), as it proves to be useful in producing high density nano-grained ceramics and it has been successfully used on ZnO (Mazaheri, Simchi, et al., 2008). The reason why TSS produces materials with better mechanical property is because by sintering it to a temperature of T1 will allow the ceramic to achieve its critical density. The decrease in temperature to T2 however increases densification but limited grain growth leading to better mechanical property (Chen & Wang, 2000b).

It has been widely reported that the addition of transitional metal oxide in Y-TZP as sintering aid was found to enhance sintering at low temperature while improving densification. Until recently, some attempt was done by firing the Y-TZP ceramic with short holding time with addition of dopant. For example, Ramesh et al. (2011) compared effects of various holding times (12 and 120 min) between the plain and doped (1 wt.% MnO<sub>2</sub>) of 3Y-TZP sintered over a temperature range 1150 – 1600 °C. They discovered that short sintering time (12 min) coupled with low temperature (1250 °C) was beneficial in densification without sacrificing the properties including the ageing resistance as the result of the formation of transient liquid during the sintering of MnO<sub>2</sub> doped Y-TZP ceramics. Similar work was conducted by Kwa et al. (2015) by preparing 3Y-TZP doped with 0, 0.5 and 1 wt.% MnO<sub>2</sub> sintered at 1350 °C and comparison was done at different holding times range from 1 to 120 min. The results

revealed that the undoped Y-TZP sintered with short holding time (1 & 12 min) was not favorable for densification and mechanical properties as compared to the sample with 120 min. but the ageing resistance was enhanced which was attributable to the smaller grain size ( $\sim 0.33 \mu\text{m}$ ). Conversely, the 0.5 wt.%  $\text{MnO}_2$  doped Y-TZP exhibited enhanced properties (Relative density =  $>97\%$ ,  $E = \sim 187 \text{ GPa}$ ,  $H_v = \sim 13.5 \text{ GPa}$ ,  $K_{IC} = \sim 5.2 \text{ MPam}^{1/2}$ ) and excellent ageing resistant without traces of monoclinic phase after 200 hr exposure in superheated steam at  $180 \text{ }^\circ\text{C}$  when sintered at short holding time (1 and 12 min). Regardless of holding time, Y-TZP ceramic doped with 1.0 wt.%  $\text{MnO}_2$  was less effective in densification and ageing resistance enhancement. In term of microstructure, the holding time enhanced grain growth i.e. the grain sizes ranged  $0.32 - 0.35 \mu\text{m}$  and  $0.40 - 0.43 \mu\text{m}$  for short and long holding period respectively that showed 20 - 30% enlargement with long holding period. However dopant had marginal effect on the grain growth which was  $< 10 \%$  as compared to the undoped. Consequently, due to the smaller grain, Y-TZP ceramic with short holding time had better ageing resistance than the long holding as less monoclinic content was detected on the former ( $< 1.3\%$ ) as compared to the latter (2 - 6%).

#### 2.4.6.1 Pressure Assisted Fast Sintering

Pressure assisted fast sintering method such as Spark plasma sintering (SPS) or High Pressure-Field Assisted Sintering (HP-FAST) is a type of sintering method (Figure 2.12), which is known to produce ceramics with very small grain size, on a nanometric scale (Tredici et al., 2016). Spark plasma sintering is based on electrical spark discharges to generate heat, such that heat is produced from spark discharges to cause solidification of particles. A high energy but low voltage pulse current generates the spark plasma at high temperature. A direct current (DC) pulse is passed through the

punch electrodes, then to a die compacted to powdered ceramics. The figure showed the construction of spark plasma sintering furnace. A special feature that SPS compared to conventional sintering is that SPS has a very high sintering rate. This causes the heating rate to be considerably high, up to 300°C/min as compared to a conventional sintering which has a heating rate of a maximum 10°C/min. This allows SPS to heat up substances at least 30 times faster than conventional sintering. Such high sintering rate by SPS means that it requires a very short amount of time for a substance to be heated to its required temperature. It also allows uniform sintering since all the heat is being compacted into a die, thus allow uniform heat distribution across the material. SPS has been proven to obtain high relative densities materials especially in processing nanostructured materials.

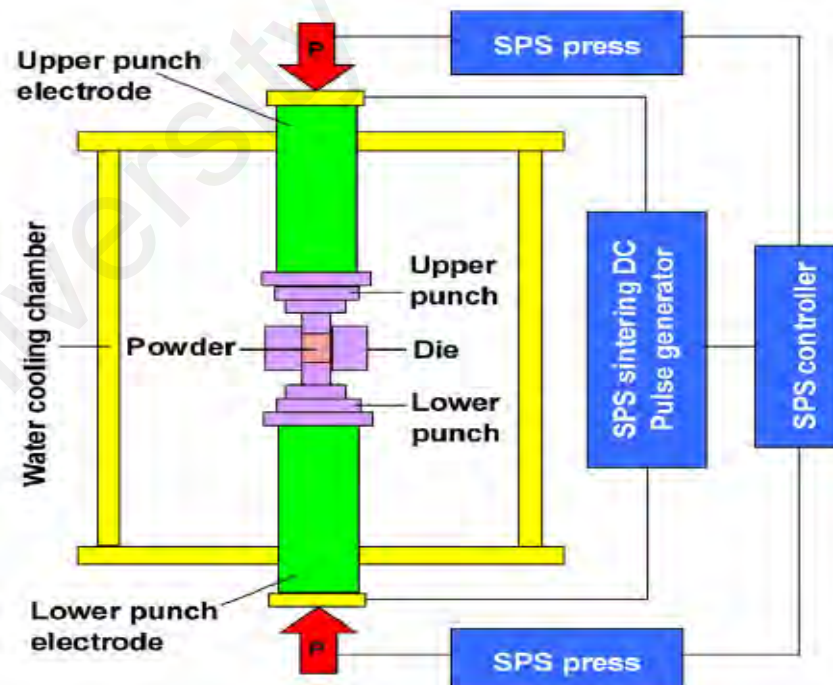


Figure 2.12: Spark Plasma Sintering Process (Chintapalli et al., 2010).

Experiment was done by Chintapalli et al. (2010) to compare the stability of YSZ ceramic using the SPS and conventional sintering method. In this work, 3Y-TZP powder with a crystallite size of 29 nm was used where 4 of the 5 samples were subjected to SPS at different temperature, while the 5<sup>th</sup> sample was subjected to conventional sintering at standard temperature of 1450°C (Figure 2.13). Table 2.1 below shows the results obtained from the 5 samples. The results show that increasing sintering temperature increases the relative density as well as the grain size. In terms of hardness, the sample SPS-65 has the least amount of Vickers hardness attributed to the present of porosity which is susceptible towards indentation due to the imperfect structure (Lawn et al., 1980).

Table 2.1: Conditions and measured properties of the different specimens (Chintapalli et al., 2010).

<b>Sample Code</b>	<b>SPS 65</b>	<b>SPS 90</b>	<b>SPS 120</b>	<b>SPS 800</b>	<b>AS 300</b>
<b>Sintering Temperature (°C)</b>	1100	1150	1175	1600	1450
<b>Density (g/cm<sup>3</sup>)</b>	5.42	5.71	6.00	6.05	6.10
<b>Mean Grain Size (nm)</b>	65	90	120	800	300

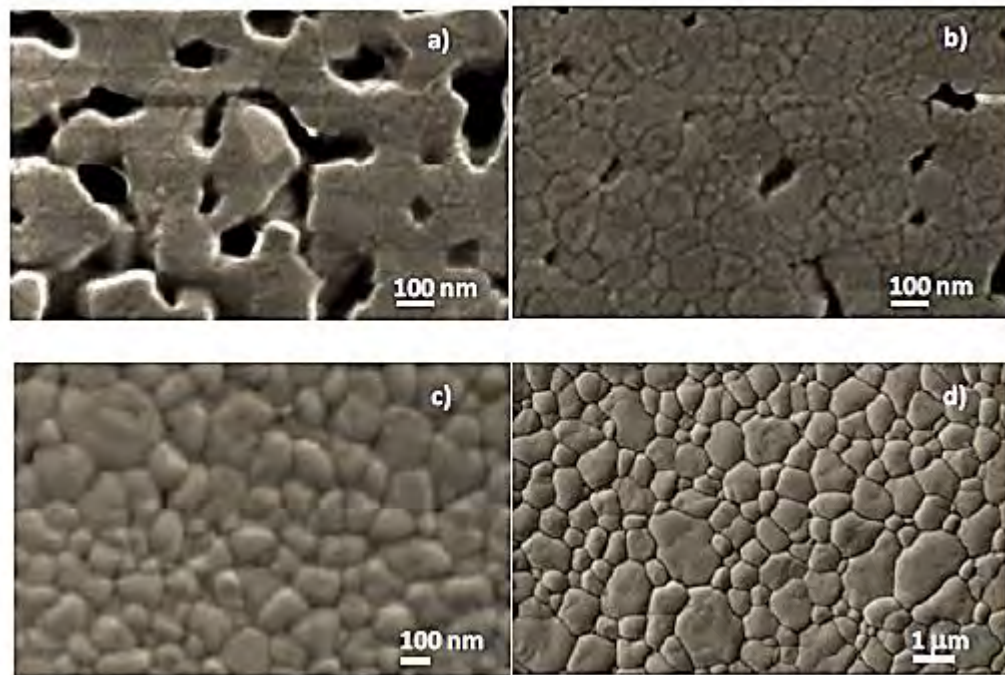


Figure 2.13: Microstructure of thermally etched samples observed from electron microscope: (a) SPS-65, (b) SPS-90, (c) SPS-120 and (d) SPS-800 (Chintapalli et al., 2010).

It is found that SPS-800 and AS-300 is extremely susceptible to LTD with 71.4% and 65.4% of monoclinic volume fraction respectively while the samples SPS-65, SPS-90 and SPS-120 retain 100% tetragonal grains after 60 hours of hydrothermal aging. 3Y-TZP with grain size below 300nm is highly resistant to degradation whereas those with larger than 300nm shows severe degradation. SPS-65 and SPS-90 showed no sign of monoclinic phase although porosities were found in these ceramics. This concludes that porosity do not affect LTD for samples of grain size in nanometric scale.

Despite the advantages of SPS being able to produce materials with nanostructured grain size in a very short amount of time, there are drawbacks in using SPS. The first drawback is that only simple and symmetric shape can be prepared. This means that complicated and unique shape die is not possible since it can cause uneven

sintering. The second drawback is that the cost of operation is extremely expensive. A large energy is required for operation as it requires a standard operating current of over 1000A to cause spark discharge despite low voltage. Since spark plasma sintering relies on a pulsed current, a pulsed DC generator is required in spark plasma sintering and it is extremely costly. Spark plasma sintering is not favourable in for most industrial application mainly due to high production costs (as it requires expensive DC pulse generator) as well as small product size capacity (Wang & Gao, 2005).

#### 2.4.6.2 Microwave Sintering

Microwave sintering is another type of sintering technique which requires the use of a microwave. Microwave is common in variety of applications for more than 50 years ranging from industry to domestic usage such as microwave oven. These applications include communication, food processing, wood drying, rubber vulcanization, medical therapy, polymers, etc. In materials science and processing, microwave technology is not rather new as it involved in process control, drying of ceramic sanitary wares, calcination, and decomposition of gaseous species by microwave plasma, power synthesis and sintering (Agrawal, 2006).

Microwave sintering is very much different from conventional sintering. In conventional sintering, direct heat transfer such as conduction and convection is the main driving force for densification during sintering. However this differs from microwave sintering as it relies on the conversion of electromagnetic radiation into heat by the materials due to its dielectric properties (Presenda et al., 2015). In the mechanism of a microwave oven, the energy from microwave is transferred to materials via interaction of electromagnetic field. Such field is dependent on the dielectric properties of the materials that is to be sintered. The molecular dipoles in the material will rotate

and vibrate continuously in order to align itself with the electromagnetic field, hence microwave is said to be exciting the molecules. Heat is generated from friction during the continuous vibration and rotation of the molecules (Thostenson & Chou, 1999), thus creating a rise in temperature. The higher the energy, the higher the excitation and thus the more heat is produced in the process, resulting in higher sintering temperature.

Microwave sintering generates heat from the very core of the material (inside out) to the surface as contrast to conventional sintering where heat is being transferred from the surface of the material towards the interior. Using microwave sintering improves the heating rate. The temperature rise can go above 100°C/min compared to conventional sintering whose heating rate is around 10°C/min. With high heating rate, highly dense materials can be obtained via microwave sintering without any significant grain growth due to short sintering time and dwell time needed to achieve required temperature which is similar to spark plasma sintering. As such it improves the mechanical properties of 3Y-TZP due to the small grain size it can be achieved after sintering (Presenda et al., 2017).

In Presenda et al. (2015) research, experiments were conducted to compare the mechanical properties of 3Y-TZP that were sintered via microwave sintering (MW) and conventional sintering (CS). Hardness, fracture toughness and grain size were used for comparison purpose in the study. Three different brands of 3Y-TZP were taken into comparison, namely LAVA, VITA and TOSOH from different manufacturer. From Table 2.2, it can be seen that samples that were sintered using microwave sintering has smaller grain size as compared to conventional sintering (less than 200nm). This is mainly due to the short dwell time in microwave sintering. Longer dwell time means a higher tendency to promote grain growth and it is inevitable due to the small heating rate in conventional sintering as compared to microwave sintering. It was found out that

samples that were sintered using microwave sintering shows the higher relative density (99%) as compared to the ones with conventional sintering. This shows that microwave sintering provides a higher degree of densification. Hardness test was conducted on each sample, and it was also found out that the hardness is higher in samples that were sintered via microwave sintering rather than conventional sintering which was expected. Fracture toughness was found to be higher in samples that were microwave sintered compared to conventional sintered 3Y-TZP (Presenda et al., 2015).

Table 2.2: Summary of sintering parameters and final grain size determined for all materials after conventional and microwave sintering (Presenda et al., 2015)

3Y-TZP Manufacturer	Sintering Method	Final Temperature (°C)	Dwell time (min)	Average grain size (nm)
LAVA	CS	1300	120	238 ± 54
		1400	120	343 ± 43
	MW	1200	10	146 ± 64
		1300	10	162 ± 98
VITA	CS	1300	120	229 ± 67
		1400	120	286 ± 68
	MW	1200	10	173 ± 49
		1300	10	186 ± 43
TOSOH	CS	1300	120	203 ± 43
		1400	120	199 ± 85
	MW	1200	10	174 ± 67
		1300	10	194 ± 88



Menezes and Kiminami (2008) consolidated the zirconia ceramics containing 1, 3 and 5 vol.% of alumina by microwave hybrid fast sintering. Ceramic samples with density more than 99.0% of theoretical density were produced after sintering period around 35 min. Microstructural observation indicated that uniform grain size distribution without any observable cracks or pores and no abnormal grain growth were found. The results showed that microwave hybrid heating has a great potential method in fabricating alumina-zirconia nanocomposites with uniform microstructures, even at the short sintering period as well as for suppressing grain growth in ceramic nanocomposites (Menezes & Kiminami, 2008).

In recent work by Borrell et al. (2012), 3 mol%  $Y_2O_3$ -stabilized zirconia ceramic were densified using conventional sintering (CS) and non-conventional sintering for instant, microwave (MW) and pulsed electric current-assisted-sintering (PECS) at 1300 and 1400 °C. The MW materials attain a bulk density 99.4% theoretical density (t.d.) at 1300 °C, while the CS materials attain only 92.5% t.d. and PECS 98.7% t.d. Finer grain sizes (135 nm) was achieved by PECS followed by MW with average grain size of 188 nm and CS with 225 nm. Though PECS showed smallest average grains size among other sintering methods, the carbon rich atmosphere from the die diffused into the sample causing full black colour on the surface of the sample. Figure 2.14 shows that all the sintered specimens exhibited equiaxed grain microstructures and MW shows a better homogeneous microstructure than the others (Figure 2.14b).

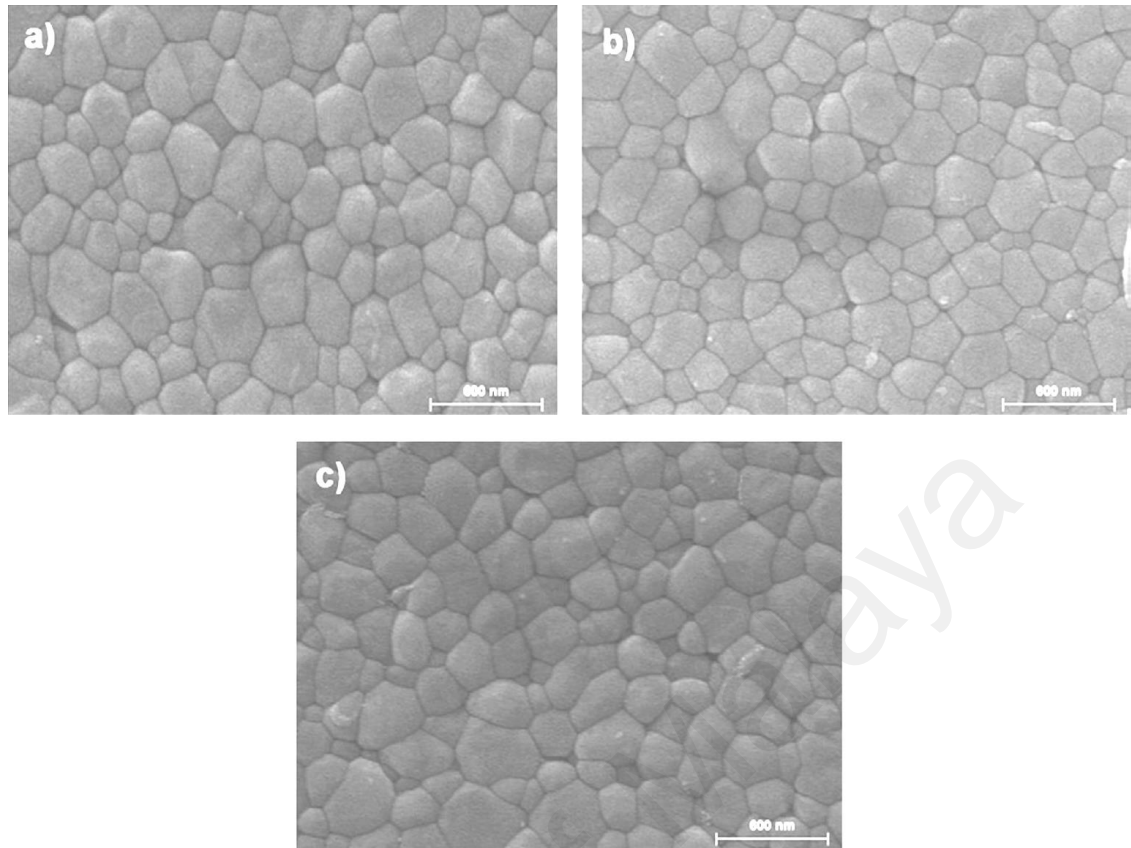


Figure 2.14: FE-SEM micrographs of near full dense specimens sintered by PECS at 1400 °C/1min (a), MW at 1400 °C/10 min (b), and CS at 1400 °C/60 min (c) (Borrell et al., 2012).

Microwave sintering results in ceramics with improved densification, better mechanical properties and suppressed grain growth due to a fast heating rate at lower sintering temperature. Therefore it can be inferred and predicted that microwave sintered materials results in higher aging resistance due to the small grain size of materials. Microwave sintering is a considerable option for as a sintering method to manufacture 3Y-TZP as it reduces processing time as well as energy consumption. A review of microwave versus conventional sintering was done by (Oghbaei & Mirzaee, 2010) and they conclude with the following summary:

- Microwave sintering consumes much lower energy as compared to conventional sintering.
- Owing to its enhanced mechanism, the diffusion process is enhanced by microwave sintering.
- Higher heating rates can be achieved via microwave sintering, thus reduces the sintering duration.
- Higher density and better grain distribution can be achieved via microwave sintering method.
- Better physical and mechanical properties can be obtained by using microwave sintering.

Along with the evident energy savings, reduction in process duration, low sintering temperature (1200 °C) and high rates of microwave heating has the potential of enhanced the product quality, resulting in the final materials without substantial grain grow couple with less defective microstructures and improved densification as compare to conventional sintering. Further to this, almost 100% conversion of electromagnetic energy into heat largely with in the sample itself (Agrawal, 1998; Menezes & Kiminami, 2008; Monaco et al., 2015).

## **2.5 Summary**

Different approaches were used to enhance the ageing resistance of YSZ ceramic such as altering the content and distribution of the stabilizer, decreasing the grain size, and reducing the residual stress. Nevertheless, these methods on the other hand deteriorated the mechanical properties and required high cost or even labour intensive. Many studies on YSZ ceramic were focused either only on the mechanical properties or

on the LTD behavior. It is essential to maintain the intrinsic mechanical properties, particularly the fracture toughness, when improving LTD resistance of YSZ ceramic at low temperature in humid environment. Sintering conditions of zirconia ceramics especially sintering temperature was found to be most substantial on the mechanical properties and ageing resistance on the sintered YSZ ceramic. Hence, the modifications of the material with suitable sintering profile are possible to prepare ceramics of an optimum grain size and phase composition that minimizes transformation and thus reduces degradation under hydrothermal environment without sacrificing the mechanical properties of YSZ ceramic.

University of Malaysia

## CHAPTER 3: METHODOLOGY

### 3.1 Introduction

In this Chapter, all the standard experimental apparatus and techniques in the present research work are described in detail. The pictures of equipment used are shown in Appendix B.

### 3.2 Powder Preparation

The 3 mol% yttria-stabilized zirconia powder, 3YSZ (co-precipitated type) employed in current work with the code name KZ-3YF was manufactured by Kyoritsu Co. Ltd., Japan based on hydrolysis method and spray-dried to achieved free-flowing for mechanical pressing such as cold isostatic pressing (CIP) process. The as received powder contains 0.1 wt% of impurity which comprises SiO<sub>2</sub>, Fe<sub>2</sub>O<sub>3</sub>, TiO<sub>2</sub> and Al<sub>2</sub>O<sub>3</sub> as the major impurities. 99.0% pure manganese oxide (MnO<sub>2</sub>) powder by R&M Chemicals, UK was used as dopant. The starting 3YSZ ceramic powder without dopant is labelled as “undoped”. The chemical analysis and properties of these powders are given in Table 3.2 and Table 3.3.

The starting powders were prepared in 120 g for each batch of different MnO<sub>2</sub> addition and was calculated based on the equation (3.1) and (3.2). As tabulated in Table 3.1, the entire research required 1.80 g of MnO<sub>2</sub> and 358.20 g of 3YSZ to prepare all the three batches of powders.

$$\text{MnO}_2 \text{ (g)} = \frac{\text{MnO}_2(\text{wt}\%)}{100} \times 120\text{g} \quad (3.1)$$

$$3\text{YSZ (g)} = 120\text{g} - \text{MnO}_2 \text{ (g)} \quad (3.2)$$

Table 3.1: Starting powders compositions.

<b>Batch</b>	<b>MnO<sub>2</sub></b> <b>(wt%)</b>	<b>MnO<sub>2</sub></b> <b>(g)</b>	<b>3YSZ</b> <b>(g)</b>	<b>Total</b> <b>(g)</b>
1	0	0.00	120.00	120.00
2	0.5	0.60	119.40	120.00
3	1.0	1.20	118.80	120.00
	<b>Total</b>	1.80	358.20	

Manganese oxide (MnO<sub>2</sub>) was measured according to different composition required and mixed with the 3YSZ powder in ethanol medium through a process involving ultrasonification and followed by mechanical milling. During the ultrasonification process, the required amount of dopant was poured into a beaker containing approximately 150 mls of ethanol for about 5 minutes followed by the zirconia powder for another 25 minutes subject to ultrasonication at frequency 28 – 34 kHz to increase the homogeneity mixture of the MnO<sub>2</sub> in the zirconia. The mixture was ball milled with milling balls for 1 hour in a high density polyethylene (HDPE) bottle. Sieve was used to separate the milling balls from the slurry prior to the drying process. After 24 hours drying in the oven at 60°C, the dried cake of powder mixture was crushed and sieved through a stainless steel sieve of 212 μm mesh into powder form for green body preparation.

Table 3.2: Characteristic of the starting 3 mol% yttria-stabilized zirconia powder.

Powder Properties	
Yttria / Y <sub>2</sub> O <sub>3</sub> (mol%)	3
Y <sub>2</sub> O <sub>3</sub> (wt.%)	5.4
Al <sub>2</sub> O <sub>3</sub> (wt.%)	0.25
Specific surface area (m <sup>2</sup> /g)	12
mean particle diameter (nm)	200
Characteristic of sintered body (Sintered at 1450 °C)	
Sintered density (g/cm <sup>3</sup> )	6.07
Bending strength (MPa)	1000
Hardness (GPa)	12.5
Fracture Toughness (MPam <sup>1/2</sup> )	4-5
Forming method	Mechanical pressing, CIP

Table 3.3: Characteristic of the doping MnO<sub>2</sub> powder.

Chemical composition	
Manganese oxide (%)	99.0
Barium (%)	0.3845
Calcium (%)	0.25
Cadmium (%)	0.0003
Niobium (%)	0.07
Phosphorous (%)	0.27
Plumbum (%)	0.006
Strontium (%)	0.0002
Zirconium (%)	0.019
Mean particle size (nm)	5.0
Theoretical density (g/cm <sup>3</sup> )	3.9

### 3.3 Green Body Preparation

All the powders were pressed uniaxially at 0.3 MPa into the form of discs (20 mm diameter and 5 mm thickness) and rectangular bars (4 mm x 13 mm x 32 mm) with each sample weighing 2.5 g. Then the green compacts were marked using the sample identification codes shown in Table 3.4. The samples subsequently were cold isostatically pressed (CIP) at 200 MPa (Riken Seiki, Japan) with holding time of 1 minute. The CIP process is to ensure homogeneous compaction and to induce uniform shrinkage and ultimately improve densification.

Table 3.4: Samples labelling used in present study.

Sintering Temperature (°C)	Composition of MnO <sub>2</sub> doped YSZ (wt%)	Sintering Holding Time (min)				
		12	60	120	240	480
1100	0	A1M	A11	A12	A14	A18
	0.5	C1M	C11	C12	C14	C18
	1.0	D1M	D11	D12	D14	D18
1150	0	A2M	A21	A22	A24	A28
	0.5	C2M	C21	C22	C24	C28
	1.0	D2M	D21	D22	D24	D28
1200	0	A3M	A31	A32	A34	A38
	0.5	C3M	C31	C32	C34	C38
	1.0	D3M	D31	D32	D34	D38
1250	0	A4M	A41	A42	A44	A48
	0.5	C4M	C41	C42	C44	C48
	1.0	D4M	D41	D42	D44	D48



### **3.4 Sintering**

Sintering of green samples was done in air atmosphere using a box furnace (Carbolite, UK) at seven different temperatures, 1200, 1250, 1300, 1350, 1400, 1450, and 1500 °C for 2 hours with heating rate of 10 °C/min. In order to elucidate the efficacy of dopant and sintering holding time in enhancing densification of 3YSZ, selected samples were sintered at four different temperatures (1100, 1150, 1200 and 1250 °C) for five sintering holding times (12, 60, 120, 240 and 480 min) with standard heating and cooling rate of 10 °C/min.

### **3.5 Grinding and Polishing**

Silicon Carbide (SiC) abrasive papers of 120, 240, 600, 800, 1000 and 1200 grades were used to perform grinding on one surface of sintered disc specimens with running tape water as coolant. Finally the ground samples were polished with 5 and 1 µm diamond paste to achieve a fine surface finish prior to XRD, SEM evaluation, Vickers hardness and fracture toughness testing.

### **3.6 X-Ray Diffraction (XRD)**

X-ray diffraction (XRD) is a versatile, non-destructive analytical technique for identification and quantitative determination of the various crystalline forms known as phases of compounds present in powder and solid. Besides that, XRD method is capable of providing qualitative and quantitative information about the crystalline phase exists in the sample (Rahaman, 1995).

In the present work, the sample was held fixed while the X-ray source and detector will rotate at different angles. The tetragonal and monoclinic phase analysis of the powders and sintered samples were done by X-ray diffraction (SHIMADZU, X-ray diffractometer, XD-3A Series, Japan) within the  $2\theta$  range  $27-36^\circ$  at  $0.02^\circ$   $2\theta$  step size

and a count time of 0.5 s per step under ambient conditions using Cu-K $\alpha$  as the radiation operating at 35 kV and 35 mA. Within this 2 $\theta$  range, monoclinic (m) phase at  $\sim 28.2^\circ$  and  $\sim 31.5^\circ$  as well as the tetragonal (t) phase at  $\sim 30.2^\circ$  where covered. The presence of monoclinic content in the samples was calculated using the integrated peak intensities of the cubic/tetragonal line (1 1 1) and monoclinic lines (1 1 1), (1 1  $\bar{1}$ ) by applying the method of Toraya et al. (1984):

$$V_m = \frac{1.311 X_m}{1 + 0.311 X_m} \times 100 \% \quad (3.3)$$

Where,  $V_m$  represent volume fraction of monoclinic zirconia and  $X_m$  represent integrated intensity ratio as shown below:

$$X_m = \frac{I_m^{(1\bar{1}\bar{1})} + I_m^{(111)}}{(I_m^{(1\bar{1}\bar{1})} + I_m^{(111)}) + I_t^{(111)}} \quad (3.4)$$

Where,  $X_m$ , monoclinic fraction;  $I_m^{(111)} \sim 31.5^\circ$ ,  $I_m^{(1\bar{1}\bar{1})} \sim 28.2^\circ$  and, monoclinic peak intensity;  $I_t^{(111)} \sim 30.2^\circ$ , tetragonal peak intensity.

The reported tetragonal content usually included cubic phase that present in the system (if any), as the (1 1 1) peaks for both phases overlap each other between  $30^\circ - 31^\circ$  2 $\theta$  range. the XRD data sheet was analyzed by compared with the standard JCPDS-ICDD files (Joint Committee of Powder Diffraction Standard International Center for Diffraction Data) to identify the phases present in steatite body.

The cubic phase was identified by referring the peaks at  $\sim 73^\circ$  and  $\sim 74.4^\circ$  correspond to line (0 0 4) and (4 0 0) reflections of the transformable tetragonal zirconia while for the non-transformable tetragonal zirconia, the peaks at  $\sim 73.4^\circ$  and  $\sim 73.9^\circ$  correspond to line  $t'(0\ 0\ 4)$  and  $t'(4\ 0\ 0)$  were referred respectively. In present study, for cubic phase measurement, the 2 $\theta$  range 72-76 $^\circ$  at 0.02 $^\circ$  2 $\theta$  step size and a count time of

5.0 s per step was employed. The volume fraction of the cubic phase was then determined from the following equation (Paterson & Stevens, 1986):

$$V_c = \frac{I_{t'}^{(4\ 0\ 0)} + I_{t'}^{(0\ 0\ 4)}}{I_{t'}^{(4\ 0\ 0)} + I_{t'}^{(0\ 0\ 4)} + I_t^{(4\ 0\ 0)} + I_t^{(0\ 0\ 4)}} \times 100 \% \quad (3.5)$$

Where,  $V_c$  denoted volume fraction of cubic phase while volume fraction of the metastable tetragonal phase,  $V_t$  can then be obtained by:

$$V_c \% = V_{c,t} \% - V_t \% \quad (3.6)$$

### 3.7 Bulk Density Measurement

Density is a measure weight of a material for a given unit of volume. Bulk density is one of the various ways to interpret density which is defined as the measured density of a ceramic body, which includes all lattice defects, phases, and fabrication porosity. Due to the existence of the polycrystalline phase in most ceramics, bulk density is the most suitable ways to measure the density in order to consider the porosity present in the materials (Richerson, 1992).

The bulk density of the sintered samples was measured by water immersion method using an analytical balances fitted with a density measurement accessory (Vibra HT, Japan) and the relative density was obtained by referring the theoretical density of YSZ ceramic as 6.10 g/cm<sup>3</sup>. The procedures to conduct the water immersion technique are stated below:

1. The temperature of the distilled water was recorded to determine the density of the distilled water based on the density table of water.

2. The dry weight of the sample was measured.
3. Same sample was immersed into the distilled water and recorded the value only when the reading from the balance stops to increase. The weight of the sample in water will gradually increase due to the reason that the water is penetrating the pores in the sample.
4. The sample was removed from the water. The excess liquid was wiped out from the sample with a cloth saturated with the liquid. The weight of the fluid-saturated sample was then measured.

The bulk density of the samples can be calculated using equation (3.4):

$$\rho = \left( \frac{W_a}{W_{sat} - W_w} \right) \rho_w \quad (3.4)$$

Where,

$\rho$  = sample's bulk density

$W_a$  = sample's weight which measured in air

$W_w$  = sample's weight which measured in water

$\rho_w$  = density of distilled water (Refer to Appendix A for density values base on the testing temperature)

### 3.8 Young's Modulus Determination

The Young's modulus of the rectangular samples was determined using a non-destructive method called sonic resonance method. In this method, the flexural resonant

frequency of each bar samples were collected using a commercial testing instrument (GrindoSonic: MK5 “Industrial”, Belgium).

The testing instrument enables direct measurement of the resonant frequency of the bar samples by a transducer via monitoring and evaluating the vibrational harmonics of the samples. The vibrations are generated in the sample by tapping. The modulus of elasticity is then determined with the experimentally determined resonant frequencies applying the equation (3.5) (ASTM E1876–97).

$$E = 0.9465 \left( \frac{mF^2}{b} \right) \left( \frac{L}{t} \right)^3 T \quad (3.5)$$

Where,

E = Young’s modulus (Pa)

m = Mass of bar (g)

F = Fundamental resonant frequency of the bar in flexural (Hz)

b = Width of bar (mm)

L = Length of bar (mm)

t = Thickness of bar (mm)

T = Correction factor for fundamental flexural mode to account for finite thickness of bar and material’s Poisson’s ratio based on equation (3.6):

$$T = 1 + 6.585(1 + 0.0752\mu + 0.8109\mu^2) \left( \frac{t}{L} \right)^2 - 0.868 \left( \frac{t}{L} \right)^4 - R \quad (3.6)$$

Where,

$$R = \frac{8.34(1 + 0.2023\mu + 2.173\mu^2)\left(\frac{t}{L}\right)^4}{1 + 6.338(1 + 0.1408\mu + 1.536\mu^2)\left(\frac{t}{L}\right)^2} \quad (3.7)$$

$\mu$  = Poisson's ratio taken as 0.23 (Brook, 1991)

### 3.9 Vickers Hardness Determination

Vickers hardness ( $H_v$ ) and fracture toughness ( $K_{IC}$ ) were measured on the polished disc samples using the Vickers indentation method (Bowers, China). Indentations were made by using a pyramidal diamond indenter that has a  $136^\circ$  tip with load of 10 kgf was applied and held slowly for 10 seconds without impact to create an impression (Figure 3.1). The physical quality of the indenter and the accuracy of the applied load as defined clearly in ASTM E384-99 and ISO 14705 must be controlled to obtain the correct results.

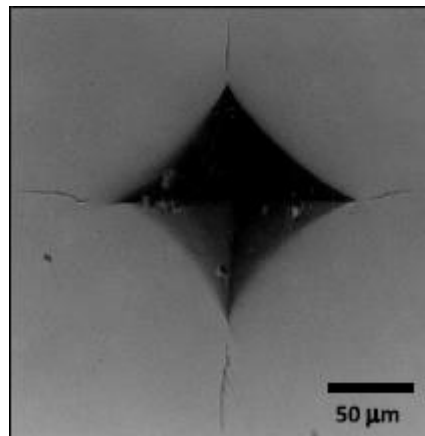


Figure 3.1: Optical Image of Polished Y-TZP Surface Containing the Vickers Impression.

As shown in Figure 3.2, the two impression diagonals,  $D_1$  and  $D_2$  were measured with the built in filar micrometer at the microscope attached on the Vickers machine to the nearest  $0.1 \mu\text{m}$  and average value is obtained from three measurements. The Vickers hardness ( $H_v$ ) is obtained from the surface area of indentation created based on equation (3.8):

$$H_v = \frac{1.854P}{d^2} \quad (3.8)$$

Where,

$P$  = applied load (N)

$d$  = average diagonals =  $\frac{D_1 + D_2}{2}$

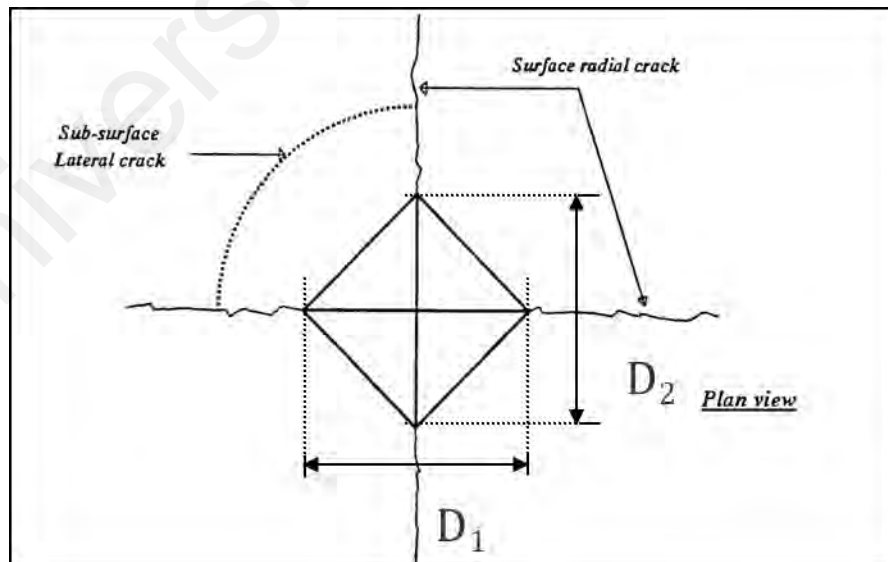


Figure 3.2: Schematic Indentation Fracture Pattern of an Idealized Vickers Palmqvist Crack System.

### 3.10 Fracture Toughness Determination

Fracture toughness ( $K_{Ic}$ ) is the ability of a material that contains cracks to resist the propagation of cracks. Its unit is  $\text{MPam}^{1/2}$ . After each Vickers indentation, the length ( $l$ ) of four cracks as shown in Figure 3.3 were measured and average crack length of the indentation was identified. Fracture toughness ( $K_{Ic}$ ) of the samples was calculated by using equation (3.9). (Niihara, et al., 1981). The average value was taken from three measurements for each sample.

$$K_{Ic} = 0.035 \left(\frac{a}{l}\right)^{1/2} \left(\frac{E\phi}{Hv}\right)^{2/5} \left(\frac{Hv}{\phi}\right) a^{1/2} \quad (3.9)$$

Where,

$K_{Ic}$  = Fracture toughness

$E$  = Young's Modulus (GPa)

$H_v$  = Vickers's Hardness (GPa)

$P$  = Indentation load (N)

$l$  = Average crack length ( $\mu\text{m}$ ) =  $\frac{l_1+l_2+l_3+l_4}{4}$

$\phi$  = Constraint factor, taken as 3 (ISO 14705, 2000)



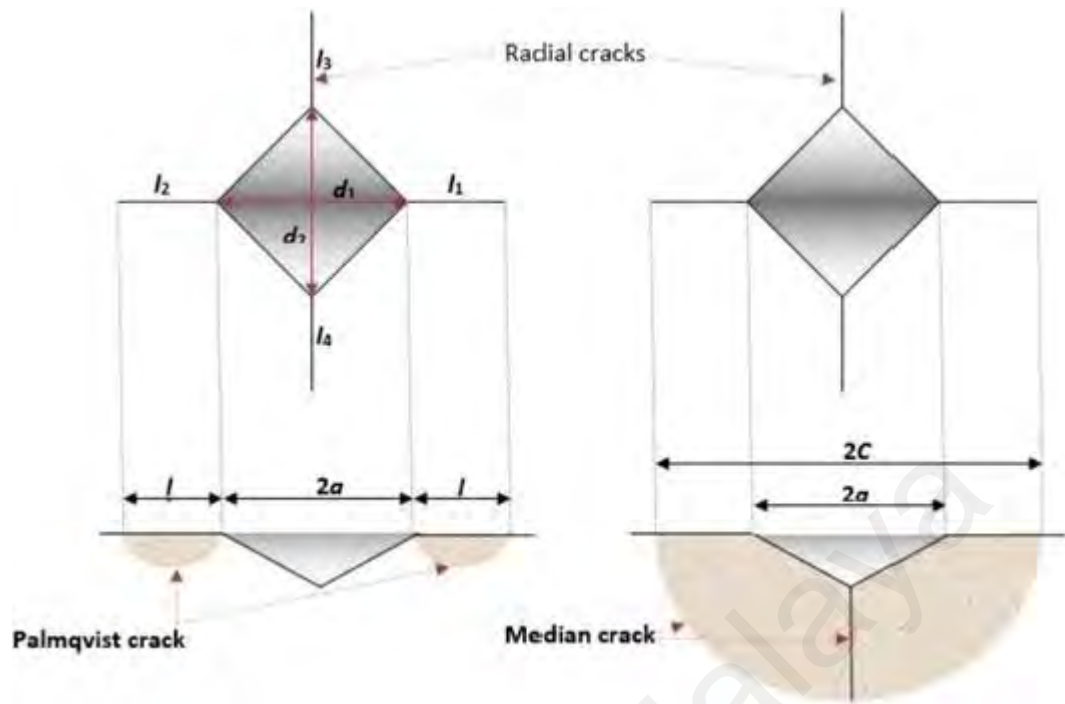


Figure 3.3: Schematic Indentation Fracture Pattern of an Idealized Vickers Palmqvist Crack System. (Khan et al., 2014)

### 3.11 Microstructure Examination

#### 3.11.1 Scanning Electron Microscopy

The SEM focuses a small spot of electrons on a chemically etched sample and then scans this across the sample surface, in a series of lines, using electrostatic or electromagnetic forces. Electrons emerging from the upper specimen surface were collected by an electron detector and used to produce image on a T.V. monitor as a series of lines. The image produced is of a 3-D surface and has much greater depth of field at magnifications as high as 15,000 times. (Joy, 1992; Zhou *et al.*, 2006).

The morphology of the starting powders and microstructural evolution of the sintered samples were observed by scanning electron microscopy (SEM, Shimadzu, USA). Prior to SEM analysis, the disc samples with surface polish up to mirror finish

were thermally etched 50 °C below the sintering temperature of the sample at heating and cooling rate of 10 °C/min, with holding time of 30 min prior to cooling to reveal the grain boundaries. Subsequently a thin layer of gold palladium coating was applied by sputtering process to prevented charging at the ceramic samples during scanning process. This is to obtain a clear microstructure especially the grain boundary.

### 3.11.2 Grain Size Measurement

The grain size was measured from scanning electron micrographs by the linear intercept technique. Diagonal line (test line) will be sketched on an SEM micrograph printed on the A4 size paper that cover at least 50 grains. The intercept points between the test line and grain boundaries are counted. The measurement is repeated three times with the lines are drawn at different locations to obtain the average value. Figure 3.4 shows the sketch of diagonal line on SEM micrograph.

The average grain size is determined with the equation (3.10) proposed by Mendelson:

$$\bar{D} = 1.56\bar{L} \quad (3.10)$$

Where  $\bar{D}$  is the average grain size and  $\bar{L}$  is the measured average interception length over a large number of grains which can be represented by:

$$\bar{L} = \frac{C}{MN} \quad (3.11)$$

Where  $C$ ,  $M$  and  $N$  are the total length of the test line, the magnification of the SEM micrograph and the number of intercepts respectively.

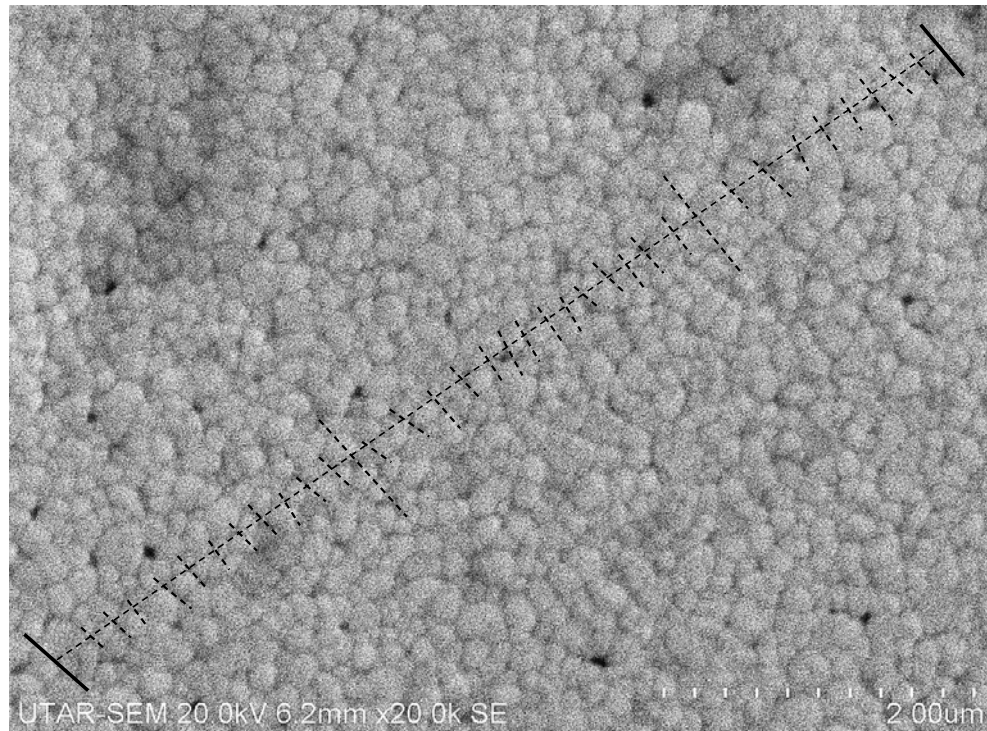


Figure 3.4: Sketch of Diagonal Line on SEM Micrograph.

The international standard measurement method was used for linear intercept counting (ASTM E112-96, 2000) to quantify the number of intersection points. Basically, the end points of a test line that touch a grain boundary is scored as a '1' intersection point or else no score shall be counted without intersection point, while a '1.5' intersection point for intersection coinciding with triple junction of 3 grains as illustrated in Figure 3.5.

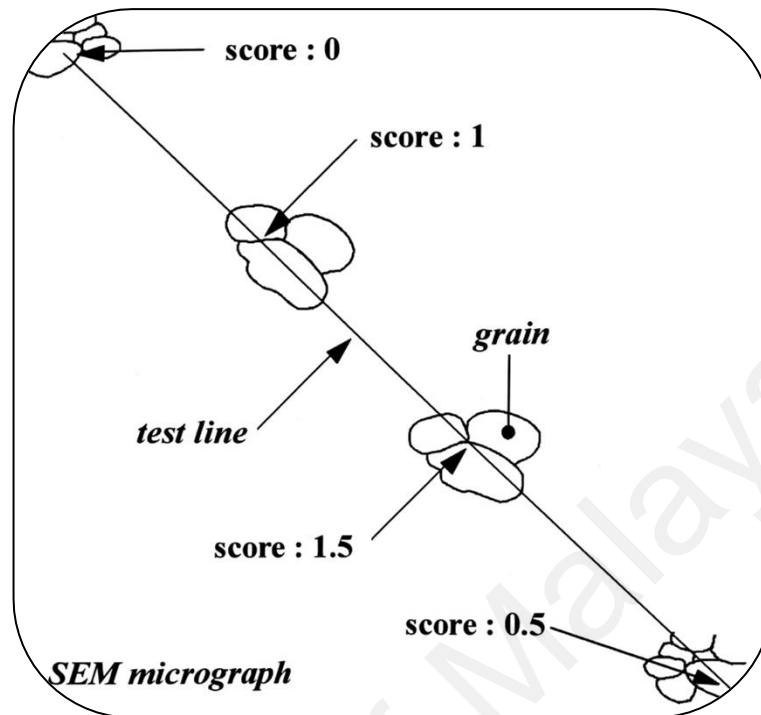


Figure 3.5: Schematic diagram of the score for several type of line interception.

The line intercept method applied to determine the average grain size is only restricted to polycrystalline ceramics comprising equiaxed grains which have developed normally to fully dense single-phase microstructure. However, minute of porosity or second phase (i.e. < 10 vol%) present in the microstructure have negligible influence on the accuracy of the measurement with condition the size distribution and shape of the grains are not significantly affected. This technique is also relevant for material with two-phase microstructures by applying a correction factor when calculating the grain size (Wurst & Nelson, 1972).

### 3.12 Hydrothermal Ageing Experiment

Both undoped and MnO<sub>2</sub> doped 3YSZs disc samples (sintered) were exposed to autoclave conditions for selected periods in order to examine the low temperature degradation (LTD) behavior of the ceramics in pressurized steam environment. The samples were placed in a pressurized reactor containing 20 mls of distilled water and then placed in an oven with temperature 180 °C to form superheated steam at 10 bar for periods up to 300 hours. The amount of formed monoclinic phase was determined by XRD analysis as a function of ageing time of 0, 3, 6, 12, 24, 48, 120, 150, 200 and 300 hours progressively.

University of Malaya

## CHAPTER 4: RESULTS AND DISCUSSION

### 4.1 Introduction

The results and discussion are discussed in three sections. The first section focuses on the evaluation of the densification behaviour and properties of the undoped YSZ ceramics via standard sintering profile (heating/cooling: 10 °C/min, holding time 240 min and temperature between 1200 to 1500 °C). In the second section, the impact of MnO<sub>2</sub> concentration (0, 0.5 and 1.0 wt.%) within the YSZ ceramic was varied at low temperatures (1100, 1150, 1200 & 1250 °C) with holding times (12, 60, 120, 240 and 480 min) were studied. The ageing behaviour of the YSZ ceramics will be presented in the third section. The final part of the work will build on the above sections to optimise the property sets and hydrothermal ageing resistance of the produced YSZ ceramics.

### 4.2 YSZ Powder Characteristic

The SEM micrograph showed that the starting YSZ powder agglomerate comprises of small particles with size varying up to ~150 nm as shown in Figure 4.1.

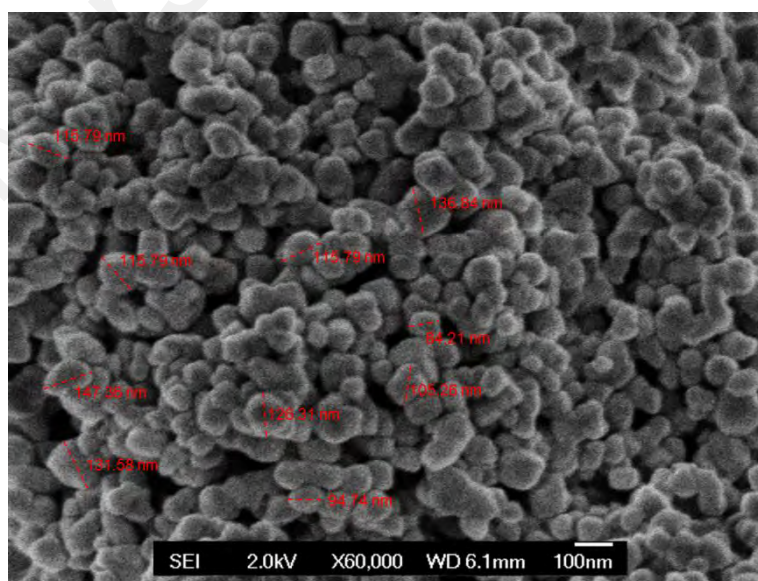


Figure 4.1: SEM micrographs of agglomerates as-received YSZ powder.

### 4.3 Sintering Temperature Effect on Undoped YSZ Ceramic

#### 4.3.1 Tetragonal Phase Retention

Phase analysis was carried out by X-ray diffraction after each hydrothermal ageing process for various durations up to 300 hr. The XRD traces of undoped YSZ ceramics did not show t – m phase transformation before hydrothermal ageing as depicted in Figure 4.2.

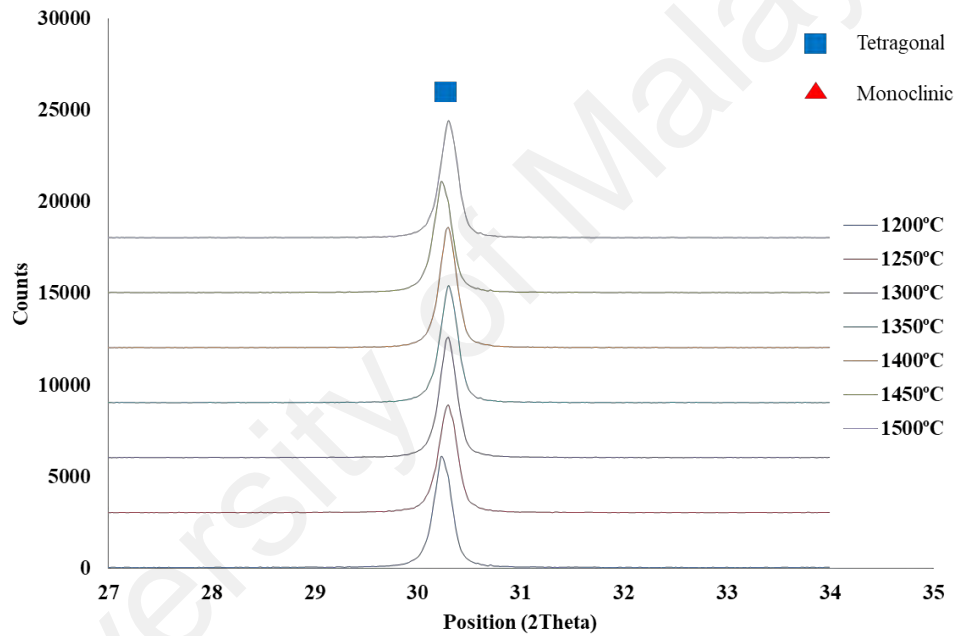


Figure 4.2: XRD plots of the undoped YSZ ceramics sintered at 1200 °C to 1500 °C

revealing tetragonal (t) symmetry.

The X-ray diffraction results of all investigated sintered YSZ ceramics showed that they were primarily tetragonal with small amounts of a cubic phase. As the sintering temperature increased, more cubic was developed and the amount of tetragonal phase declined as shown in Figure 4.3.

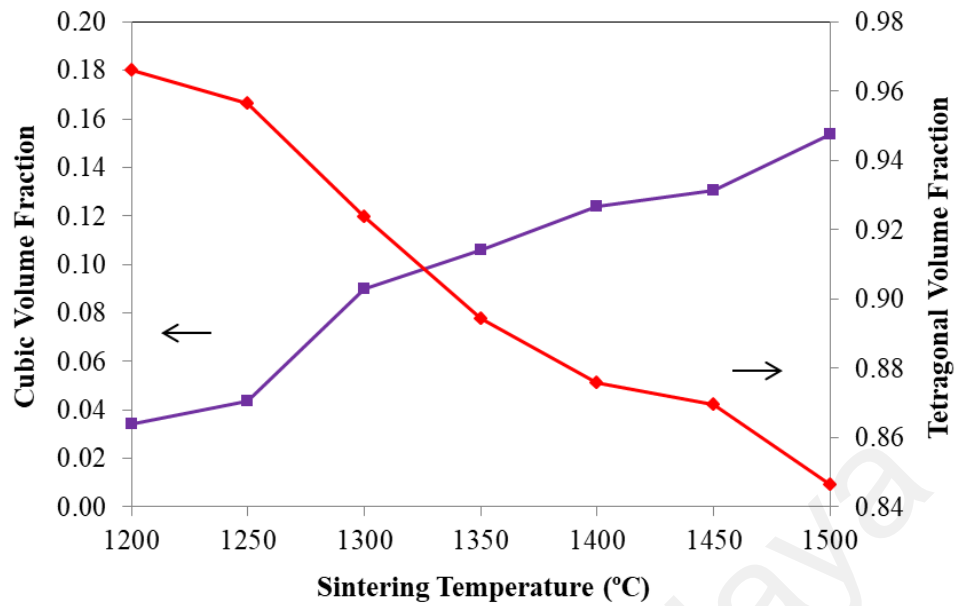


Figure 4.3: Phase analysis of as-received YSZ ceramics sintered at 1200 °C to 1500 °C.

#### 4.3.2 Density

The effect of sintering temperature on relative density of the samples is shown in Figure 4.3. The lowest relative density measured was approximately 94% and was produced at a sintering temperature of 1200 °C. The density initially increased as sintering temperature increased. All the samples had a comparative density, in the range of 98 - 99% for the sintering temperatures above 1250 °C. The maximum density was achieved for sintering temperatures between 1400 to 1450 °C before decreasing slightly when sintered at 1500 °C. (Hannink et al., 2000b) decrease in density could be associated with grain coarsening at higher temperatures. According to Inokoshi et al. (2014), the decrease in bulk density of YSZ samples when sintered at temperatures as high as 1650 °C resulted in the partial transformation of the tetragonal phase into cubic and monoclinic phases thus resulting in a decreased density of the YSZ ceramics.



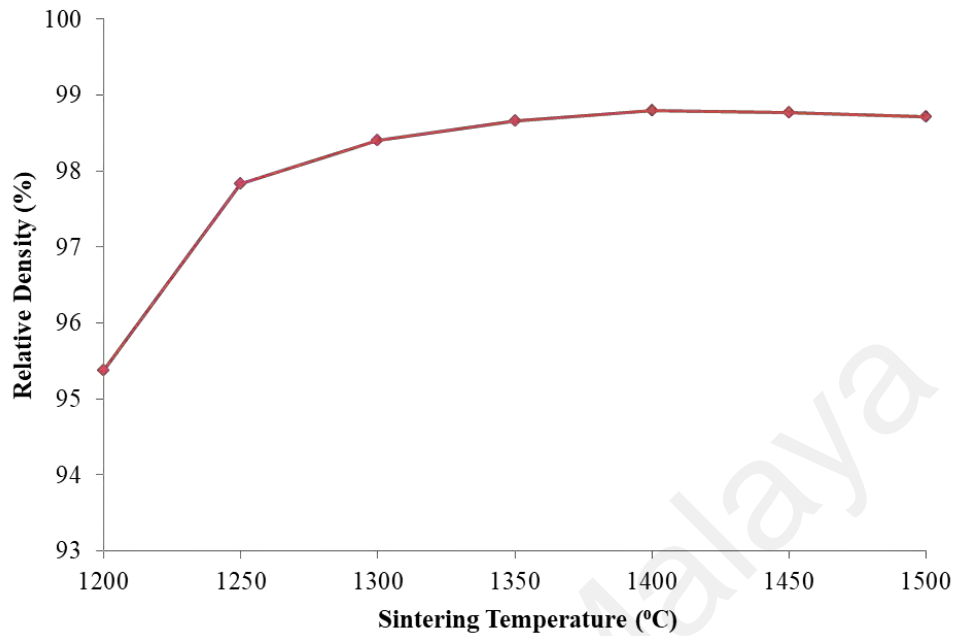


Figure 4.4: The relationship of sintering temperatures and the relative density of the YSZ ceramics.

### 4.3.3 Young's Modulus

The effect of sintering temperature on the Young's modulus of YSZ ceramics is illustrated in Figure 4.5. The Young's modulus of YSZ ceramics was relatively low (178 GPa) when sintered at 1200 °C but increased sharply (~207 GPa) as the sintering temperature was increased to between 1250 – 1350 °C. The highest modulus (211 GPa) was obtained with a sintering temperature of 1400 °C.

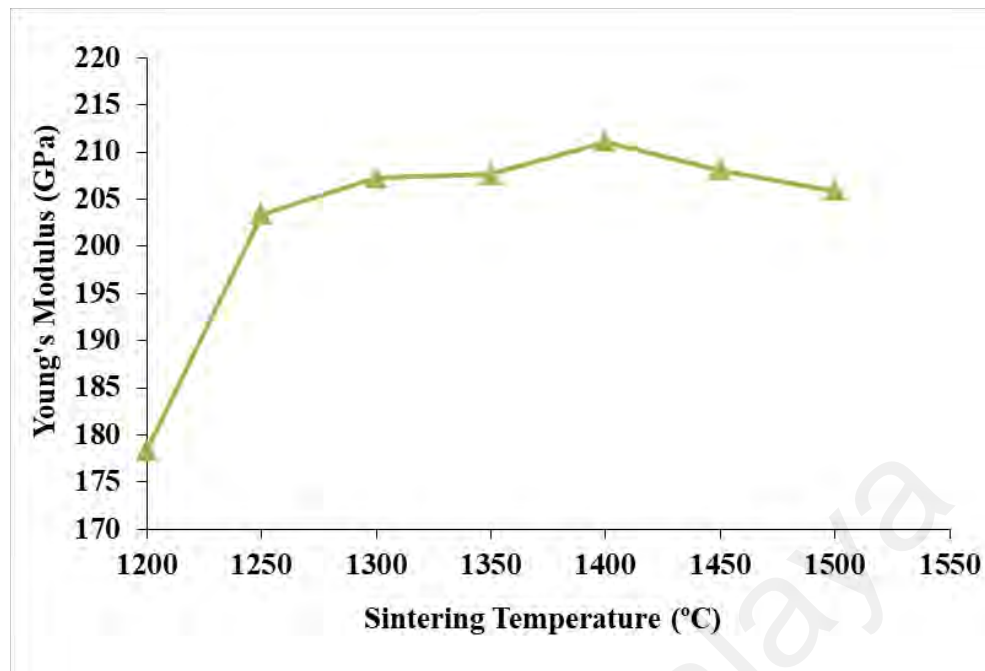


Figure 4.5: Young's modulus variation as a function of sintering temperature.

There is strong linear correlation between the sintered bulk density and Young's modulus as shown in Figure 4.6. The results in this work are in general agreement with the findings of other researchers (Khan et al., 2014; Ramesh et al., 2013; Siva Kumar et al., 2016). The matrix stiffness of the YSZ is strongly dependent on the bulk density of the ceramics. The current results was used to estimate the Young's modulus values required to obtain the other mechanical properties such as hardness and fracture toughness in Section 4.4.3 and 4.4.4 of this thesis.

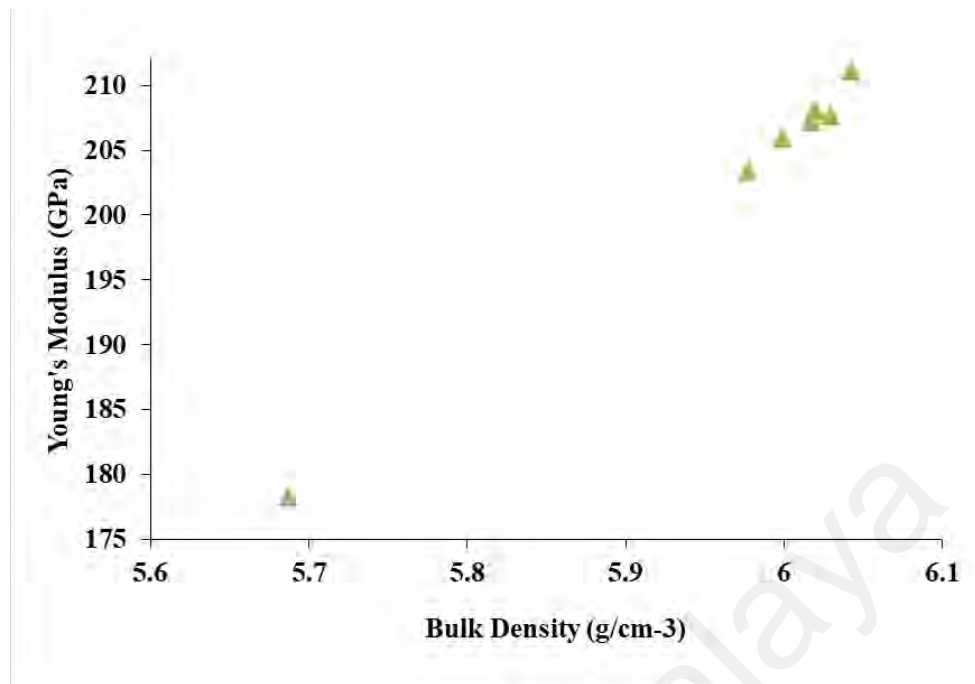


Figure 4.6: The linear relationship of Young's modulus and bulk density of YSZ ceramics.

#### 4.3.4 Vickers Hardness

The effect of sintering temperature on the Vickers hardness of the YSZ ceramics is illustrated in Figure 4.7. The hardness of the YSZ ceramic increases from 12.2 GPa at 1200 °C to 13.9 GPa at 1250 °C reaching a maximum of 14.4 GPa at 1350 °C. It can be inferred from the work of (Ramesh et al., 2011) which showed that hardness improvement in zirconia ceramic was due to the enhanced densification of the sintered body. Figure 4.7 shows the relationship between the hardness and density of the ceramic samples. However, the hardness began to decline when sintering temperature exceeded 1350 °C and it was believed to be associated with grain coarsening as well as formation of cubic phase. This trend of Vickers hardness observed in the present work is in agreement with that reported by other researchers (Hodgson et al., 1999a, 1999b; Ramesh et al., 2011).

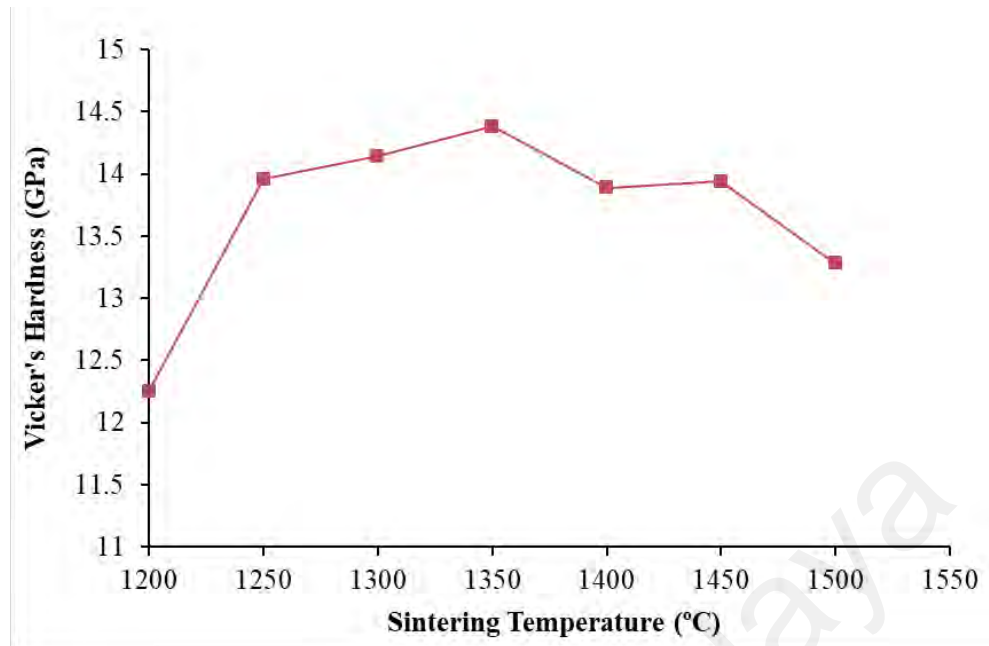


Figure 4.7: Influence of sintering temperatures on the Vickers hardness of YSZ ceramic.

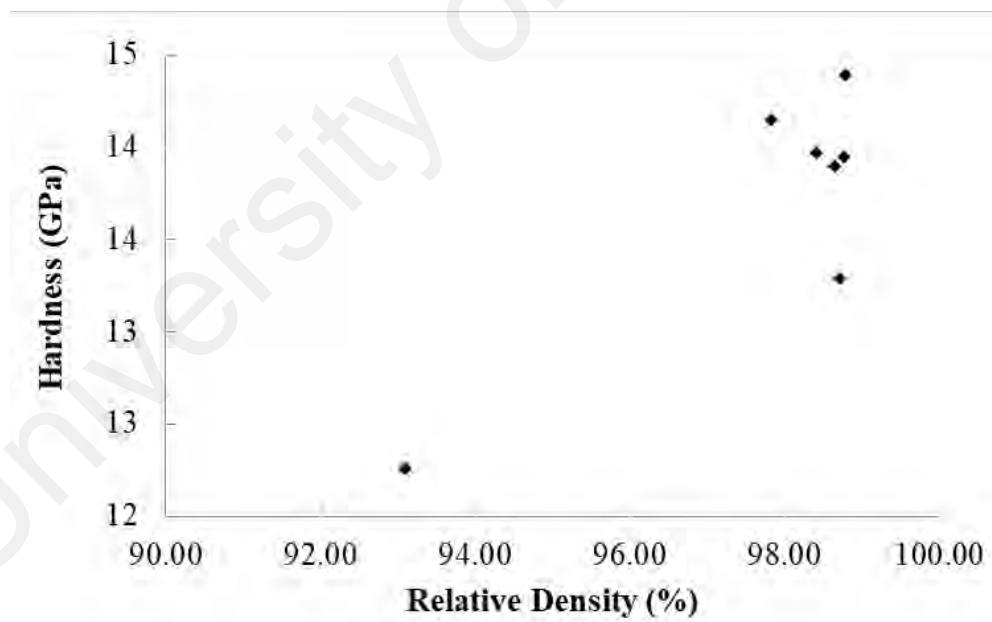


Figure 4.8: Changes of Vickers hardness and density in YSZ ceramic with sintering temperature.

### 4.3.5 Fracture Toughness

The influence of sintering temperature on the fracture toughness,  $K_{Ic}$  of YSZ ceramic is shown in Figure 4.9. The  $K_{Ic}$  of the sintered samples increased gradually with temperature reaching a maximum of  $5.07 \text{ MPam}^{1/2}$  at  $1350^\circ\text{C}$ . In general, the fracture toughness varied between  $4.91$  to  $5.03 \text{ MPam}^{1/2}$  when sintered above  $1400^\circ\text{C}$ . These results indicate that the sintering temperature had only a marginal effect on the fracture toughness of the YSZ ceramic. Similar result was observed by Kwa et al. (2015) who suggested that it was attributed to homogenisation of stabilizer within the  $\text{ZrO}_2$  grains of the YSZ powder, thus resulting in a more stable tetragonal phase.

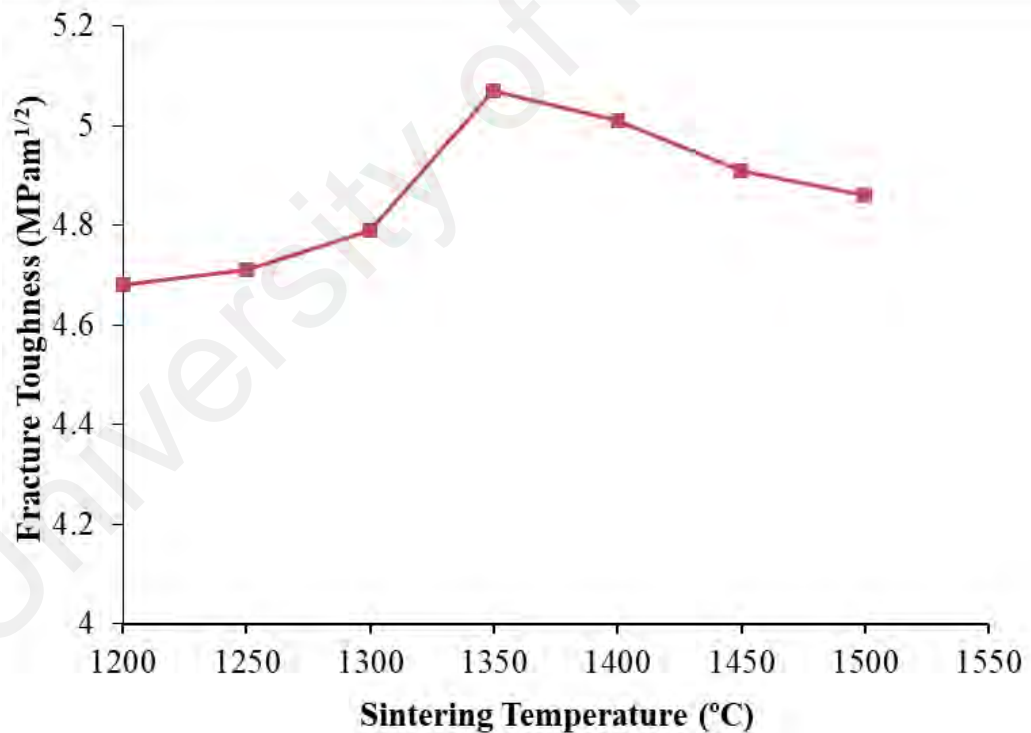


Figure 4.9: Variation of fracture toughness for YSZ ceramic sintered at various temperatures.

The relationship between the fracture toughness,  $K_{Ic}$  of YSZ ceramic and grain size is shown in Figure 4.10. The samples can be categorized into two regions, region 2 with average  $K_{Ic}$ ,  $<4.80 \text{ MPam}^{1/2}$  and Region 1 with  $>4.80 \text{ MPam}^{1/2}$ . Samples in region 1 had a broader range of grain sizes ( $0.28 - 0.71 \mu\text{m}$ ) compared to those in region 2 ( $0.14 - 0.25 \mu\text{m}$ ). Although there was a small difference in  $K_{Ic}$  ( $4.68 - 5.07 \text{ MPam}^{1/2}$ ) between the regions the average grain increased significantly  $0.139$  to  $0.714 \mu\text{m}$ . This result revealed that the effect of grain size on fracture toughness of the YSZ ceramics and it can be seen that sintering temperature has direct impact to fracture toughness of the ceramic samples as reported in literature (Eichler et al., 2007; Ho & Tuan, 2012).

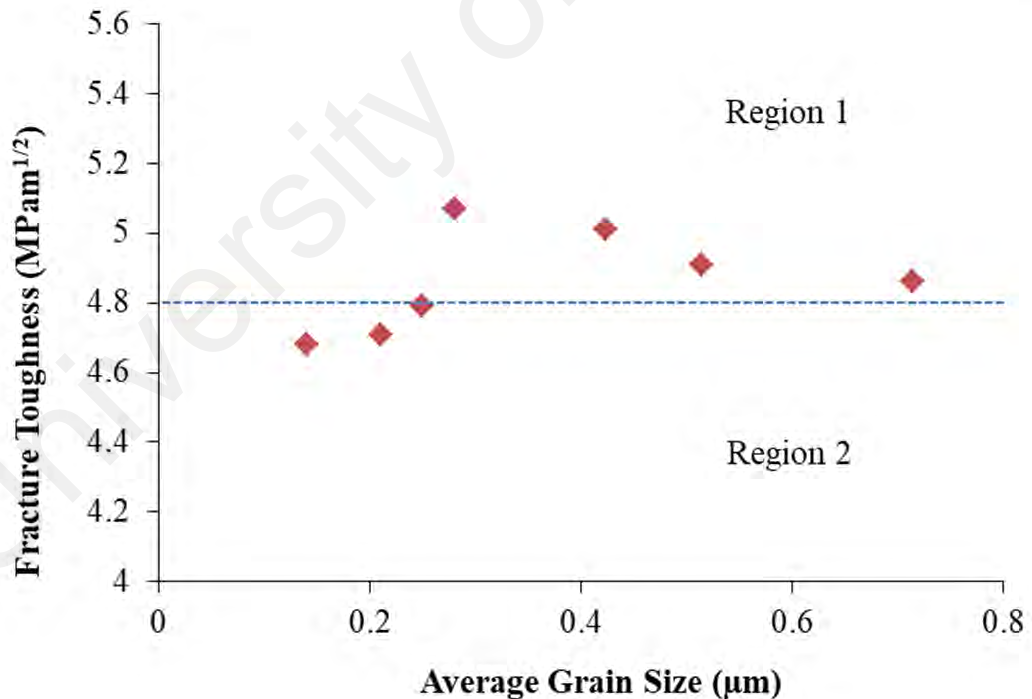


Figure 4.10: Variation of fracture toughness for YSZ ceramic sintered at various grain sizes.

#### 4.3.6 Microstructural Evolution & Grain Size

Figure 4.12 shows the effect of sintering temperature on the average grain size of YSZ ceramics. In general, it was found that the grain size increases with increasing sintering temperature from 0.14  $\mu\text{m}$  to 0.71  $\mu\text{m}$  as the sintering temperature increases from 1200  $^{\circ}\text{C}$  to 1500  $^{\circ}\text{C}$ .

The YSZ sintered samples exhibited typical unimodal grains with no pores or inclusions. A uniform microstructure, composed of equiaxed grains was observed when sintered at 1250  $^{\circ}\text{C}$  and above. However, the grain growth rate for a small percentage of the grains was higher than that observed in the surrounding grains. This was especially true for samples sintered at higher temperatures  $\geq 1350$   $^{\circ}\text{C}$  as evident from the SEM micrograph in Figure 4.11. Grains with a faceted shape were also evident with the increase of sintering temperature as depicted in Figure 4.11 (d, e, f & g). The larger grains were 3 to 5 times larger than the smaller grains for the sample sintered at 1500 $^{\circ}\text{C}$ . Larger grain size was generally observed for higher sintering temperatures and/or longer sintering times (above 2 hours) which could be the cubic grains (Chevalier et al., 2004; Denry & Kelly, 2008; Hallmann, Mehl, et al., 2012; Ruiz & Readey, 1996).

Figure 4.13 shows the changes in relative density and average grain size of YSZ with sintering temperature. Small grain growth rates  $\sim 3.0 \times 10^4$   $\mu\text{m}/^{\circ}\text{C}$  was observed for samples that showed a sharp increase from 93% to 98% as sintering temperatures increased from 1200 to 1250  $^{\circ}\text{C}$ . However when sintering temperature was elevated above 1300  $^{\circ}\text{C}$ , the ceramic samples showed a minimum enhancement in density but relatively large grain growth rate  $\sim 3.0 \times 10^3$   $\mu\text{m}/^{\circ}\text{C}$ .

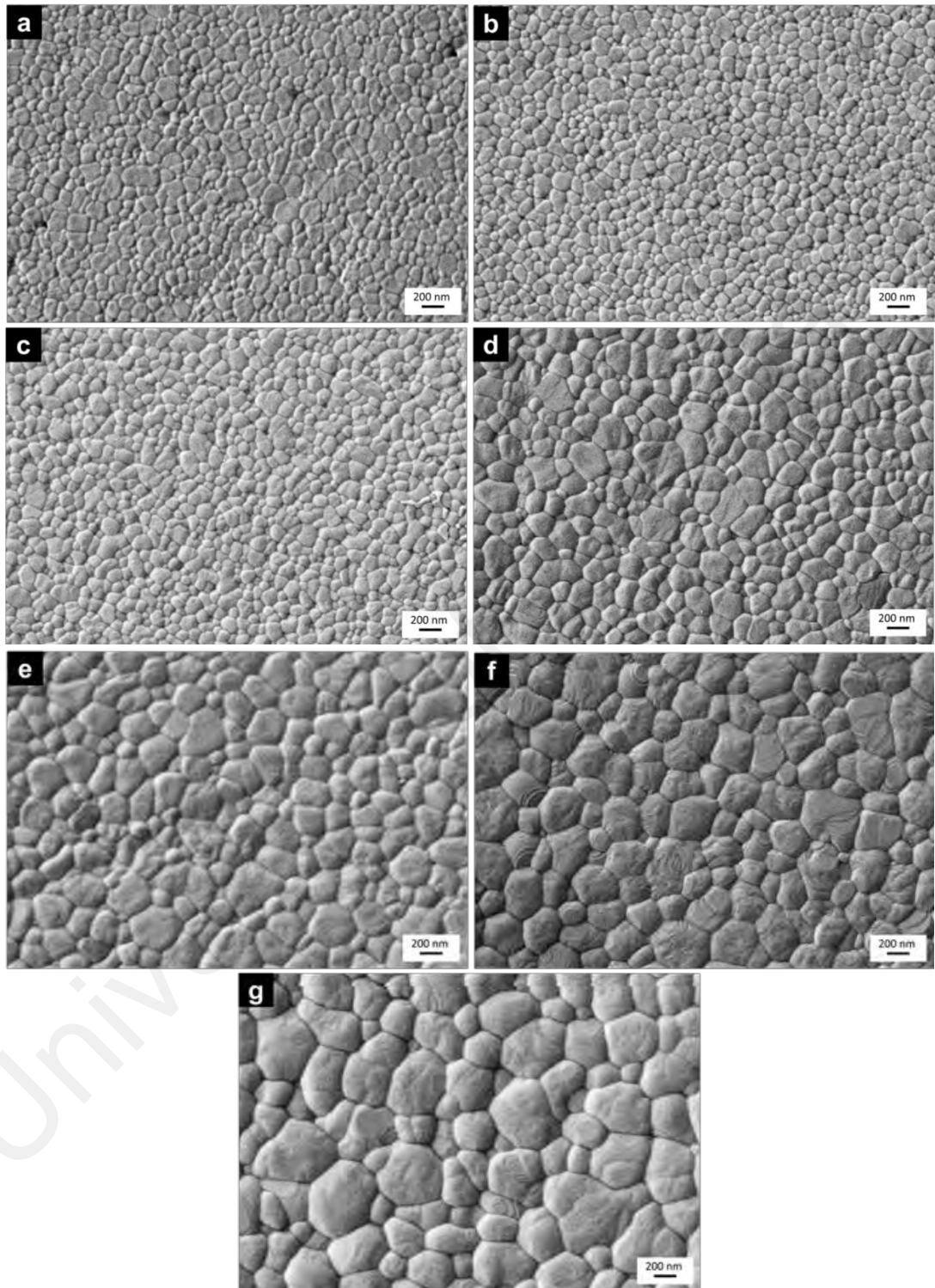


Figure 4.11: Microstructure evolution of YSZ ceramics sintered at (a) 1200 °C, (b) 1250 °C, (c) 1300 °C, (d) 1350 °C, (e) 1400 °C, (f) 1450 °C and (g) 1500 °C.



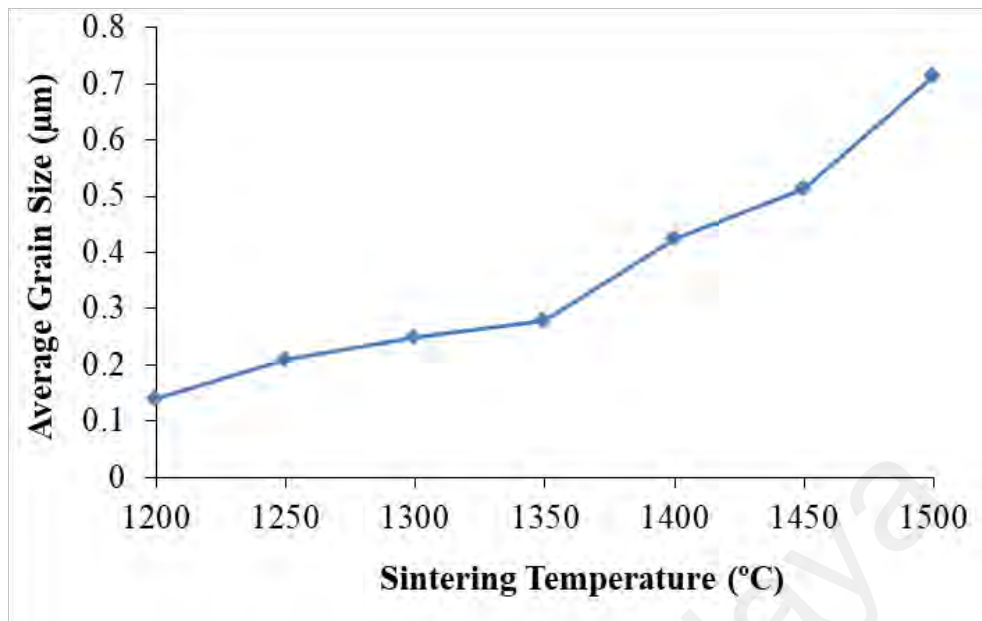


Figure 4.12: Effect of sintering temperatures on the average grain size of the YSZ ceramics.

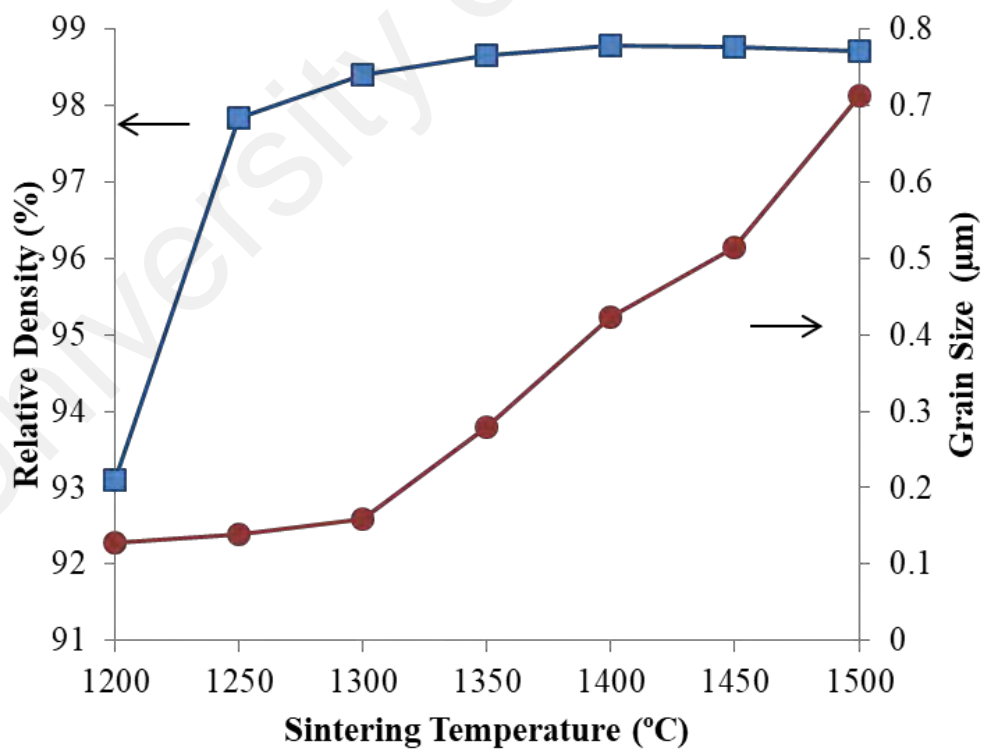


Figure 4.13: Effect of sintering temperatures on the density and grain size of the YSZ ceramics.

#### **4.4 Isothermal Sintering Effect at Low Sintering Temperature with MnO<sub>2</sub> Dopant**

Addition of sintering additives are able to fabricate YSZ ceramics with enhanced densification at low sintering temperatures (Lawson, 1995). Studies have shown that additions of small amounts of dopant to zirconia based ceramics promote full densification at the lower sintering temperature, e.g. SiO<sub>2</sub>, Al<sub>2</sub>O<sub>3</sub>, Fe<sub>2</sub>O<sub>3</sub>, CuO, MnO<sub>2</sub>. Moreover these additives are able to suppress the hydrothermal degradation by controlling the microstructure and improving the properties of the ceramic. Wu et al. (2013) reported that the addition of 0.25 wt% Al<sub>2</sub>O<sub>3</sub> could effectively retard the ageing of 3Y-TZP (Bravo-Leon et al., 2002). Guo and Xiao (2012) successfully produced high relative densities (>95 %) in 3Y-TZP ceramics sintered at 1150 °C when doped up to 2 mol% of Fe<sub>2</sub>O<sub>3</sub>. On the other hand, Ramesh et al. (2013) discovered that high relative densities (>97.5%) of 3Y-TZP could be obtained at < 1300 °C with the 0.5 wt% of MnO<sub>2</sub> dopant. Therefore, through modifications of materials with suitable sintering profiles it is possible to prepare ceramics with an optimum grain size and phase composition that minimizes transformation and thus reduces degradation under hydrothermal environment.

##### **4.4.1 Tetragonal Phase Retention**

The X-ray diffraction patterns of the investigated sintered YSZ ceramics showed that all ceramics were primarily tetragonal with a smaller amount of cubic phase. Generally the cubic phase content of the ceramics increased from 4 to 12 % with holding time at various sintering temperatures (1100, 1150, 1200 and 1250 °C) as shown in Figure 4.14, 4.15 and 4.16. Larger percentage of cubic phase was detected in YSZ ceramics doped with MnO<sub>2</sub> as compared to the undoped YSZ ceramics. YSZ

doped with 1.0 wt.% MnO<sub>2</sub> had 10 - 12 % of cubic phase when sintered at 1250 °C with holding time >60 min while by YSZ doped with 0.5 wt.% MnO<sub>2</sub> had of 8 – 10 %.

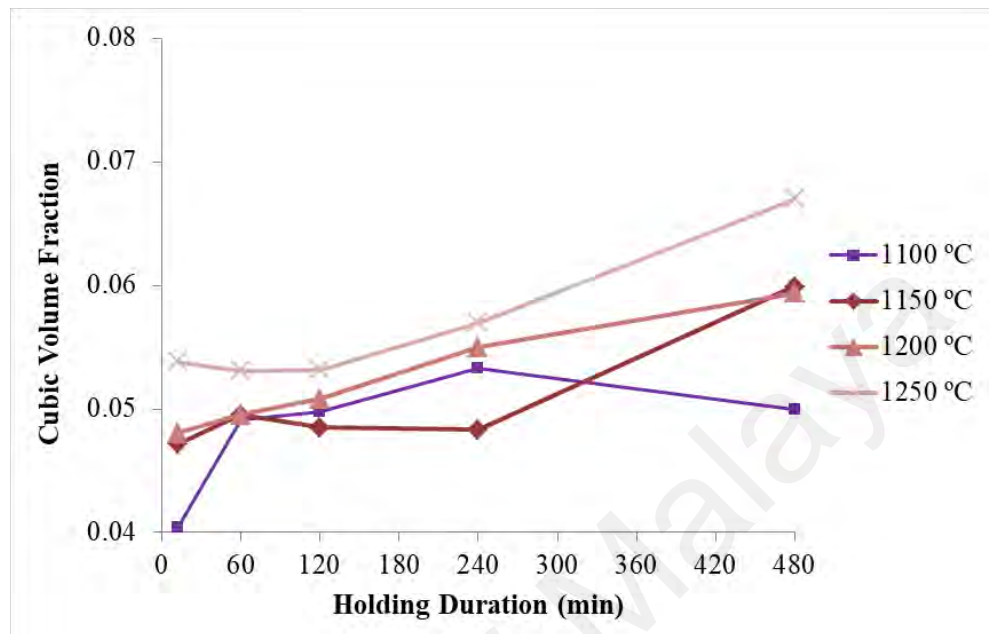


Figure 4.14: Cubic phase content of sintered undoped-YSZ ceramic.

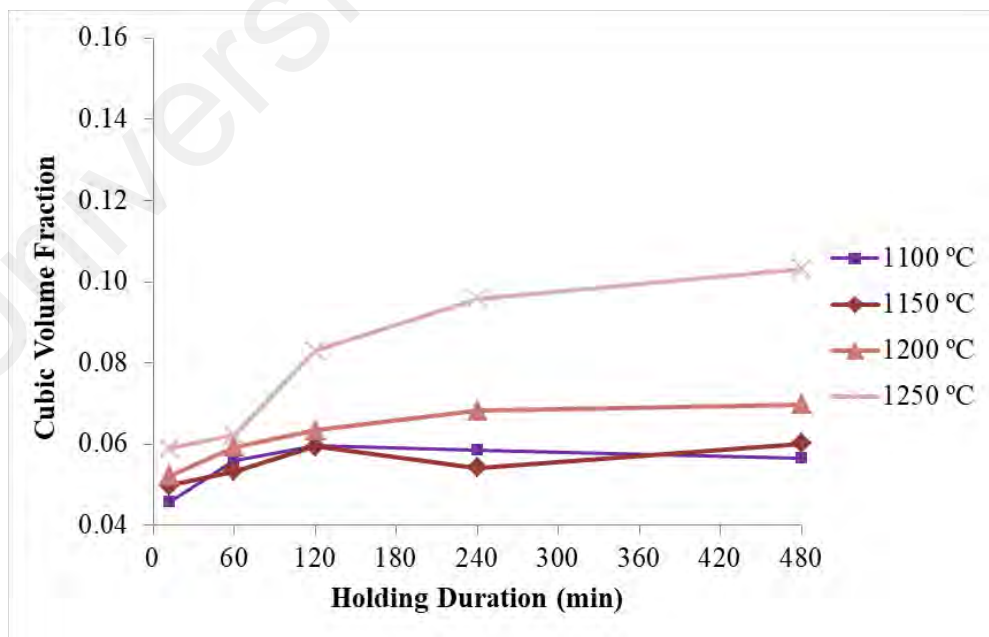


Figure 4.15: Cubic phase content of sintered 0.5 wt.% MnO<sub>2</sub> doped-YSZ ceramic.

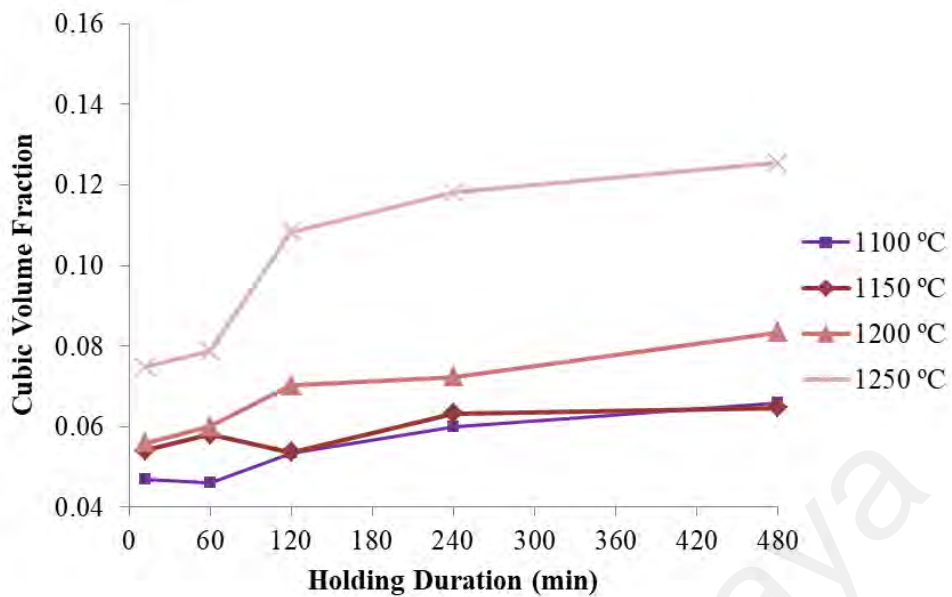


Figure 4.16: Cubic phase content of sintered 1.0 wt.% MnO<sub>2</sub> doped-YSZ ceramic.

#### 4.4.2 Relative Density

The relative density of 3 different samples (0, 0.5 and 1.0 wt.% MnO<sub>2</sub>) sintered at various temperatures and holding times are depicted in Figure 4.17. Overall, the relative density of the samples increased with sintering temperature and holding time. The impact of temperature was more pronounced than that of hold time on densification. Within limits the MnO<sub>2</sub> dopant had a beneficial effect on densification of YSZ ceramics. For example, at a sintering temperature 1200 °C, for the undoped YSZ to achieve >90 % relative density the minimum required holding time was 120 min while the MnO<sub>2</sub> doped (0.5 and 1.0 wt.%) samples attained a similar density after only 12 min. Nevertheless, at lower sintering temperature (1100 °C), the doped samples (1.0 wt.% MnO<sub>2</sub>) took longer time (240 min) to attain the same density. At higher sintering temperatures (1250 °C), the relative density of all YSZ ceramics investigated except undoped YSZ remained constant at ~97 % regardless of holding time. The undoped YSZ ceramic showed a slight improvement (93 – 97 %) when the holding times were extend beyond 12 min.

The effect of MnO<sub>2</sub> dopant in promoting high densification of YSZ ceramics during low temperature sintering is in general agreement with other researchers (Ramesh et al., 2011; Ramesh et al., 2013; Sakka et al., 2004) who used manganese oxide as sintering additive. Zhou et al. (2011) postulated the diffusion activation energy was reduced as the result of Mn<sup>4+</sup> substitution in the crystal structure of zirconia. The results also indicated that larger amounts of MnO<sub>2</sub> dopant (1.0 wt.%) aid densification of YSZ ceramics at low temperature with longer holding time at temperature 1100 - 1150 °C but no effect was observed at high temperatures (>1200 °C). Indeed at higher sintering temperatures MnO<sub>2</sub> resulted in adverse effects on the properties of YSZ ceramic under prolonged sintering. Ramesh et al. (2008) found that 1 wt.% MnO<sub>2</sub> doped Y-TZP caused a decline in the density due to formation of cubic (c) phase when sintered above 1300 °C. In their later work, the formation of cubic phase was prevented in 1 wt.% MnO<sub>2</sub> doped 3Y-TZP samples under similar sintering conditions but with shorter holding times (12 min) (Ramesh et al., 2011).

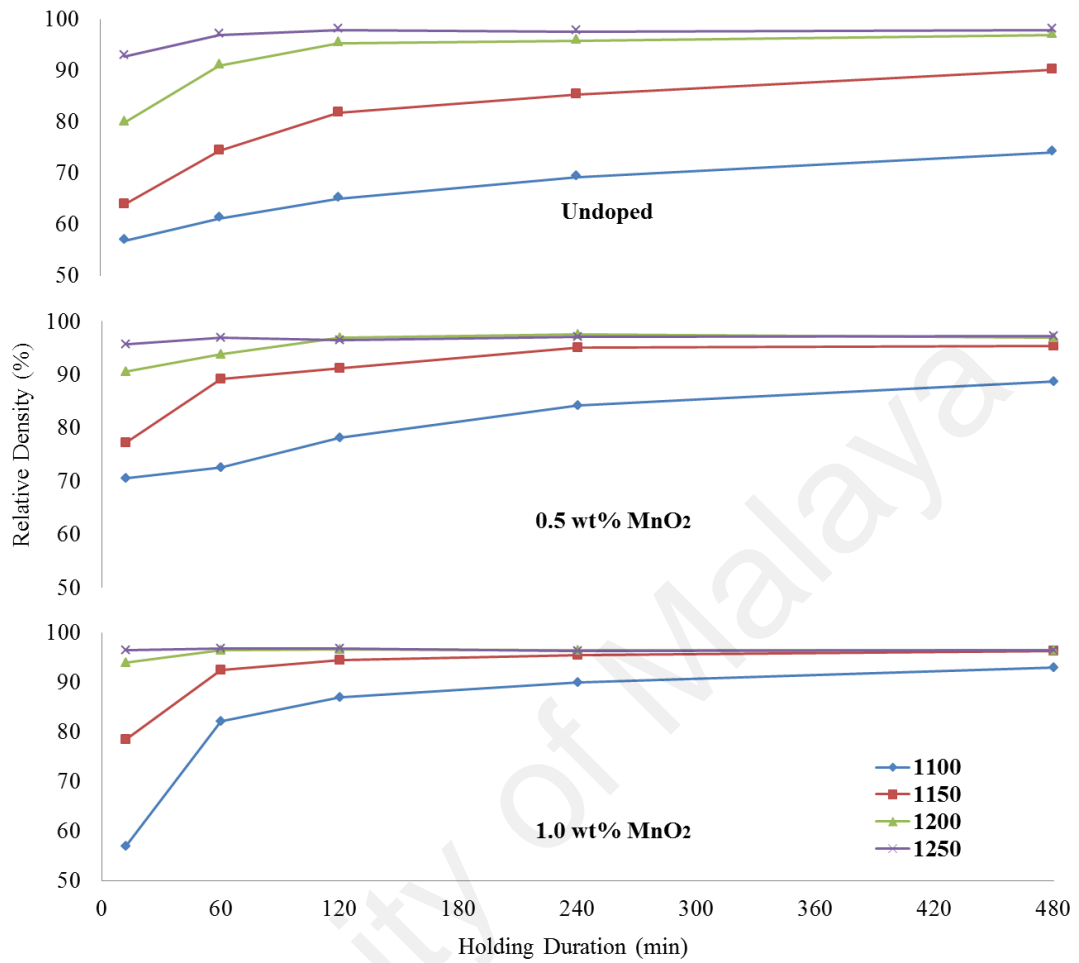


Figure 4.17: Effect of sintering temperature and holding time on the relative density of MnO<sub>2</sub> doped (0, 0.5 & 1.0 wt%) YSZ ceramics.

#### 4.4.3 Fracture Toughness

Figure 4.18 shows the variation of the fracture toughness of the MnO<sub>2</sub> (0, 0.5 and 1.0 wt.%) doped YSZ ceramics with increasing sintering holding times and temperatures. At higher sintering temperatures (1200 and 1250 °C) the fracture toughness, ( $K_{Ic}$ ) of the undoped and 0.5 wt.% MnO<sub>2</sub> doped YSZ ceramics did not vary significantly (4.9 to 5.6 MPam<sup>1/2</sup>) with holding time. The  $K_{Ic}$  of all YSZ sintered at lower temperatures (1100 and 1150 °C) was increased (1.6 to 5.2 MPam<sup>1/2</sup>) with the

increasing holding time. In order to achieve  $K_{Ic} > 5 \text{ MPam}^{1/2}$  at sintering temperature 1150 °C, the holding time for undoped YSZ was 480 min while the holding time for  $\text{MnO}_2$  (0.5 and 1.0 wt.%) doped YSZ was only 60 min. Longer holding times (480 and 240 min) were required for  $\text{MnO}_2$  (0.5 and 1.0 wt.%) doped YSZ ceramics sintered at 1100 °C to obtain  $K_{Ic} > 5 \text{ MPam}^{1/2}$ . At sintering temperatures between 1200 to 1250 °C, all the YSZ samples (undoped and doped) exhibited a constant toughness regardless of increasing the holding time. This behavior has been attributed to the more homogeneous distribution of stabilizer within the  $\text{ZrO}_2$  grains. The consequence of which is that the tetragonal grains are more stable with less transformability (Zhou et al., 2011). It can therefore be concluded that the stability of tetragonal grains in YSZ ceramics was not affected by the addition of  $\text{MnO}_2$  up to 1 wt.% sintered at the temperature profile employed. In contrast, other researchers have shown that tetragonality of the YSZ ceramics was disrupted by high content of  $\text{MnO}_2$  (> 0.5 wt.%) at temperatures > 1450 °C when spontaneous t to m phase transformation occurred upon cooling to room temperature (Ramesh et al., 2008).

Figure 4.19 shows the relationship between the fracture toughness of the YSZ ceramics as a function of grain size. The results show that the grain size of all the samples was relatively consistent and the fracture toughness of the YSZ ceramics was independent of grain size. At lower sintering temperatures, the low toughness of the ceramic was increased by longer sintering time and further enhanced by doping with  $\text{MnO}_2$ . However, sintering temperature becomes dominant above 1200 °C and the holding period and level of dopant have zero effect on further enhancement of toughness of the YSZ ceramics.

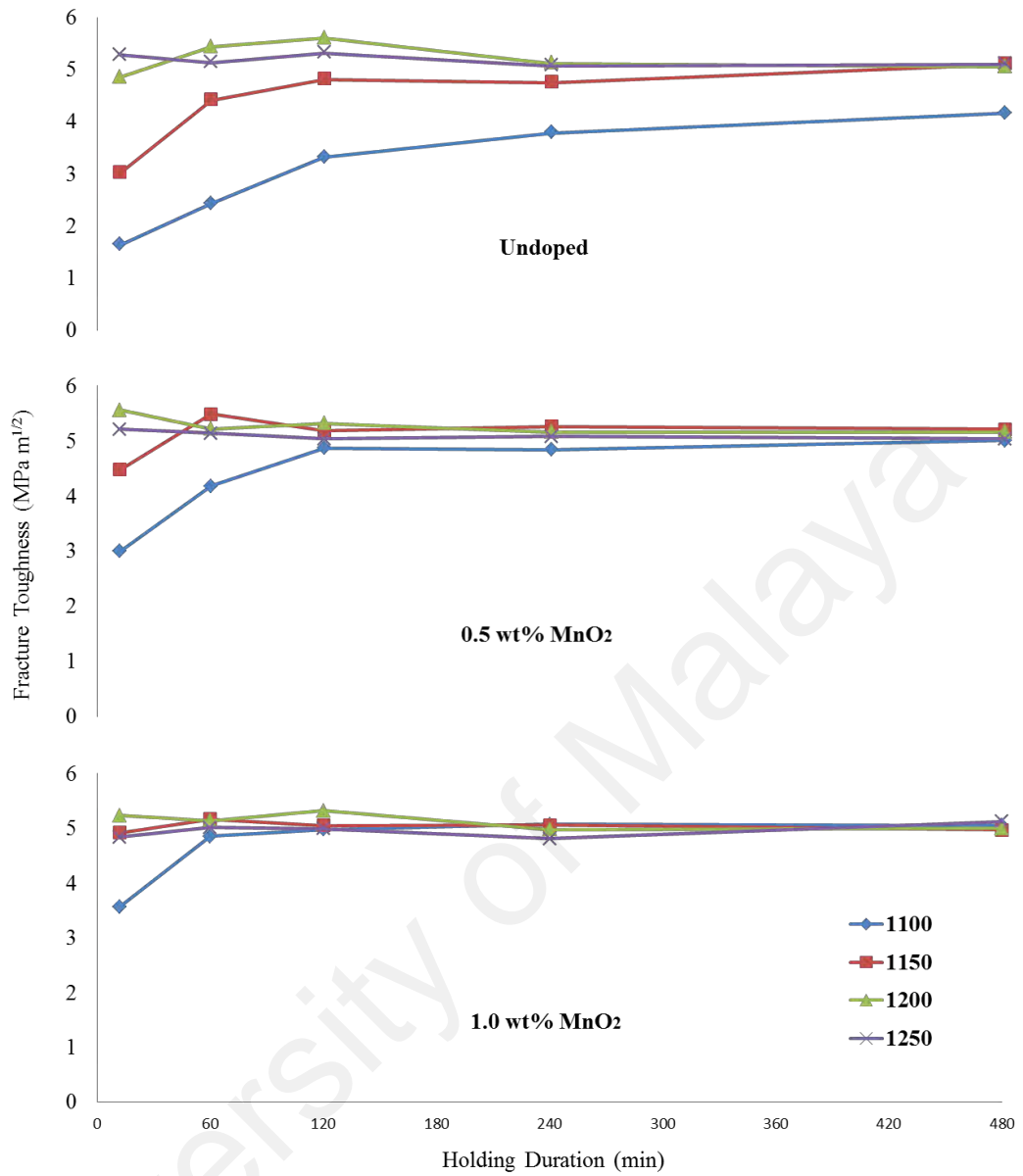


Figure 4.18: Effect of sintering temperature and holding time on fracture toughness of MnO<sub>2</sub> (0, 0.5 & 1.0 wt%) doped 3Y-TZP.



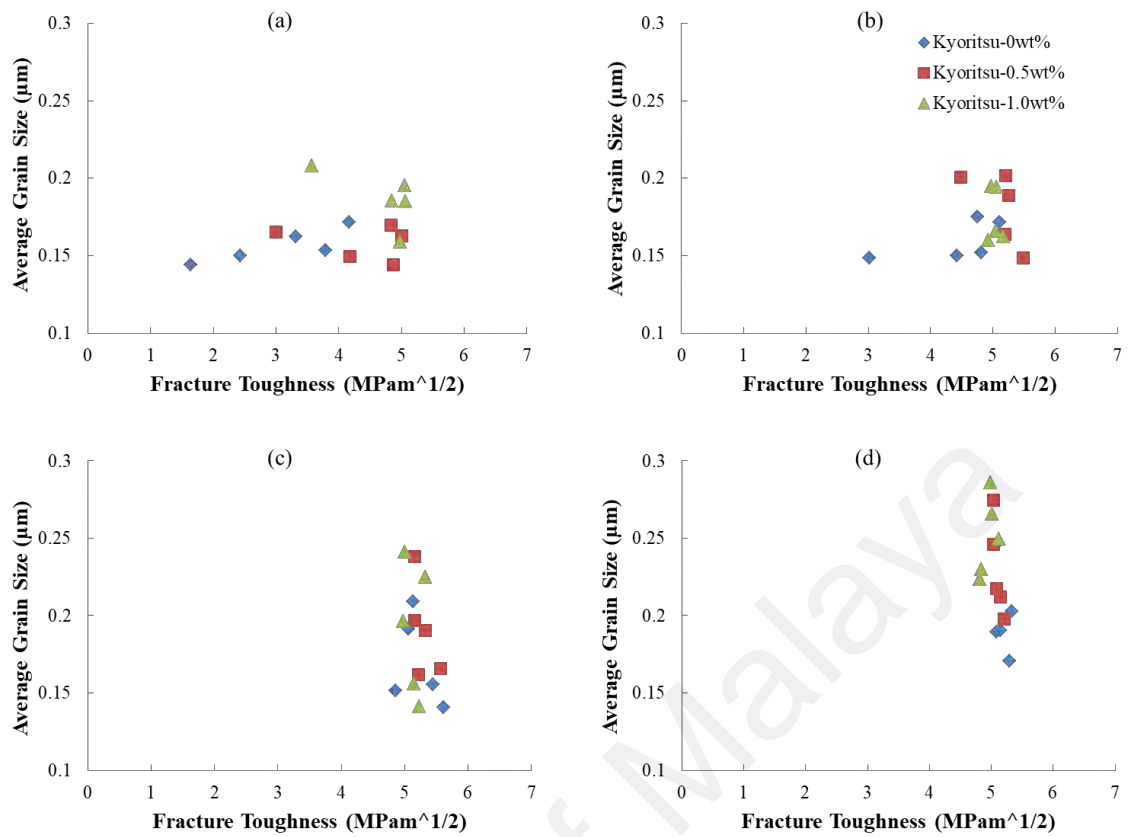


Figure 4.19: The influence of grain size on the fracture toughness of YSZ ceramics for various sintering temperatures (a) 1100 °C, (b) 1150 °C, (c) 1200 °C & (d) 1250 °C.

#### 4.4.4 Vickers Hardness

The Vickers hardness variation of YSZ ceramics (0, 0.5 and 1.0 wt.% MnO<sub>2</sub>) with sintering temperature and holding time (Figure 4.20). In the present work, hardness was improved from 6 to 12 GPa for both undoped YSZ ceramics sintered at temperatures of 1200 °C and 1250 °C with holding times of 480 and 60 min respectively. The effect of MnO<sub>2</sub> was evident at shorter holding times especially for samples doped with 1.0 wt% which required only 60 and 1 min for temperatures 1200 °C and 1250 °C respectively to obtain hardness >14 GPa. All YSZ sintered at low temperatures (1100 and 1150 °C) did not achieve hardness values above 14 GPa even with longer holding time coupled with addition of MnO<sub>2</sub>. Hardness values above 12 GPa were successfully achieved for

1.0 wt% MnO<sub>2</sub> doped YSZ sintered at 1100 °C with 8 hrs holding time, while 0.5 wt% MnO<sub>2</sub> doped samples sintered at 1150 °C but shorter holding time 4 hrs.

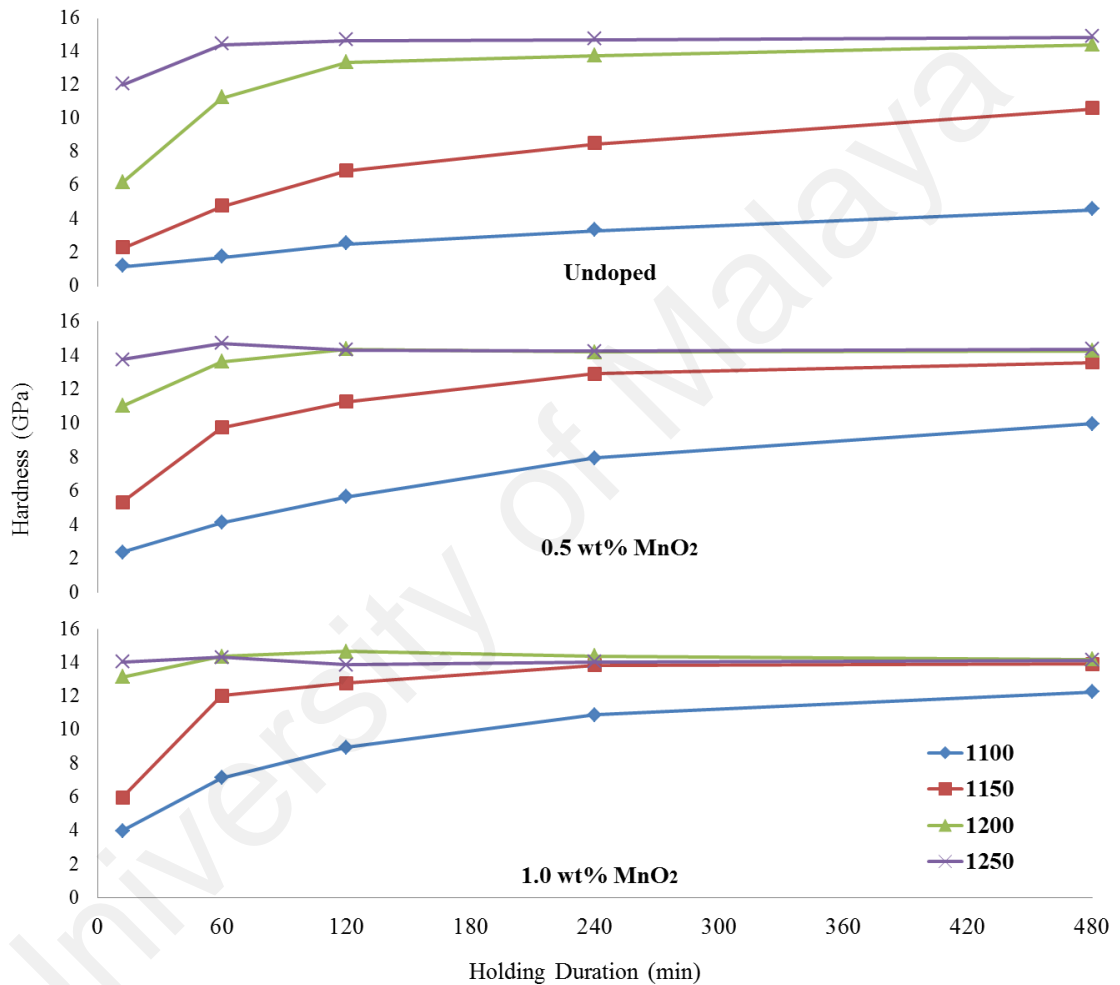


Figure 4.20: Effect of sintering temperature and holding time on the Vickers hardness of MnO<sub>2</sub> doped (0, 0.5 & 1.0 wt%) YSZ ceramics.

The hardness of the ceramic for structural application is correlated with the densification of the sintered body as depicted in Figure 4.21. Based on Fig. 4.17 and 4.20, hardness of the YSZ ceramics at sintering temperatures in the range of 1100 -

1150 °C exhibited low hardness mainly due to the existence of pores. Pores are inevitable for ceramic bodies with low density or those which are not fully consolidated.

MnO<sub>2</sub> doped YSZ ceramics has slightly lower hardness as compared to the undoped samples with sintering holding time beyond 240 min at temperature 1250 °C. This could be due to the higher amount of cubic phase was formed (8 – 10 %) which lead to reduction of densification and this was confirmed by the result of present work in Section 4.4.1. The formation of cubic grain with relatively lower density as compared to tetragonal grain is possible (Matsui et al., 2009, 2014). However, there was no sign of extra-large grains in the ceramics samples that usually exist at elevated sintering temperature (Inokoshi et al., 2014; Ruiz & Readey, 1996).

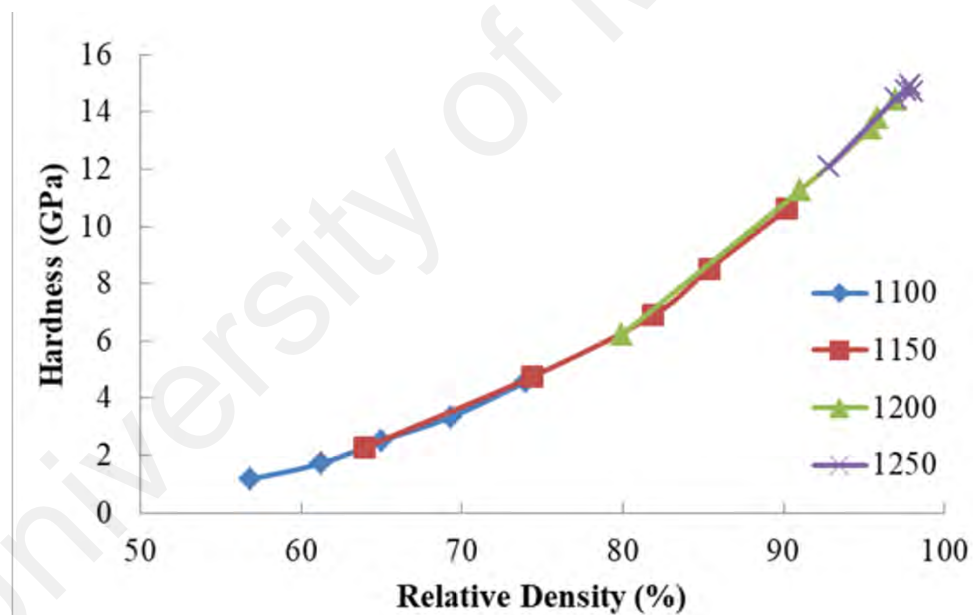


Figure 4.21: Changes of Vickers hardness and density in undoped YSZ for various sintering temperatures (1100, 1150, 1200 and 1250°C).

#### 4.4.5 Microstructure Evolution

FESEM micrographs of the polished surface of YSZ samples after thermal etching are shown in Figure 4.22, 4.23 & 4.24. Uniform rounded fine grain microstructures were observed for all samples. The average grain size ranged from 0.14 to 0.28  $\mu\text{m}$  (Figure 4.24). The average grain size fluctuated 0.15 – 0.20  $\mu\text{m}$  for samples sintered at 1100 - 1150  $^{\circ}\text{C}$ . However, for YSZ ceramics sintered at 1200 - 1250  $^{\circ}\text{C}$ , prominent grain growth was evident (0.20 – 0.28  $\mu\text{m}$ ). The long sintering time was promoting grain growth in both the doped and undoped samples. However, in the doped samples significantly higher growth rate were observed especially in samples doped with 1.0 wt%  $\text{MnO}_2$ . From the result, samples doped with  $\text{MnO}_2$  had a larger grain size as compared to the undoped samples especially at higher sintering temperatures. In the present, the  $\text{MnO}_2$  doped YSZ ceramics showed slight grain growth rate ( $\sim 15$  to 35 %) as compared to the sintering temperature and holding time but not to the extent of abnormal grain growth as there was no sight of grain coarsening ( $> 100$  %).

To minimize the excessive grain growth in YSZ ceramic during high sintering temperature, a relatively low temperature (1100, 1150, 1200 and 1250 $^{\circ}\text{C}$ ) was selected. Various holding times (12, 60, 120, 240 and 480 min) and  $\text{MnO}_2$  doping were used to understand the grain growth rates. A low sintering temperature couple with elongated holding time leads to an increase in densification without significant grain growth in the undoped YSZ samples as illustrated in Figure 4.26. However, this is not the case for the  $\text{MnO}_2$  doped YSZ ceramics where higher densification was achieved at shorter sintering duration (Figure 4.27 & 4.28). Grain enlargement occurred at longer sintering times and higher sintering temperatures were employed with the latter parameter showed greater impact on grain growth.

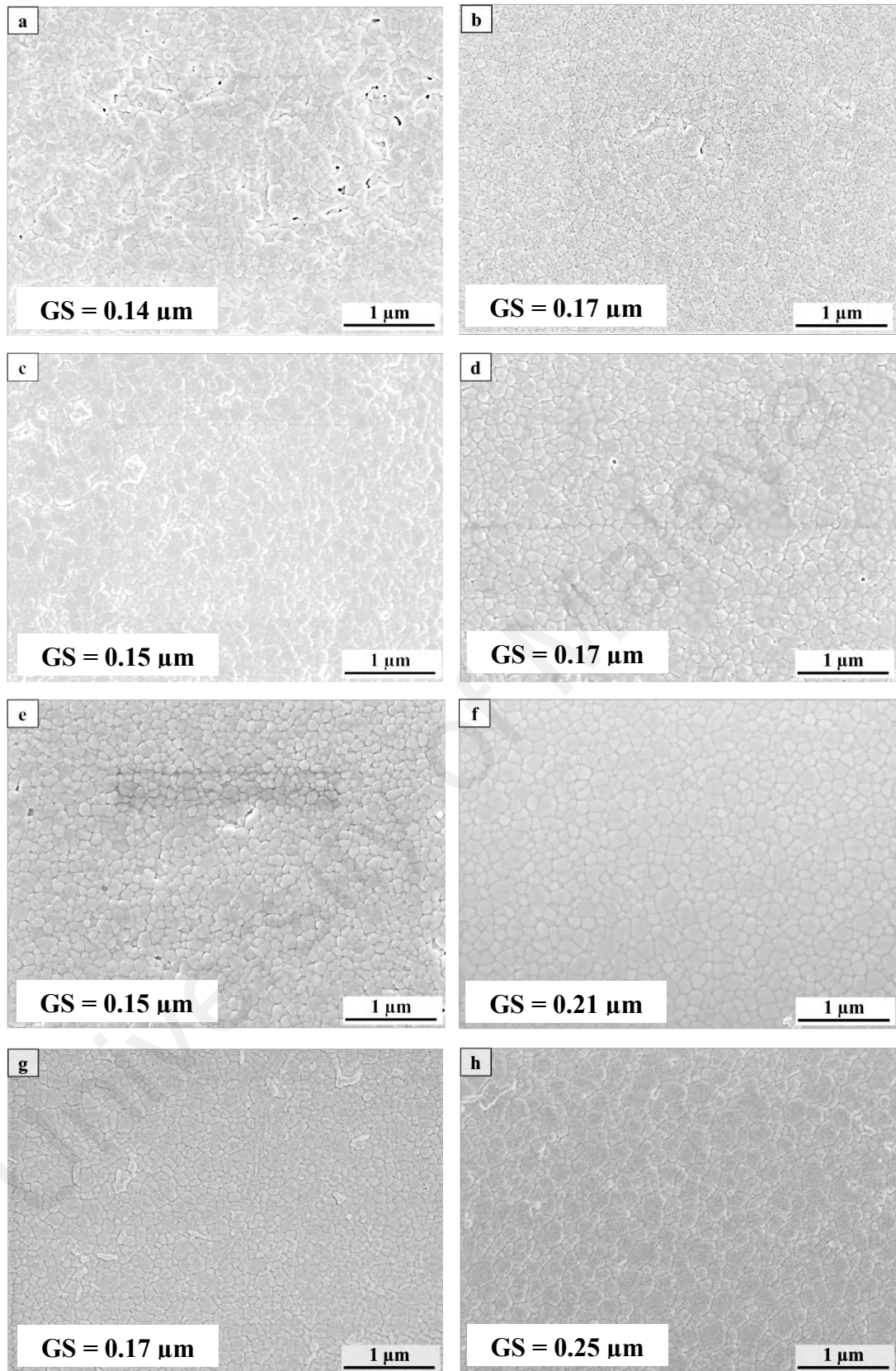


Figure 4.22: Microstructure evolution of undoped YSZ ceramics sintered at 1100°C: (a) 12 min, (b) 480 min, 1150°C: (c) 12 min, (d) 480 min, 1200°C: (e) 12 min, (f) 480 min & 1250°C: (g) 12 min, (h) 480 min. (GS) Indicate grain size.

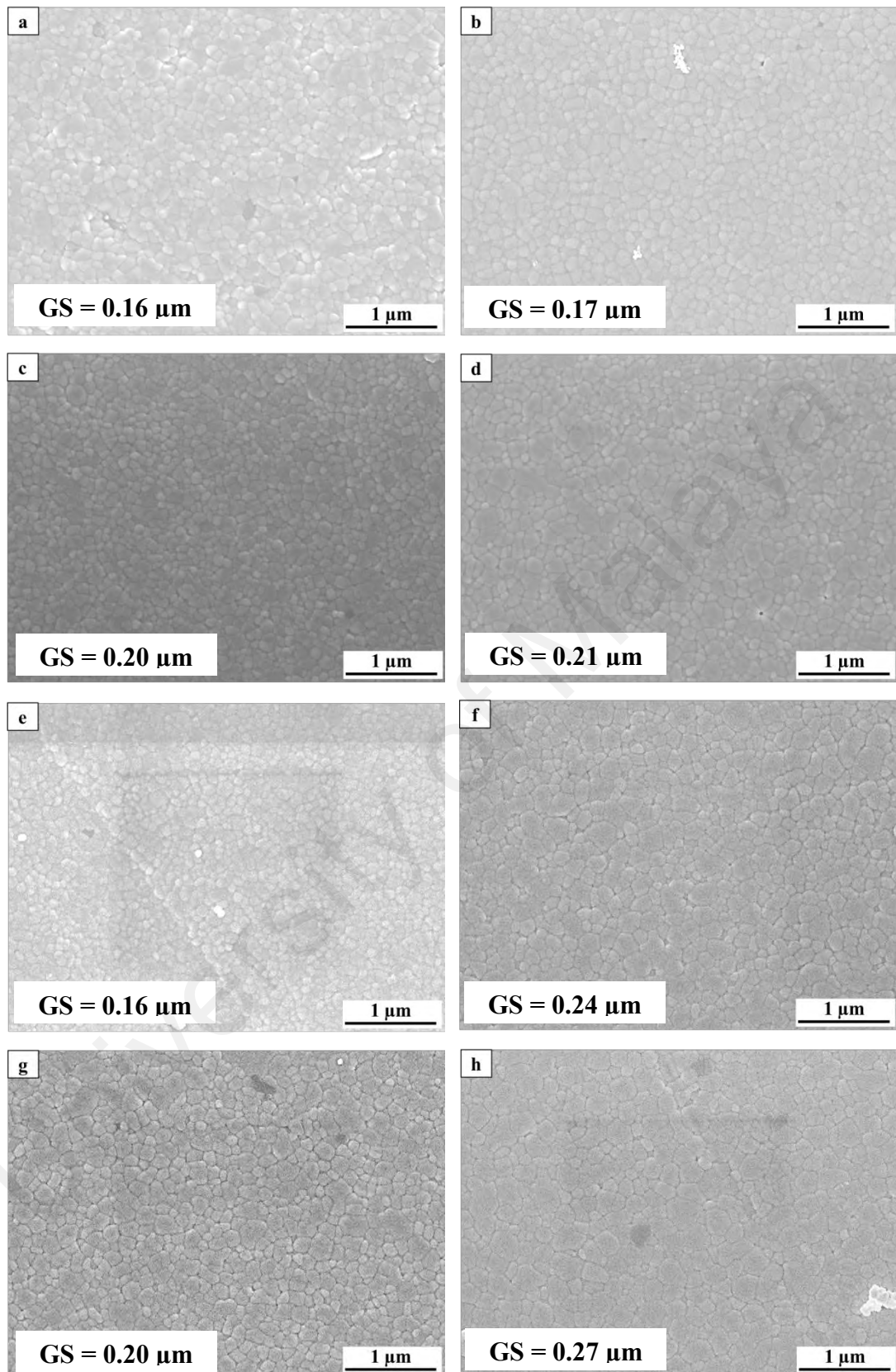


Figure 4.23: Microstructure evolution of 0.5 wt% MnO<sub>2</sub>-doped YSZ ceramics sintered at 1100°C: (a) 12 min, (b) 480 min, 1150°C: (c) 12 min, (d) 480 min, 1200°C: (e) 12 min, (f) 480 min & 1250°C: (g) 12 min, (h) 480 min. (GS) Indicate grain size.

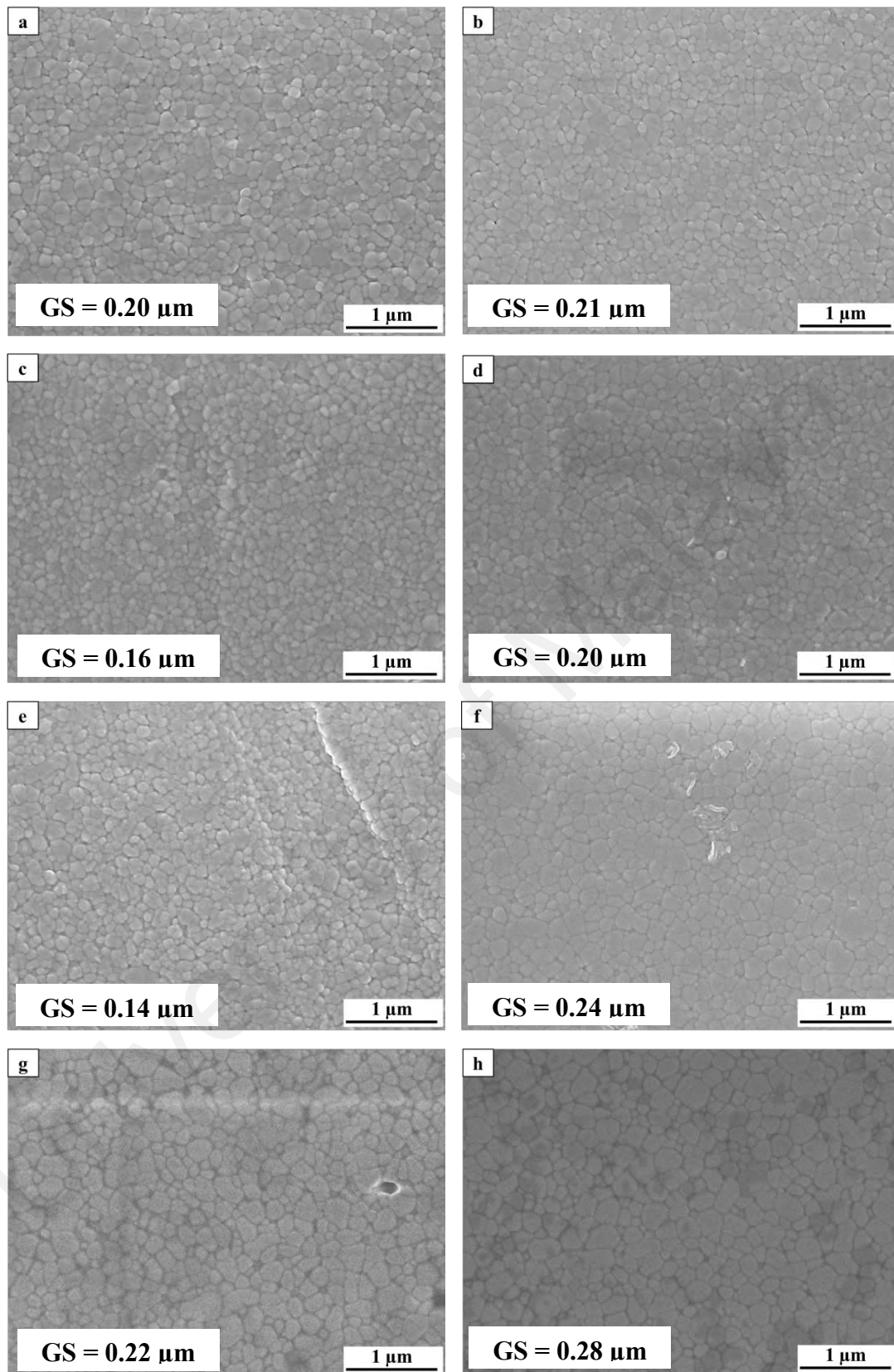


Figure 4.24: Microstructure evolution of 1.0 wt% MnO<sub>2</sub>-doped YSZ ceramics sintered at 1100°C: (a) 12 min, (b) 480 min, 1150°C: (c) 12 min, (d) 480 min, 1200°C: (e) 12 min, (f) 480 min & 1250°C: (g) 12 min, (h) 480 min. (GS) Indicate grain size.

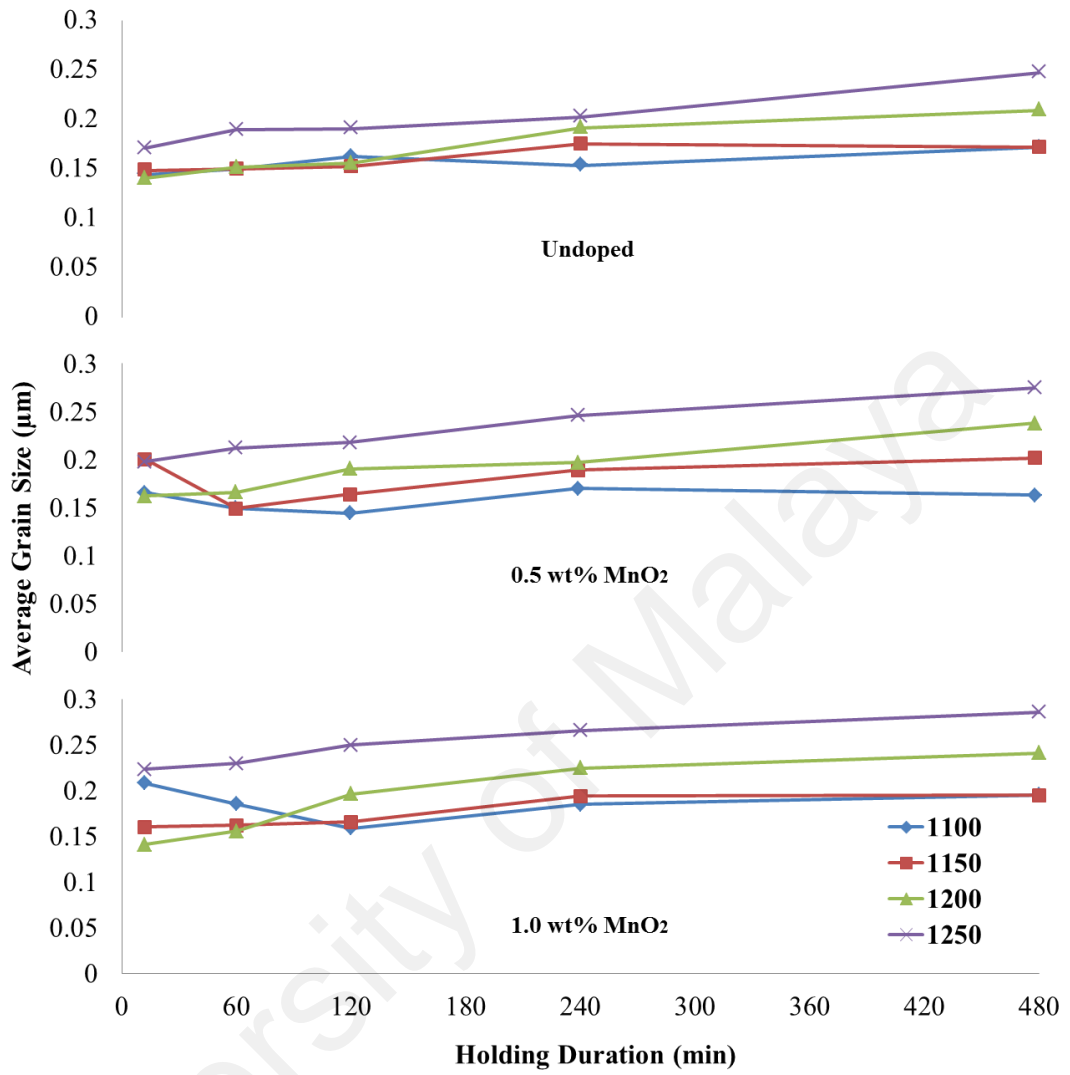


Figure 4.25: Effect of sintering temperature and holding time on the average grain size of the MnO<sub>2</sub> doped (0, 0.5 & 1.0 wt%) YSZ ceramics.



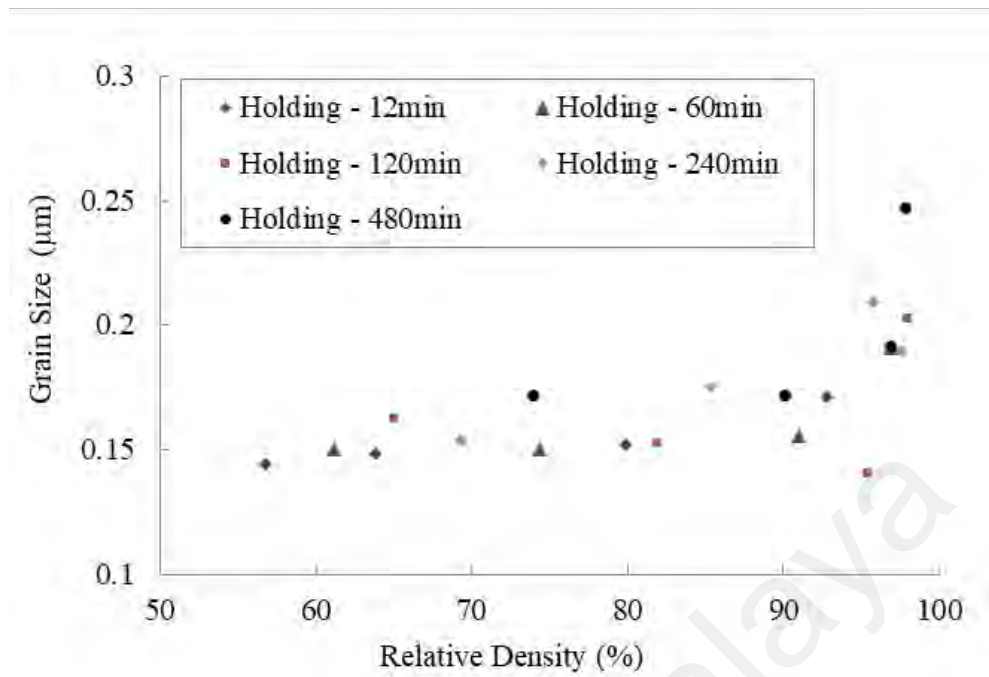


Figure 4.26: Changes of grain size and density in undoped YSZ for various sintering temperatures (1100, 1150, 1200, 1250°C).

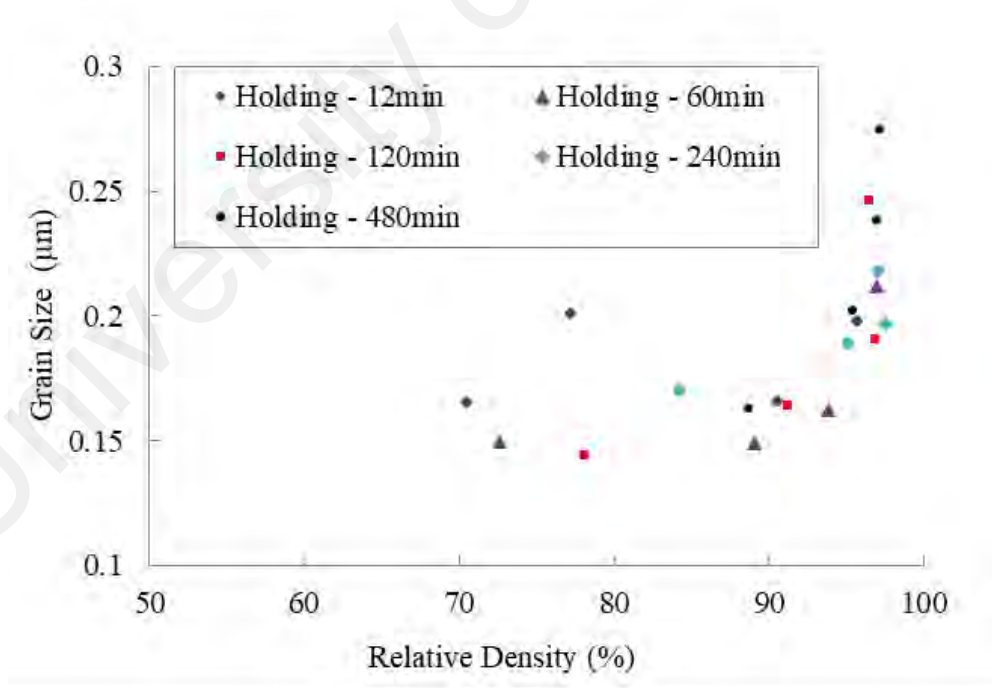


Figure 4.27: Changes of grain size and density in 0.5wt.% MnO doped YSZ for various sintering temperatures (1100, 1150, 1200, 1250°C).

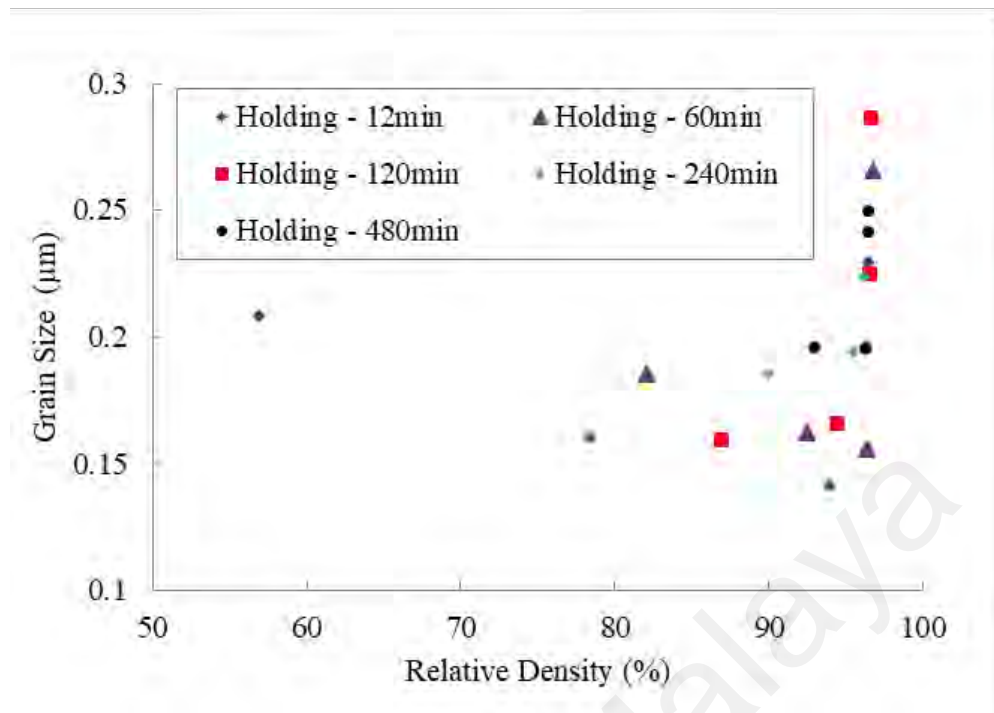


Figure 4.28: Changes of grain size and density in 1.0wt.% MnO doped YSZ for various sintering temperatures (1100, 1150, 1200, 1250°C).

#### 4.5 Hydrothermal Behaviour

In this chapter, the influence of various sintering temperatures, holding times and MnO<sub>2</sub> dopant content on the ageing resistance of YSZ ceramics was studied. The stability of tetragonal phase of the ceramics was determined by measuring the monoclinic phase content in hydrothermal ageing condition at designated intervals. Discussion was done based on the relationship of the sintering temperatures, holding time, grain size and cubic content (distribution of the stabiliser, yttria) on the low temperature degradation LTD induced t to m phase transformation in YSZ ceramics.

#### 4.5.1 Sintering Temperature Effect of Undoped YSZ Ceramic

The effect of superheated steam (180°C and 10 bar pressure) on the tetragonal (t) to monoclinic (m) phase transformation of the YSZ samples as illustrated in Figure 4.29. It was found that all samples sintered below 1250 °C exhibited good resistance to LTD with no traces of monoclinic phase found after ageing up to 120 hr. On the contrary, samples sintered  $\geq 1300^{\circ}\text{C}$  were susceptible to LTD but at different rates. The rate of LTD was highest for samples sintered at 1500 °C, immediately reaching a saturated monoclinic level of about 80% within 3 hr of exposure while samples with sintering temperature of 1400 °C and 1450 °C both showed lower LTD kinetics with 28 to 34% monoclinic phase before achieving monoclinic saturation level at 90% within 12 hr of exposure. Both samples sintered at 1300 °C and 1350 °C showed delayed degradation as 6% and 29% of monoclinic phase were formed after ageing for 48 hr and 12 hrs respectively where the latter reached saturation level after 48 hr with ~85% (m) phase. The YSZ ceramic sintered at 1200 and 1250 °C conversely did not experience the t to m phase transformation even after hydrothermal testing for 120 hr.

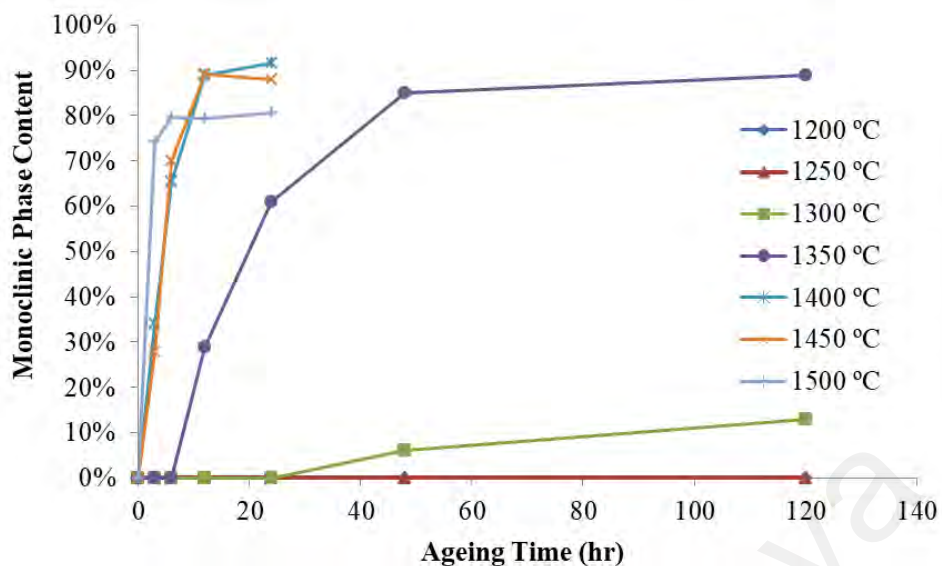


Figure 4.29: Low temperature degradation (LTD) on the monoclinic phase formation in YSZ ceramics when exposed to 120 hr superheated steam at various sintering temperatures.

The current work has shown that samples with an average grain size of about 0.7  $\mu\text{m}$  and sintered at 1500  $^{\circ}\text{C}$  were most sensitive to LTD. In contrast, YSZ ceramics having grain sizes of 0.14 to 0.21  $\mu\text{m}$  did not experience LTD as shown in Figure 4.29. However, samples with grains larger than 0.21  $\mu\text{m}$  showed considerable phase transformations. These observations indicate that average grain size of the order of 0.25  $\mu\text{m}$  was the critical grain size below which the YSZ ceramic is not susceptible to hydrothermal ageing. This critical grain size observation has also been reported for other YSZ ceramics when exposed to hydrothermal ageing tests (Hallmann, Ulmer, et al., 2012; Kosmač & Kocjan, 2012; Kwa et al., 2015; Lawson, 1995; Ramesh et al., 2011; Ramesh et al., 1999; Singh et al., 1996).

It is well documented that ageing resistance relates closely to grain morphology of the YSZ ceramics and is attributable to residual stresses originated from the thermal

expansion anisotropy (Lawson, 1995). According to Schmauder and Schubert (1986), the stresses originated from thermal expansion anisotropy were lower in the smaller grains compared to the larger grains, these larger stresses lead to less stable grains. In addition, the grain shape for spherical grains or those with rounded edges have less stresses compared to the faceted grains with flat surfaces.

The present work reveals that the saturation monoclinic volume fraction of YSZ ceramics sintered at 1400°C and 1450°C reached about 90% after 12 hr of hydrothermal ageing and the remaining 10% is believed to be tetragonal and/or cubic phases (Inokoshi et al., 2014). However, samples sintered at 1500°C have achieved saturated monoclinic content of about 80% after exposure for 3 hr in superheated steam. It is envisaged that the cubic grains in this sample could act as a getter to draw out yttria stabiliser from the adjacent stable tetragonal grains, resulting in an enrichment of the yttria at grain boundary regions of the cubic grains. As a result, the tetragonal grains that suffered from yttria depletion could become unstable and prone to hydrothermal ageing (Chevalier et al., 2004; Scott, 1975).

Matsui et al. attributed the formation of the cubic grains in YSZ ceramic to the redistribution of stabilizer during sintering process. They noticed a homogeneous distribution of yttria in the grains of the YSZ ceramics sintered at 1300 °C but higher amount of yttria was found within the larger cubic grains of ceramics sample sintered at 1500 °C. The cubic phase region were formed from grain boundaries and triple junctions where the yttria ions segregated (Matsui et al., 2003b; Matsui et al., 2008; Matsui et al., 2009). Samples with higher cubic content were more susceptible to LTD as the formation of cubic phase will drain the yttria content in the tetragonal grains adjacent to the cubic grain. This drain in yttria content can occur to an extent that causes YSZ ceramic to be less resistant to LTD (Chevalier et al., 2004).

Matsui et al. reported the tetragonal (t) to cubic (c) phase transformation during densification was due to the grain boundary segregation of  $Y^{3+}$  ions and termed the phenomena as the grain boundary segregation-induced phase transformation (GBSIPT). Sintering temperature above 1300 °C will trigger GBSIPT where  $Y^{3+}$  ions stabilizer would be drained from the core of tetragonal grain to the outer grain adjacent to the grain boundary leaving behind the unstable tetragonal grains that are vulnerable to LTD as the stabilizer fall below 3 mol% (Matsui et al., 2014). Therefore, sintering at a higher temperature leads to uneven distribution of the yttrium-stabilizing ions that cause cubic phase formation and is not desirable in YSZ ceramics.

The sintering temperature is found to affect the mechanical properties (Figure 4.3, 4.4, 4.6 and 4.8) and hydrothermal degradation (Figure 4.28) of the YSZ ceramic samples. The tetragonal phase stability decreased tremendously as sintering temperature increased. This can be attributed to an increase the size of grains, higher content of cubic phase and a decline in stabilizer content in the remnant tetragonal grains. Enhancing LTD resistance of YSZ ceramic is possible by lowering the sintering temperature but at the expense of fracture toughness. This was confirmed in Figure 4.9 which depicted that the fracture toughness of the YSZ ceramics was reduced with decreasing sintering temperature (<1350 °C) and a smaller grain size which is in good agreement with the observation made by many researcher (Bravo-Leon et al., 2002; Ruiz & Readey, 1996; Stawarczyk et al., 2013). Furthermore, low temperature sintering (<1300 °C) of YSZ ceramics resulted in formation of residual porosity which results in low density that compromises hardness. Table 4:1 shows that 1400 °C is the optimum sintering temperature for YSZ ceramics based on density and hardness but the ceramic samples suffered severe LTD with 93 % monoclinic phase after 48 hr of ageing.

Many works reported that improvement of ageing resistance while preserving the mechanical properties of the zirconia was made possible through low temperature sintering with the use sintering additives (Mecartney, 1987; Ramesh et al., 2013; Sakka et al., 2004; Wu et al., 2013).

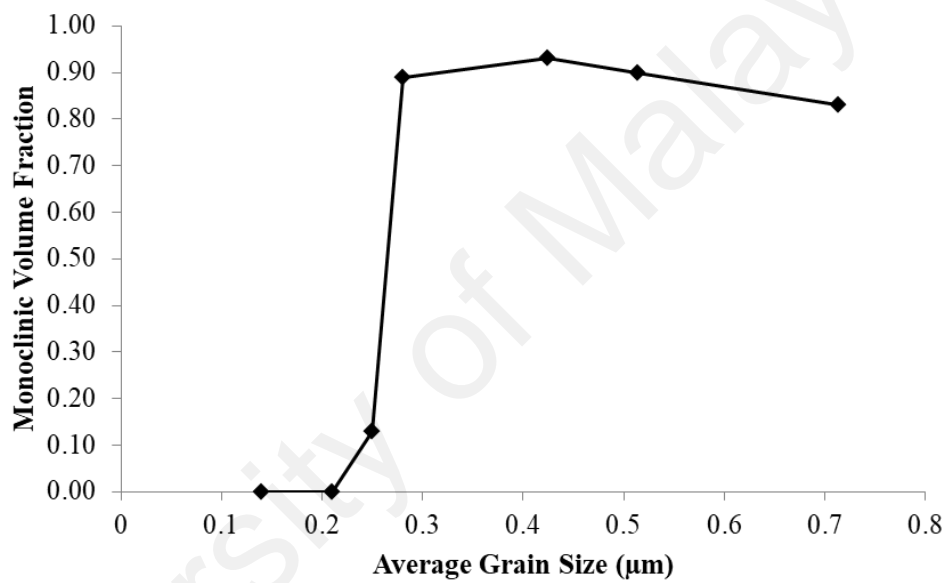


Figure 4.30: Grain size dependence on the LTD induced monoclinic phase development in YSZ ceramics after exposure for 120 h in superheated steam.

Table 4.1: The properties of YSZ samples sintered at various temperatures.

Sintering Temperature (°C)	Relative Density (%)	Young's Modulus (GPa)	Vickers Hardness (GPa)	Fracture Toughness (MPam <sup>1/2</sup> )	Average Grain Size (µm)	Cubic Content (%)	Monoclinic Content (%)
						Sintered Sample	After ageing for 48 h
1200	93.10	178.32	12.25	4.68	0.14	3.40%	0.00
1250	97.84	207.25	13.96	4.71	0.21	7.35%	0.00
1300	98.41	203.43	14.14	4.79	0.25	7.61%	6.00
1350	98.66	207.61	14.38	5.07	0.280	10.58%	85.00
1400	98.79	211.12	13.89	5.01	0.424	12.41%	93.00
1450	98.77	205.90	13.94	4.91	0.514	13.04%	90.00
1500	98.71	208.09	13.28	5.03	0.714	15.36%	83.00



## 4.5.2 Hydrothermal Ageing Behaviour of Undoped and MnO<sub>2</sub>-doped YSZ

### Ceramic Isothermal Sintering at Low Temperature

As illustrated in Figures 4.31 and 4.32, undoped YSZ ceramics sintered at low temperatures (1100 – 1250 °C) with various holding times (12 – 480 min) exhibited good LTD resistance without any monoclinic phase formation even after 300 hrs of hydrothermal ageing. However, monoclinic phase began to form in MnO<sub>2</sub> doped YSZ ceramics at a sintering temperature of 1250 °C with holding time more than 60 min after 6 hr of hydrothermal. While the 1.0 wt.% MnO<sub>2</sub> doped sample sintered at 1200 °C for 480 min showed delayed ageing, after 12 hr ~ 0.8 % of monoclinic phase was formed after 300 hr of ageing. The ageing resistance of MnO<sub>2</sub> doped samples was affected by the sintering holding time as well as the content of dopant. The LTD resistance of YSZ decreased with the increase of sintering holding time and also the amount of dopant in YSZ. Generally, MnO<sub>2</sub> doped YSZ ceramics sintered at higher sintering temperatures (> 1200 °C) and longer holding time (> 120 min) were susceptible to the hydrothermal ageing environment. The same ceramic sample with a short sintering time (12 min and 60 min) was resistant to ageing.

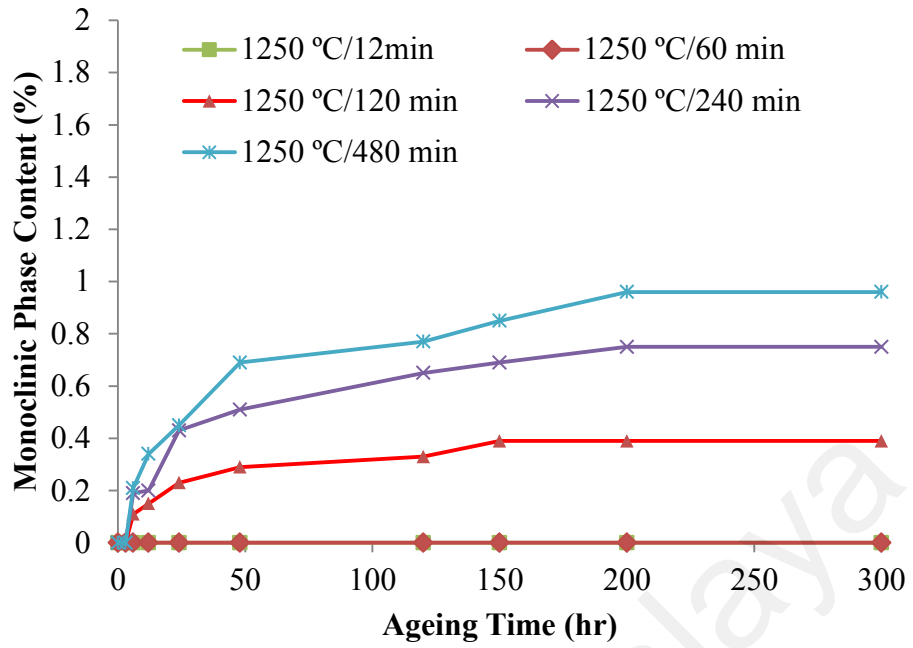


Figure 4.31: Hydrothermal ageing on the monoclinic phase formation in 0.5 wt% MnO<sub>2</sub> doped YSZ ceramics when exposed to superheated steam sintered at 1250 °C.

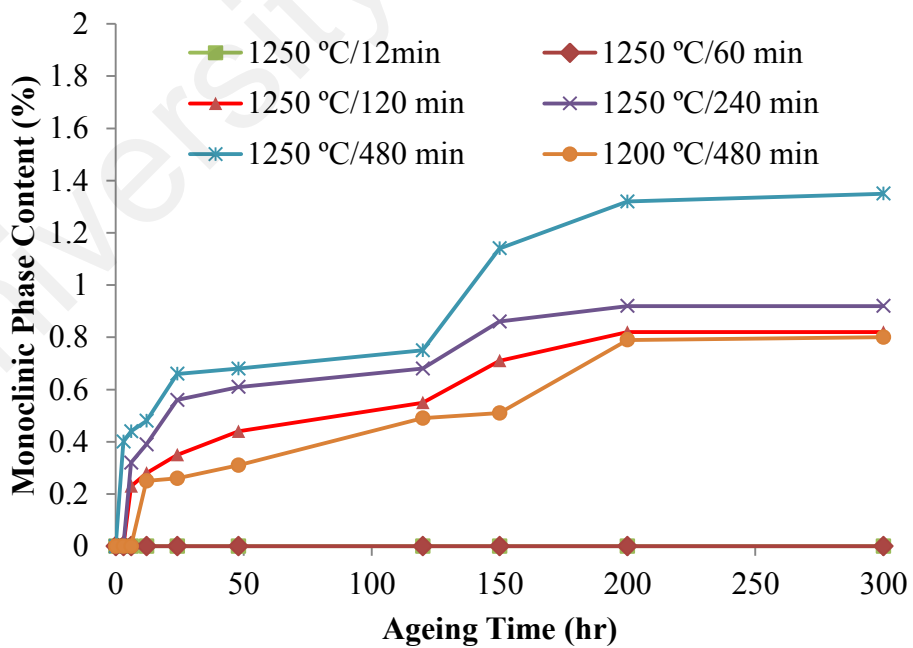


Figure 4.32: Hydrothermal ageing on the monoclinic phase formation in 1.0 wt% MnO<sub>2</sub> doped YSZ ceramics when exposed to superheated steam sintered at 1200 and 1250 °C.

The relationship between grain size and the monoclinic phase content of the YSZ ceramics sintered at temperature 1250 °C can be seen in Figure 4.33. The undoped YSZ ceramics displayed good ageing resistance at hydrothermal degradation environment with average grain sizes (0.17 to 0.25  $\mu\text{m}$ ) below the critical grain size, 0.25  $\mu\text{m}$  which trigger LTD as reported earlier in Section 4.5.1. The monoclinic phase began to form in both 0.5 and 1.0 wt.% of  $\text{MnO}_2$  doped YSZ samples with an average grain size 0.21 and 0.25  $\mu\text{m}$  respectively after 300 hr of hydrothermal ageing. An interesting observation was found on the  $\text{MnO}_2$  doped YSZ ceramics where the LTD occurred at average grain size slightly below the critical grain size of the undoped YSZ ceramic.

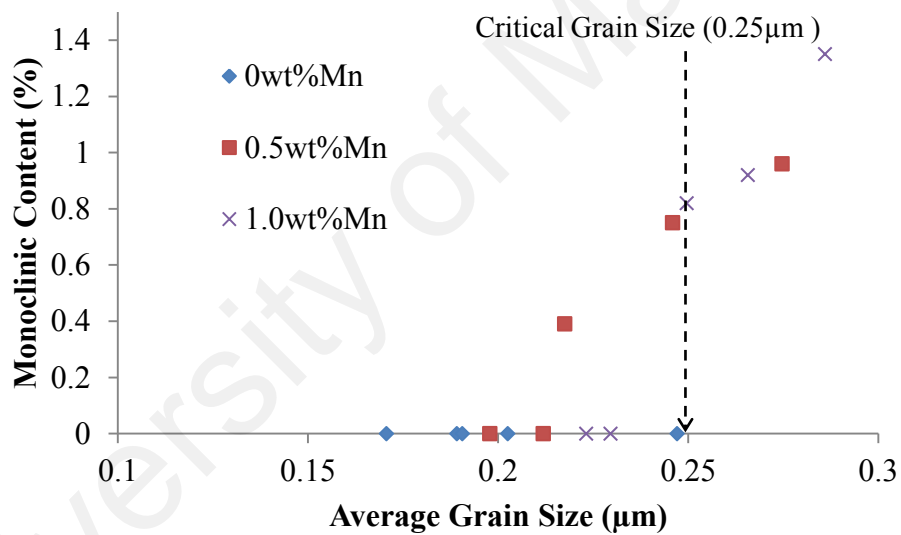


Figure 4.33: Grain size dependence on the LTD induced monoclinic phase development in YSZ ceramics sintered at 1250 °C for various holding time (12, 60, 120, 240 & 480 min) after exposure for 300 hr in superheated steam.

Similar observation made by many researchers on the YSZ ceramics where no phase transformation would occur below the critical grain. This was not the case in the present work. From these observations it can be inferred that the transformability of the

tetragonal grains is not only governed by the grain size factor but also to the redistribution of stabiliser (yttria content) in the tetragonal grains. The presence of  $\text{MnO}_2$  in the YSZ ceramic has contributed to the yttria segregation and redistribution and is further enhanced by the extended sintering holding time ( $> 60$  min). Furthermore, YSZ ceramic with higher dopant content showed greater tetragonal to monoclinic transformation rate with increasing grain size due to the long sintering holding time. While others ceramics were resistant to LTD induced t to m phase transformation attributed to the stable tetragonal grains as result of homogeneous distribution of yttria in the structure of the ceramics. This observation indicates that the transformability of the tetragonal grains is not only governed by grain size but is also dependent on redistribution of yttria in the grains and grain boundaries. This can be estimated from amount of cubic phase formed in the YSZ ceramic as depicted in Figure 4.14, 4.15 & 4.16.

Figure 4.34 shows factors of the cubic volume fraction and grain size of the YSZ ceramic on the (m) phase development. Some of the tetragonal grains on the surface of the ceramic were disrupted as monoclinic phase and began to form in the samples that contained cubic phase of more than 8 %. The monoclinic phase of those samples showed a small increase in cubic phase content but ceramics with less than 8 % cubic phase were resistant to LTD.

It can be noted that cubic grains are formed in the YSZ ceramics when subject to high sintering temperature ( $> 1400$  °C) but also occurred at a low sintering temperature  $\sim 1300$  °C with long holding time. (Matsui et al., 2018) in their recent work observed that the cubic phase region was formed without grain growth in isothermal sintering at 1300 °C.

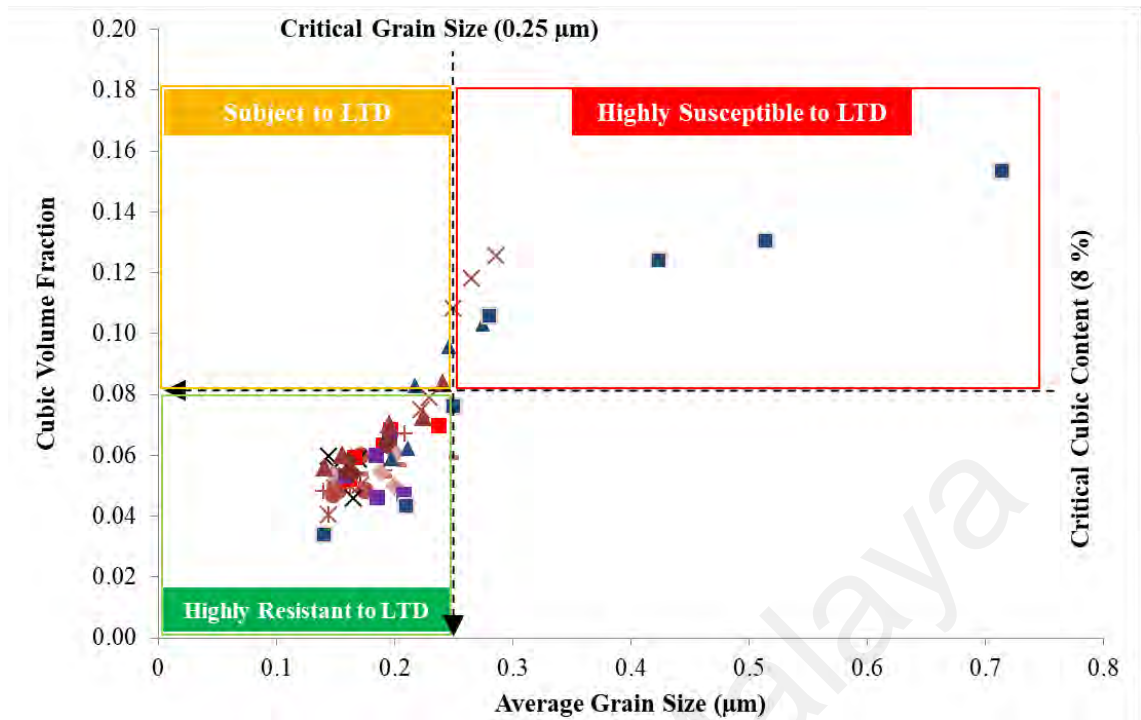


Figure 4.34: The relationship between the cubic phase content and average grain size on the (m) phase development for of the YSZ ceramic.

The EDAX analysis performed at the grain interior of the 1.0 wt%  $\text{MnO}_2$ -doped YSZ ceramic indicated that the Mn content was located mainly at grain boundary regions as illustrated in Figure 4.35 as  $\text{Mn}^{+}$  ion was not detected in the grain.

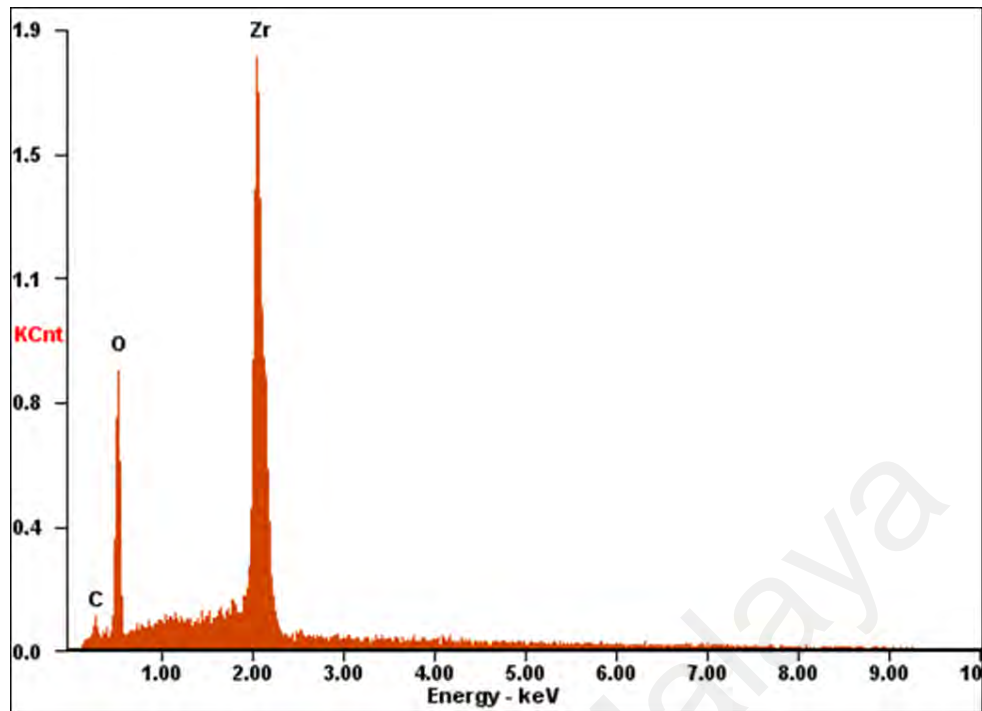


Figure 4.35: EDAX analysis at the grain interior of the 1.0 wt% MnO<sub>2</sub>-doped YSZ ceramic sintered at 1250 °C with holding time, 480 min.

### 4.5.3 Hydrothermal Ageing Mechanism

From the evidences obtained in the present study, the grain size and redistribution of Ytria content of the YSZ ceramic were found to have an effect on the LTD transformation. Hence, according to the literature findings and experimental results attained in the present work, the following LTD mechanism is proposed:

- 1) Microstructure of the YSZ ceramic especially grain size and shape has been shown to affect ageing induced phase transformation. The grain growth due to high temperature sintering resulted in smaller nucleation barrier for transformation owing to residual stresses generated by the thermal expansion anisotropy with the tetragonal grain. As illustrated in Figure 4.30, the experimental results in current work concur with the theory that all YSZ ceramics which have an average grain

sizes of more than 0.25  $\mu\text{m}$  experience LTD induced t to m transformation. The phase transformation rate increases with increasing grain size. Hence, the increasing grain size is expected to reduce the stability of the tetragonal grains during LTD.

- 2) The stability of the tetragonal phase is also governed by the yttria content in the grain interior and grain size. Cubic phase are formed in the grains when sufficient yttria was drawn from the adjacent tetragonal grains and results in tetragonal grains to be unstable during LTD. The quantity of cubic phase formed in the grain is directly influenced by the sintering profile i.e. sintering temperature and sintering holding time as shown in Figures 4.3, 4.14, 4.15 & 4.16. Therefore tetragonal grains of the ceramic became less resistant to LTD when higher volume of cubic phase was formed with increasing sintering temperature beyond 1300  $^{\circ}\text{C}$ . Redistribution and segregation of yttria which triggered the formation of cubic phase in  $\text{MnO}_2$ -doped YSZ ceramic sintered at low temperature sintering (1250  $^{\circ}\text{C}$ ) couples with long sintering time ( $> 60$  min) is shown in Figure 4.34 as small amount of monoclinic was detected in the ceramic with the cubic phase exceeded 8 % threshold.
- 3) Preferential redistribution of stabiliser in the zirconia matrix as well as possible reaction between Mn and  $\text{Y}_2\text{O}_3$  forming an amorphous grain boundary phase could have occurred simultaneously, thus resulting in enhanced LTD of the ceramic. This idea is supported by the experimental results shown in Figure 4.33 where the YSZ ceramics contained  $\text{MnO}_2$  were susceptible to LTD as a greater content of cubic phase was formed in these samples compared with undoped ceramic as illustrated in Figure 4.34. This result could be attributed to the redistribution of  $\text{Y}^+$  ions in the tetragonal grains which are originally homogeneous in the YSZ powder. During sintering, segregation of  $\text{Y}^+$  ions in the

grain begins followed by tetragonal-cubic phase partitioning at sintering temperature 1250 °C. The segregation of  $Y^+$  ions in the grain interior adjacent to the grain boundary and triple junction was enhanced in the presence of  $Mn^+$  ions at the grain boundary causing part of the tetragonal phase in YSZ ceramic to become cubic when sufficient  $Y^+$  ions are gathered. The tetragonal phase with lower  $Y^+$  ions concentration leads to a decrease in stability that will eventually causes LTD in YSZ ceramic. Moreover, the stability of the tetragonal grains further declines when greater concentrations of  $MnO_2$  are added and with longer sintering periods. The depletion of yttria in the grain could have occurred concurrently with the formation of amorphous phase due to the chemical reaction between Mn and  $Y_2O_3$  at the grain boundary. This reaction intensifies as the sintering holding time increases especially beyond 60 min. while more  $Y_2O_3$  is drained from the tetragonal grain for such reaction as more  $MnO_2$  was added to the ceramic.

To improve the LTD resistance of YSZ ceramic, the redistribution of the  $Y^+$  ions and the grain growth during sintering should be suppressed while maintaining the intrinsic mechanical strength of the YSZ ceramic. Densification and mechanical properties of the YSZ ceramics were improved when longer sintering times were used. Further enhancement resulted when doped with  $MnO_2$  (0.5 & 1.0 wt.%) with higher dopant concentrations showing better results (Figures 4.17, 4.18 & 4.20). These benefits diminished as the sintering temperatures were increased beyond 1200 and 1250 °C with holding times longer than 4 and 2 hr respectively. Dopant additions showed better results compared to the undoped YSZ ceramics when sintered at lower temperatures (1100 and 1150 °C) however the mechanical properties were not viable for engineering application especially. Several sintering profiles and dopant strategies for YSZ powder that achieve fully dense (> 95% relative density) ceramics with high ageing resistance



(0% monoclinic phase after 300 hr hydrothermal ageing) and good mechanical properties (Hardness > 14 GPa & fracture toughness > 5 MPam<sup>1/2</sup> ) are proposed in Table 4.2.

University of Malaya

Table 4.2: The properties of YSZ ceramics doped with MnO<sub>2</sub>, sintered at various sintering profiles.

Dopant MnO <sub>2</sub> (wt%)	Sintering		Relative Density (%)	Vickers Hardness (GPa)	Fracture Toughness (MPam <sup>1/2</sup> )	Average Grain Size (μm)	Cubic Content (%)	Monoclinic Content (%)
	Temperature (°C)	Time (min)					Sintered Sample	After Ageing for 120 hr
1.0	1200	12	94.00	13.13	5.23	0.141	5.59	0
1.0	1200	60	96.40	14.35	5.14	0.156	6.01	0
1.0	1200	120	96.60	14.64	5.32	0.196	7.02	0
1.0	1250	12	96.50	14.04	4.84	0.223	7.47	0
1.0	1250	60	96.80	14.29	5.01	0.229	7.87	0
0.5	1200	120	96.60	14.38	5.32	0.190	6.34	0
0.5	1200	240	97.60	14.20	5.16	0.196	6.83	0
0.5	1200	480	97.00	14.27	5.16	0.238	6.99	0
0	1200	480	97.00	14.43	5.06	0.209	6.70	0
0	1250	60	97.00	14.47	5.14	0.229	5.31	0
0	1250	120	97.20	14.40	5.33	0.249	5.32	0
0	1250	240	97.60	14.77	5.08	0.265	5.70	0
0	1250	480	97.90	14.92	5.11	0.286	5.94	0

## CHAPTER 5: CONCLUSION & FURTHER WORK

### 5.1 Conclusions

The densification behavior and properties of YSZ ceramics were investigated. YSZ ceramic sintered at low sintering temperature ( $<1300\text{ }^{\circ}\text{C}$ ) for various holding times (12, 60, 120, 240 & 480 min) with  $\text{MnO}_2$  (0.5 & 1.0 wt.%) sintering additives were prepared. Comparisons were made with the undoped-YSZ ceramic via standard sintering route, phase analysis, bulk density, Vickers hardness, fracture toughness, microstructural and hydrothermal ageing behavior were all examined. The results were analyzed and the overall effects are summarized as follow:

1. The tetragonal phase stability of the all the YSZ ceramics was not affected by the sintering temperature or holding time as no monoclinic phase was found in all the sintered samples. On the other hand, small amount of cubic phase (3 – 15 %) was formed in all the ceramics samples and increased with the sintering temperature. Furthermore, the addition of  $\text{MnO}_2$  was found to promote the formation of cubic phase even though at low sintering temperature  $1250\text{ }^{\circ}\text{C}$  and further increased with longer holding time ( $>60$  min).
2. The relative density and Young's modulus of the YSZ correlated well and increased with sintering temperature before reaching the maximum value at 98.9% and 211 GPa, respectively at  $1400^{\circ}\text{C}$ . The undoped YSZ ceramic required sintering temperature at least  $1200\text{ }^{\circ}\text{C}$  to achieved relative density above 95% and holding time of 240 min but similar density can be achieved by sintering temperature as low as  $1150\text{ }^{\circ}\text{C}$  with sintering period 120 min required by the  $\text{MnO}_2$ -doped (0.5 & 1.0 wt.%) YSZ. However, both 0.5 and 1.0 wt.%  $\text{MnO}_2$  doped YSZ ceramics showed no enhancement in densification at sintering temperature  $1250\text{ }^{\circ}\text{C}$  and holding time longer than 120 min.

3. Sintering with holding time (120 min), the maximum Vickers hardness, 14.4 GPa and fracture toughness,  $5.07 \text{ MPam}^{1/2}$  were obtained for ceramic sintered at 1350 °C. At low sintering temperature, Vickers hardness  $>14 \text{ GPa}$  was achieved with sintering temperature and holding time 1150 °C, 240 min respectively for YSZ ceramics doped with 1.0 wt%  $\text{MnO}_2$  compared to undoped YSZ ceramics that sintered at 1250 °C and 60 min of holding time. Fracture toughness  $\sim 5 \text{ MPam}^{1/2}$  could only achieved for undoped YSZ ceramics when sintered at 1150 °C, 480 min but both doped YSZ recorded shorter holding time of only 60 min at the same temperature. Even lower sintering temperature (1100 °C) was possible to achieve by extending the holding time for the  $\text{MnO}_2$ -doped YSZ .
4. The grain of the YSZ was found increase about 400 % from  $0.14 \mu\text{m}$  to  $0.71 \mu\text{m}$  with increasing sintering temperature from 1250 to 1500 °C. For ceramics sintered at low temperature ( $< 1300 \text{ °C}$ ), less than 100 % grain growth rate was observed on all YSZ ceramics ( $0.14 - 0.28 \mu\text{m}$ ).
5. The microstructure of YSZ ceramics composed of fine equiaxed grains. A few pores were found at the triple junction of the grain boundary of undoped YSZ ceramics sintered below  $1300\text{°C}$  and the pores diminished as the ceramics were enhanced in bulk density by long holding time and dopant. However a bimodal distribution of grains consisting of larger grains in the vicinity of the finer grains became substantial in terms of size and quantity as sintering temperature increased to  $1500\text{°C}$ . The large cubic grains were formed as the result of redistribution of yttria from the core of the tetragonal grains at high temperature. Large faceted grains were also evolved from the fine grains with rounded edge at high sintering temperature.
6. All the undoped YSZ ceramics showed ageing-induced monoclinic phase development after exposure in superheated steam at  $180 \text{ °C}$  and  $1 \text{ MPa}$  pressure

for 120 hr except for samples sintered below 1300 °C. Overall, larger grain size was found promoting the hydrothermal ageing process. It was revealed that samples having grain sizes above 0.25 μm were susceptible to hydrothermal ageing. The amount of monoclinic formed increases with increasing tetragonal grain size as the result of building up or residual stress that destabilize the tetragonal grains. On the other hand, high temperature also promoting inhomogeneous redistribution of stabilizer causing the formation of cubic phase that affect the stability of the surrounding tetragonal grains during hydrothermal degradation.

7. All YSZ ceramics sintered at low temperature (< 1300 °C) were highly resistance to LTD without any formation of monoclinic phase under hydrothermal ageing up to 300 hr except the 0.5 and 1.0 wt.% MnO<sub>2</sub> doped YSZ ceramics sintered at temperature 1250 °C and holding time (120, 240 & 480 min) with small amount of monoclinic phase (<2 %). YSZ ceramics with higher level of dopant was found more sensitive to LTD even sintered at 1200 °C for 480 min. It was noticed that the t – m transformation in MnO<sub>2</sub> doped YSZ ceramic was probably due to the redistribution of stabilizer that affecting the stability of tetragonal grains under LTD instead of grain size effect.
8. Current work has revealed that YSZ ceramic resistant to LTD could be produced by incorporating MnO<sub>2</sub> in quest to aid densification at low sintering temperature and short holding time without sacrificing the mechanical properties.

## 5.2 Further Work

Following are some suggestion for further work:

1. Further work include optimization of holding time and sintering rate at low sintering temperatures,  $< 1250\text{ }^{\circ}\text{C}$  is proposed in order to evaluate the benefits of  $\text{MnO}_2$  additives while longer duration of hydrothermal exposure to examine the maximum ageing resistance limit of the 3Y-TZP ceramics.
2. In order to elucidate the sintering mechanism of  $\text{MnO}_2$ -doped YSZ ceramics, further work should focus on the use of TEM to seek evidence of the presences of any grain boundary liquid phase during sintering and redistribution of the stabilizer,  $\text{Y}_2\text{O}_3$  within the grains and the grain boundaries.
3. The results indicate that grain growth in the  $\text{MnO}_2$ -doped system was inevitable. There are reports in the literature that highlighted the beneficial effects of using a two-stage sintering cycle in suppressing the final stage of grain growth. As such, a study could be initiated to investigate the optimum sintering condition based on two-stage sintering applied to the various dopant composition.
4. Microwave sintering is well known for achieving densification in a relatively shorter time. Such studies could be carried out to compare the sintering behaviour of YSZ using advanced techniques such as pressureless sintering methods.
5. A systematic study of the possibility of optimizing the conditions among the  $\text{MnO}_2$  and the sintering conditions (temperature, rate and holding time) that result in a better mechanical properties and higher ageing resistance without inducing grain coarsening or the cubic grains formation.

## REFERENCES

- Agrawal, D. (2006). Microwave sintering of ceramics, composites and metallic materials, and melting of glasses. *Transactions of the Indian ceramic society*, 65(3), 129-144.
- Agrawal, D. K. (1998). Microwave processing of ceramics. *Current Opinion in Solid State and Materials Science*, 3(5), 480-485.
- Akasaka, S. (2016). Thin film YSZ-based limiting current-type oxygen and humidity sensor on thermally oxidized silicon substrates. *Sensors and Actuators B: Chemical*, 236, 499-505. doi: <https://doi.org/10.1016/j.snb.2016.06.025>
- Anselmi-Tamburini, U., Garay, J. E., & Munir, Z. A. (2006). Fast low-temperature consolidation of bulk nanometric ceramic materials. *Scripta Materialia*, 54(5), 823-828.
- Azim Jais, A., Muhammed Ali, S. A., Anwar, M., Rao Somalu, M., Muchtar, A., Wan Isahak, W. N. R., . . . Brandon, N. P. (2017). Enhanced ionic conductivity of scandia-ceria-stabilized-zirconia (10Sc1CeSZ) electrolyte synthesized by the microwave-assisted glycine nitrate process. *Ceramics International*, 43(11), 8119-8125.
- Barsoum, M. (2002). *Fundamentals of Ceramics* (1 ed.).
- Bartolomé, J. F., Montero, I., Díaz, M., López-Esteban, S., Moya, J. S., Deville, S., . . . Fantozzi, G. (2004). Accelerated Aging in 3-mol%-Yttria-Stabilized Tetragonal Zirconia Ceramics Sintered in Reducing Conditions. *Journal of the American Ceramic Society*, 87(12), 2282-2285.
- Basu, B. (2005). Toughening of yttria-stabilised tetragonal zirconia ceramics. *International Materials Reviews*, 50(4), 239-256.
- Basu, B., Vleugels, J., & Van Der Biest, O. (2004). Microstructure–toughness–wear relationship of tetragonal zirconia ceramics. *Journal of the European Ceramic Society*, 24(7), 2031-2040.
- Becher, P. F., & Swain, M. V. (1992). Grain-Size-Dependent Transformation Behavior in Polycrystalline Tetragonal Zirconia. *Journal of the American Ceramic Society*, 75(3), 493-502.

- Borrell, A., Salvador, M. D., Rayon, E., & Penaranda-Foix, F. L. (2012). Improvement of microstructural properties of 3Y-TZP materials by conventional and non-conventional sintering techniques. *Ceramics International*, 38(1), 39-43.
- Bravo-Leon, A., Morikawa, Y., Kawahara, M., & Mayo, M. J. (2002). Fracture toughness of nanocrystalline tetragonal zirconia with low yttria content. *Acta Materialia*, 50(18), 4555-4562.
- Butler, E. P. (1985). Transformation-toughened zirconia ceramics. *Materials Science and Technology*, 1(6), 417-432. doi: 10.1179/mst.1985.1.6.417
- Camposilvan, E., Marro, F. G., Mestra, A., & Anglada, M. (2015). Enhanced reliability of yttria-stabilized zirconia for dental applications. *Acta Biomaterialia*, 17, 36-46.
- Cattani-Lorente, M., Scherrer, S. S., Ammann, P., Jobin, M., & Wiskott, H. W. A. (2011). Low temperature degradation of a Y-TZP dental ceramic. *Acta Biomaterialia*, 7(2), 858-865.
- Chen, I. W., & Wang, X. H. (2000a). Sintering dense nanocrystalline ceramics without final-stage grain growth. *Nature*, 404(6774), 168-171.
- Chen, I. W., & Wang, X. H. (2000b). Sintering densified nanocrystalline ceramics without final stage grain growth. *Nature*, 404(168-171).
- Chen, Y., & Brook, R. J. (1989). Sintering, microstructure and mechanical properties of TZP prepared from electro-refined powders. *British ceramic. Transactions and journal*, 88(1), 7-12.
- Chevalier, J. (2006). What future for zirconia as a biomaterial? *Biomaterials*, 27(4), 535-543.
- Chevalier, J., Deville, S., Münch, E., Jullian, R., & Lair, F. (2004). Critical effect of cubic phase on aging in 3 mol% yttria-stabilized zirconia ceramics for hip replacement prosthesis. *Biomaterials*, 25(24), 5539-5545.
- Chevalier, J., & Gremillard, L. (2009). Ceramics for medical applications: a picture for the next 20 years. *Journal of European Ceramic Society*, 29(7), 1245-1255.
- Chevalier, J., Gremillard, L., Virkar, A. V., & Clarke, D. R. (2009). The tetragonal-monoclinic transformation in zirconia: lessons learned and future trends. *Journal of the American Ceramic Society*, 92(9), 1901-1920.



- Chevalier, J., Olagnon, & Fantozzi. (1996). Study of the residual stress field around Vickers indentations in a 3Y-TZP. *Journal of Materials Science*, 31(10), 2711-2717.
- Chintapalli, R., Mestra, A., García Marro, F., Yan, H., Reece, M., & Anglada, M. (2010). Stability of Nanocrystalline Spark Plasma Sintered 3Y-TZP. *Materials*, 3(2), 800.
- Cui, J., Gong, Z., Lv, M., & Rao, P. (2017). Determination of fracture toughness of Y-TZP ceramics. *Ceramics International*, 43(18), 16319-16322.
- Curtis, A. R., Wright, A. J., & Fleming, G. J. (2006). The influence of surface modification techniques on the performance of a Y-TZP dental ceramic. *Journal of Dentistry*, 34(3), 195-206.
- Denry, I., & Kelly, J. R. (2008). State of the art of zirconia for dental applications. *Dental Materials*, 24(3), 299-307. doi: 10.1016/j.dental.2007.05.007
- Deville, S., Chevalier, J., & Gremillard, L. (2006). Influence of surface finish and residual stresses on the ageing sensitivity of biomedical grade zirconia. *Biomaterials*, 27(10), 2186-2192.
- Durán, P., Villegas, M., Capel, F., Recio, P., & Moure, C. (1996). Low-temperature sintering and microstructural development of nanocrystalline Y-TZP powders. *Journal of the European Ceramic Society*, 16(9), 945-952.
- Ebeid, K., Wille, S., Hamdy, A., Salah, T., El-Etreby, A., & Kern, M. (2014). Effect of changes in sintering parameters on monolithic translucent zirconia. *Dental Materials*, 30(12), e419-e424.
- Eichler, J., Rödel, J., Eisele, U., & Hoffman, M. (2007). Effect of Grain Size on Mechanical Properties of Submicrometer 3Y-TZP: Fracture Strength and Hydrothermal Degradation. *Journal of the American Ceramic Society*, 90(9), 2830-2836.
- Evans, A. G., & Heuer, A. H. (1980). REVIEW—Transformation Toughening in Ceramics: Martensitic Transformations in Crack-Tip Stress Fields. *Journal of the American Ceramic Society*, 63(5-6), 241-248.
- Fabris, S., Paxton, A. T., & Finnis, M. W. (2002). A stabilization mechanism of zirconia based on oxygen vacancies only. *Acta Materialia*, 50(20), 5171-5178.
- Fassina, P., Zaghini, N., Bukat, A., Piconi, C., Greco, F., & Piantelli, S. (1992). Yttria and Calcia Partially Stabilized Zirconia for Biomedical Applications. In A.

Ravaglioli & A. Krajewski (Eds.), *Bioceramics and the Human Body* (pp. 223-229): Springer Netherlands.

Feder, A., & Anglada, M. (2005). Low-temperature ageing degradation of 2.5Y-TZP heat-treated at 1650 °C. *Journal of the European Ceramic Society*, 25(13), 3117-3124.

Flegler, A. J., Burye, T. E., Yang, Q., & Nicholas, J. D. (2014). Cubic yttria stabilized zirconia sintering additive impacts: A comparative study. *Ceramics International*, 40(10, Part B), 16323-16335.

Garvie, R. C., Hannink, R. H., & Pascoe, R. T. (1975). Ceramic steel? *Nature*, 258(5537), 703-704.

Garvie, R. C., & Nicholson, P. S. (1972). Structure and Thermomechanical Properties of Partially Stabilized Zirconia in the CaO-ZrO<sub>2</sub> System. *Journal of the American Ceramic Society*, 55(3), 152-157.

Guo, F., & Xiao, P. (2012). Effect of Fe<sub>2</sub>O<sub>3</sub> doping on sintering of yttria-stabilized zirconia. *Journal of the European Ceramic Society*, 32(16), 4157-4164.

Guo, X. (2003). Roles of alumina in zirconia for functional applications. *Journal of the American Ceramic Society*, 86(11), 1867-1873.

Guo, X. (2004). Property degradation of tetragonal zirconia induced by low-temperature defect reaction with water molecules. *Chemistry of materials*, 16(21), 3988-3994.

Gupta, T. (1980). Strengthening by surface damage in metastable tetragonal zirconia. *Journal of the American Ceramic Society*, 63(1-2), 117-117.

Gupta, T. K., Bechtold, J. H., Kuznicki, R. C., Cadoff, L. H., & Rossing, B. R. (1977). Stabilization of tetragonal phase in polycrystalline zirconia. *Journal of Materials Science*, 12(12), 2421-2426.

Gupta, T. K., Lange, F. F., & Bechtold, J. H. (1978). Effect of stress-induced phase transformation on the properties of polycrystalline zirconia containing metastable tetragonal phase. *Journal of Materials Science*, 13(7), 1464-1470.

Hallmann, L., Mehl, A., Ulmer, P., Reusser, E., Stadler, J., Zenobi, R., . . . Hämmerle, C. H. F. (2012). The influence of grain size on low-temperature degradation of dental zirconia. *Journal of Biomedical Materials Research - Part B Applied Biomaterials*, 100 B(2), 447-456.

- Hallmann, L., Ulmer, P., Reusser, E., Louvel, M., & Hämmerle, C. H. F. (2012). Effect of dopants and sintering temperature on microstructure and low temperature degradation of dental Y-TZP-zirconia. *Journal of the European Ceramic Society*, 32(16), 4091-4104.
- Hannink, R. H., Kelly, P. M., & Muddle, B. C. (2000a). Transformation toughening in zirconia-containing ceramics. *Journal of the American Ceramic Society*, 83(3), 461-487.
- Hannink, R. H. J., Kelly, P. M., & Muddle, B. C. (2000b). Transformation Toughening in Zirconia-Containing Ceramics. *Journal of the American Ceramic Society*, 83(3), 461-487.
- Hernandez, M. T., Jurado, J. R., Duran, P., & Fierro, J. L. (1991). Subeutectoid Degradation of Yttria-Stabilized Tetragonal Zirconia Polycrystal and Ceria-Doped Yttria-Stabilized Tetragonal Zirconia Polycrystal Ceramics. *Journal of the American Ceramic Society*, 74(6), 1254-1258.
- Heuer, A. H., Claussen, N., Kriven, W. M., & Ruhle, M. (1982). Stability of Tetragonal ZrO<sub>2</sub> Particles in Ceramic Matrices. *Journal of the American Ceramic Society*, 65(12), 642-650.
- Hjerpe, J., Vallittu, P. K., Fröberg, K., & Lassila, L. V. (2009). Effect of sintering time on biaxial strength of zirconium dioxide. *Dental Materials*, 25(2), 166-171.
- Ho, C.-J., & Tuan, W.-H. (2012). Toughening and strengthening zirconia through the addition of a transient solid solution additive. *Journal of the European Ceramic Society*, 32(2), 335-341.
- Hodgson, S. N. B., Cawley, J., & Clubley, M. (1999a). The role of Al<sub>2</sub>O<sub>3</sub> impurities on the microstructure and properties of Y-TZP. *Journal of Materials Processing Technology*, 92–93, 85-90.
- Hodgson, S. N. B., Cawley, J., & Clubley, M. (1999b). The role of SiO<sub>2</sub> impurities in the microstructure and properties of Y-TZP. *Journal of Materials Processing Technology*, 86(1–3), 139-145.
- Inokoshi, M., Zhang, F., De Munck, J., Minakuchi, S., Naert, I., Vleugels, J., . . . Vanmeensel, K. (2014). Influence of sintering conditions on low-temperature degradation of dental zirconia. *Dental Materials*, 30(6), 669-678.
- Kanellopoulos, P., & Gill, C. (2002). Hydrothermal ageing of yttria-stabilised zirconia, sintered at 1300°C–1325°C: the effects of copper oxide doping and sintering time variations. *Journal of Materials Science*, 37(23), 5075-5082.

- Keuper, M., Berthold, C., & Nickel, K. G. (2014a). Long-time aging in 3 mol.% yttria-stabilized tetragonal zirconia polycrystals at human body temperature. *Acta Biomaterialia*, 10(2), 951-959.
- Keuper, M., Berthold, C., & Nickel, K. G. (2014b). Long-time aging in 3 mol.% yttria-stabilized tetragonal zirconia polycrystals at human body temperature. *Acta Biomaterialia*, 10(2), 951-959.
- Khan, M., Ramesh, S., Bang, L., Wong, Y., Ubenthiran, S., Tan, C., . . . Misran, H. (2014). Effect of Copper Oxide and Manganese Oxide on Properties and Low Temperature Degradation of Sintered Y-TZP Ceramic. *Journal of materials engineering and performance*, 23(12), 4328-4335.
- Kim, D.-J. (1990). Effect of Ta<sub>2</sub>O<sub>5</sub>, Nb<sub>2</sub>O<sub>5</sub>, and HfO<sub>2</sub> Alloying on the Transformability of Y<sub>2</sub>O<sub>3</sub>-Stabilized Tetragonal ZrO<sub>2</sub>. *Journal of the American Ceramic Society*, 73(1), 115-120.
- Kim, D.-J. (1997). Influence of aging environment on low-temperature degradation of tetragonal zirconia alloys. *Journal of the European Ceramic Society*, 17(7), 897-903.
- Kim, D. J., Jung, H. J., Jang, J. W., & Lee, H. L. (1998). Fracture Toughness, Ionic Conductivity, and Low-Temperature Phase Stability of Tetragonal Zirconia Codoped with Yttria and Niobium Oxide. *Journal of the American Ceramic Society*, 81(9), 2309-2314.
- Kim, M.-J., Ahn, J.-S., Kim, J.-H., Kim, H.-Y., & Kim, W.-C. (2013). Effects of the sintering conditions of dental zirconia ceramics on the grain size and translucency. *The journal of advanced prosthodontics*, 5(2), 161-166.
- Kobayashi, K., Kuwajima, H., & Masaki, T. (1981). Phase change and mechanical properties of ZrO<sub>2</sub>-Y<sub>2</sub>O<sub>3</sub> solid electrolyte after ageing. *Solid State Ionics*, 3, 489-493.
- Kosmač, T., & Kocjan, A. (2012). Ageing of dental zirconia ceramics. *Journal of the European Ceramic Society*, 32(11), 2613-2622.
- Kosmaċ, T., Oblak, C. e., Jevnikar, P., Funduk, N., & Marion, L. (2000). Strength and reliability of surface treated Y-TZP dental ceramics. *Journal of biomedical materials research*, 53(4), 304-313.
- Kwa, S., Ramesh, S., Bang, L., Wong, Y., Chew, W., Tan, C., . . . Teng, W. (2015). Effect of sintering holding time on the properties and low-temperature

degradation behaviour of manganese oxide-doped Y-TZP ceramic. *Journal of Ceramic Processing Research*, 16(2), 193-198.

- Kwon, S. Y., & Jung, I.-H. (2017). Critical evaluation and thermodynamic optimization of the CaO-ZrO<sub>2</sub> and SiO<sub>2</sub>-ZrO<sub>2</sub> systems. *Journal of the European Ceramic Society*, 37(3), 1105-1116.
- Lange, Dunlop, & Davis. (1986). Degradation During Aging of Transformation-Toughened ZrO<sub>2</sub>-Y<sub>2</sub>O<sub>3</sub> Materials at 250°C. *Journal of the American Ceramic Society*, 69(3), 237-240.
- Lange, F. (1982). Transformation toughening. *Journal of Materials Science*, 17(1), 225-234.
- Lange, F. (1986). Transformation-Toughened ZrO<sub>2</sub>: Correlations between Grain Size Control and Composition in the System ZrO<sub>2</sub>-Y<sub>2</sub>O<sub>3</sub>. *Journal of the American Ceramic Society*, 69(3), 240-242.
- Lange, F. F. (2008). Densification of powder compacts: An unfinished story. *Journal of the European Ceramic Society*, 28(7), 1509-1516.
- Lange, F. F., & Kellett\*, B. J. (1989). Thermodynamics of Densification: II, Grain Growth in Porous Compacts and Relation to Densification. *Journal of the American Ceramic Society*, 72(5), 735-741.
- Lawn, B. R., Evans, A. G., & Marshall, D. B. (1980). Elastic/plastic indentation damage in ceramics: The median/radial crack system. *Journal of American Ceramics Society*, 63, 574-581.
- Lawson, S. (1995). Environmental degradation of zirconia ceramics. *Journal of the European Ceramic Society*, 15(6), 485-502.
- Leach, C. A. (1987). Sintering of magnesium partially stabilized zirconia – behaviour of an impurity silicate phase. *Materials Science and Technology*, 3(5), 321-324.
- Lee, Y.-I., Kim, Y.-W., Mitomo, M., & Kim, D.-Y. (2003). Fabrication of Dense Nanostructured Silicon Carbide Ceramics through Two-Step Sintering. *Journal of the American Ceramic Society*, 86(10), 1803-1805.
- Lei, T., Lin, G., Ge, Q., Zhou, Y., & He, X. (1997). Morphologies of monoclinic phase in ZrO<sub>2</sub> (2 mol% Y<sub>2</sub>O<sub>3</sub>) revealed by TEM in situ continuous observations. *Journal of Materials Science*, 32(4), 1105-1111.

- Lepistö, T., & Mantyla, T. (1989). *A Model for Structural Degradation of Y-TZP Ceramics in Humid Atmosphere*. Paper presented at the A Collection of Papers Presented at the 13th Annual Conference on Composites and Advanced Ceramic Materials, Part 1 of 2: Ceramic Engineering and Science Proceedings, Volume 10, Issue 7/8.
- Li, P., Chen, I. W., & Penner-Hahn, J. E. (1994). Effect of dopants on zirconia stabilization—an x-ray absorption study: I, trivalent dopants. *Journal of the American Ceramic Society*, 77(1), 118-128.
- Li, P., Chen, I. W., & Penner, H. (1994). Effect of dopants on zirconia stabilization and X-ray absorption study: I, Trivalent dopants. *Journal of American Ceramics Society*, 77, 118-128.
- Lourenço, M. A., Cunto, G. G., Figueiredo, F. M., & Frade, J. R. (2011). Model of two-step sintering conditions for yttria-substituted zirconia powders. *Materials Chemistry and Physics*, 126(1), 262-271.
- Lughi, V., & Sergio, V. (2010). Low temperature degradation -aging- of zirconia: A critical review of the relevant aspects in dentistry. *Dental Materials*, 26(8), 807-820.
- Maca, K., Pouchly, V., & Shen, Z. (2008). TWO-STEP SINTERING AND SPARK PLASMA SINTERING OF Al<sub>2</sub>O<sub>3</sub>, ZrO<sub>2</sub> AND SrTiO<sub>3</sub> CERAMICS. *Integrated Ferroelectrics*, 99(1), 114-124.
- Maca, K., & Simonikova, S. (2005). Effect of sintering schedule on grain size of oxide ceramics. *Journal of Materials Science*, 40(21), 5581-5589.
- Malkondu, Ö., Tinastepe, N., Akan, E., & Kazazoğlu, E. (2016). An overview of monolithic zirconia in dentistry. *Biotechnology & Biotechnological Equipment*, 30(4), 644-652.
- Masaki, T. (1986a). Mechanical properties of toughened ZrO<sub>2</sub>-Y<sub>2</sub>O<sub>3</sub> ceramics. *Journal of the American Ceramics Society*, 69, 638-640.
- Masaki, T. (1986b). Mechanical properties of Y-PSZ after aging at low temperature. *International Journal of High Technology Ceramics*, 2(2), 85-98.
- Matsui, K., Horikoshi, H., Ohmichi, N., Ohgai, M., Yoshida, H., & Ikuhara, Y. (2003a). Cubic-Formation and Grain-Growth Mechanisms in Tetragonal Zirconia Polycrystal. *Journal of the American Ceramic Society*, 86(8), 1401-1408.

- Matsui, K., Horikoshi, H., Ohmichi, N., Ohgai, M., Yoshida, H., & Ikuhara, Y. (2003b). Cubic-Formation and Grain-Growth Mechanisms in Tetragonal Zirconia Polycrystal. *Journal of the American Ceramic Society*, 86(8), 1401-1408.
- Matsui, K., Matsumoto, A., Uehara, M., Enomoto, N., & Hojo, J. (2007). Sintering kinetics at isothermal shrinkage: effect of specific surface area on the initial sintering stage of fine zirconia powder. *Journal of the American Ceramic Society*, 90(1), 44-49.
- Matsui, K., Yoshida, H., & Ikuhara, Y. (2008). Grain-boundary structure and microstructure development mechanism in 2–8mol% yttria-stabilized zirconia polycrystals. *Acta Materialia*, 56(6), 1315-1325.
- Matsui, K., Yoshida, H., & Ikuhara, Y. (2009). Isothermal Sintering Effects on Phase Separation and Grain Growth in Yttria-Stabilized Tetragonal Zirconia Polycrystal. *Journal of the American Ceramic Society*, 92(2), 467-475.
- Matsui, K., Yoshida, H., & Ikuhara, Y. (2014). Nanocrystalline, ultra-degradation-resistant zirconia: its grain boundary nanostructure and nanochemistry. *Sci Rep*, 4.
- Matsui, K., Yoshida, H., & Ikuhara, Y. (2018). Review: microstructure-development mechanism during sintering in polycrystalline zirconia. *International Materials Reviews*, 63(6), 375-406.
- Matsui, M., Soma, T., & Oda, I. (1983). Effect of Microstructure on the Strength of Y-TZP Components *Science and technology of zirconia II*.
- Matsui, M., Soma, T., & Oda, I. (1986). Stress-Induced Transformation and Plastic Deformation for Y<sub>2</sub>O<sub>3</sub>-Containing Tetragonal Zirconia Polycrystals. *Journal of the American Ceramic Society*, 69(3), 198-202.
- Mazaheri, M., Simchi, A., & Golestani Fard, F. (2008). Densification and grain growth of nano crystalline 3YTZP during two step sintering. *Ceramics International*, 35, 547-554.
- Mazaheri, M., Zahedi, A. M., & Sadrnezhad, S. K. (2008). Two-step sintering of nanocrystalline ZnO compacts: Effect of temperature on densification and grain growth. *Journal of the American Ceramic Society*, 91(1), 56-63.
- Mecartney, M. L. (1987). Influence of an Amorphous Second Phase on the Properties of Yttria-Stabilized Tetragonal Zirconia Polycrystals (Y-TZP). *Journal of the American Ceramic Society*, 70(1), 54-58.

- Menezes, R., & Kiminami, R. (2008). Microwave sintering of alumina–zirconia nanocomposites. *Journal of Materials Processing Technology*, 203(1), 513-517.
- Monaco, C., Prete, F., Leonelli, C., Esposito, L., & Tucci, A. (2015). Microstructural study of microwave sintered zirconia for dental applications. *Ceramics International*, 41(1), 1255-1261.
- Nogiwa-Valdez, A., Rainforth, W., Zeng, P., & Ross, I. (2013a). Deceleration of hydrothermal degradation of 3Y-TZP by alumina and lanthana co-doping. *Acta Biomaterialia*, 9(4), 6226-6235.
- Nogiwa-Valdez, A. A., Rainforth, W. M., Zeng, P., & Ross, I. M. (2013b). Deceleration of hydrothermal degradation of 3Y-TZP by alumina and lanthana co-doping. *Acta Biomaterialia*, 9(4), 6226-6235.
- Oghbaei, M., & Mirzaee, O. (2010). Microwave versus conventional sintering: a review of fundamentals, advantages and applications. *Journal of Alloys and Compounds*, 494(1), 175-189.
- Paterson, A., & Stevens, R. (1986). Phase analysis of sintered yttria–zirconia ceramics by x-ray diffraction. *Journal of Materials Research*, 1(2), 295-299.
- Picconi, C., & Maccauro, G. (1999). Zirconia as a ceramic biomaterial. *20*, 1-25.
- Piconi, C., & Maccauro, G. (1999). Zirconia as a ceramic biomaterial. *Biomaterials*, 20(1), 1-25.
- Polotai, A., Breece, K., Dickey, E., Randall, C., & Ragulya, A. (2005). A Novel Approach to Sintering Nanocrystalline Barium Titanate Ceramics. *Journal of the American Ceramic Society*, 88(11), 3008-3012.
- Presenda, Á., Salvador, M. D., Penaranda-Foix, F. L., Catalá-Civera, J. M., Pallone, E., Ferreira, J., & Borrell, A. (2017). Effects of microwave sintering in aging resistance of zirconia-based ceramics. *Chemical Engineering and Processing: Process Intensification*, 122, 404-412.
- Presenda, Á., Salvador, M. D., Peñaranda-Foix, F. L., Moreno, R., & Borrell, A. (2015). Effect of microwave sintering on microstructure and mechanical properties in Y-TZP materials used for dental applications. *Ceramics International*, 41(5), 7125-7132.
- Ramesh, S., Amiriyan, M., Meenaloshini, S., Tolouei, R., Hamdi, M., Pruboloksono, J., & Teng, W. D. (2011). Densification behaviour and properties of manganese oxide doped Y-TZP ceramics. *Ceramics International*, 37(8), 3583-3590.



- Ramesh, S., Chew, W. K., Tan, C., Purbolaksono, J., Noor, A., Hassan, M., . . . Teng, W. (2013). Influence of manganese on the sintering properties of tetragonal zirconia. *Ceram. Silik*, 57, 28-32.
- Ramesh, S., Gill, C., & Lawson, S. (1999). The effect of copper oxide on sintering, microstructure, mechanical properties and hydrothermal ageing of coated 2.5Y-TZP ceramics. *Journal of Materials Science*, 34(22), 5457-5467.
- Ramesh, S., Khan, M. M., Alexander Chee, H. C., Wong, Y. H., Ganesan, P., Kutty, M. G., . . . Niakan, A. (2016). Sintering behaviour and properties of graphene oxide-doped Y-TZP ceramics. *Ceramics International*, 42(15), 17620-17625.
- Ramesh, S., Meenaloshini, S., Tan, C., Chew, W. K., & Teng, W. (2008). Effect of manganese oxide on the sintered properties and low temperature degradation of Y-TZP ceramics. *Ceramics International*, 34(7), 1603-1608.
- Ross, I., Rainforth, W., McComb, D., Scott, A., & Brydson, R. (2001). The role of trace additions of alumina to yttria-tetragonal zirconia polycrystals (Y-TZP). *Scripta Materialia*, 45(6), 653-660.
- Rühle, M., & Evans, A. G. (1989). High toughness ceramics and ceramic composites. *Progress in Materials Science*, 33(2), 85-167.
- Ruiz, L., & Readey, M. J. (1996). Effect of heat treatment on grain size, phase assemblage, and mechanical properties of 3 mol% Y-TZP. *Journal of the American Ceramic Society*, 79(9), 2331-2340.
- Sakib Khan, M., Saiful Islam, M., & Bates, D. R. (1998). Cation doping and oxygen diffusion in zirconia: a combined atomistic simulation and molecular dynamics study. *Journal of Material Chemistry*, 8, 2299-2307.
- Sakka, Y., Ishii, T., Suzuki, T. S., Morita, K., & Hiraga, K. (2004). Fabrication of high-strain rate superplastic yttria-doped zirconia polycrystals by adding manganese and aluminum oxides. *Journal of the European Ceramic Society*, 24(2), 449-453.
- Sakuma, T., Yoshizawa, Y.-I., & Suto, H. (1985). The microstructure and mechanical properties of yttria-stabilized zirconia prepared by arc-melting. *Journal of Materials Science*, 20(7), 2399-2407.
- Samodurova, A., Kocjan, A., Swain, M. V., & Kosmač, T. (2015). The combined effect of alumina and silica co-doping on the ageing resistance of 3Y-TZP bioceramics. *Acta Biomaterialia*, 11, 477-487.

- Saremi-Yarahmadi, S., Binner, J., & Vaidhyanathan, B. (2018). Erosion and mechanical properties of hydrothermally-resistant nanostructured zirconia components. *Ceramics International*, 44(9), 10539-10544.
- Sato, T., & Shimada, M. (1985). Transformation of Yttria-Doped Tetragonal ZrO<sub>2</sub> Polycrystals by Annealing in Water. *Journal of the American Ceramic Society*, 68(6), 356-356.
- Schmauder, S., & Schubert, H. (1986). Significance of Internal Stresses for the Martensitic Transformation in Yttria-Stabilized Tetragonal Zirconia Polycrystals During Degradation. *Journal of the American Ceramic Society*, 69(7), 534-540.
- Schubert, H., & Petzow, G. (1986). *Microstructural investigations on the stability of yttria stabilized tetragonal zirconia*. Paper presented at the Zirconia'86--The 3<sup>rd</sup> International Conference on the Science and Technology of Zirconia.
- Scott, H. G. (1975). Phase relationships in the zirconia-yttria system. *Journal of Materials Science*, 10(9), 1527-1535.
- Sevilla, P., Sandino, C., Arciniegas, M., Martínez-Gomis, J., Peraire, M., & Gil, F. J. (2010). Evaluating mechanical properties and degradation of YTZP dental implants. *Materials Science and Engineering: C*, 30(1), 14-19.
- Shah, K., Holloway, J., & Denry, I. (2008). Effect of coloring with various metal oxides on the microstructure, color, and flexural strength of 3Y-TZP. *Journal of Biomedical Materials Research Part B: Applied Biomaterials*, 87(2), 329-337.
- Shin, D.-W., Orr, K. K., & Schubert, H. (1990). Microstructure-Mechanical Property Relationships in Hot Isostatically Pressed Alumina and Zirconia-Toughened Alumina. *Journal of the American Ceramic Society*, 73(5), 1181-1188.
- Singh, R., Gill, C., Lawson, S., & Dransfield, G. P. (1996). Sintering, microstructure and mechanical properties of commercial Y-TZPs. *Journal of Materials Science*, 31(22), 6055-6062.
- Siva Kumar, S., Teow, L., Ali, N., & KCL, J. (2016). Densification behavior and properties of iron oxide doped Y-TZP ceramics. *Journal of Engineering Science and Technology*, 176-187.
- Sivakumar, S., Ramesh, S., Chin, K., Tan, C., & Teng, W. (2011). Effect of sintering profiles on the properties and ageing resistance of Y-TZP ceramic. *International Journal of Automotive and Mechanical Engineering*, 4, 405-413.

- Stawarczyk, B., Özcan, M., Hallmann, L., Ender, A., Mehl, A., & Hämmerlet, C. H. (2013). The effect of zirconia sintering temperature on flexural strength, grain size, and contrast ratio. *Clinical oral investigations*, 17(1), 269-274.
- Subbarao, E. C. (1981). *ZIRCONIA - AN OVERVIEW*. Paper presented at the Advances in Ceramics.
- Suresh, A., Mayo, M. J., Porter, W. D., & Rawn, C. J. (2003). Crystallite and Grain-Size-Dependent Phase Transformations in Ytria-Doped Zirconia. *Journal of the American Ceramic Society*, 86(2), 360-362.
- Swab, J. J. (1991). Low temperature degradation of Y-TZP materials. *Journal of Materials Science*, 26(24), 6706-6714.
- Tekeli, S., & Erdogan, M. (2002). A quantitative assessment of cavities in 3 mol% yttria-stabilized tetragonal zirconia specimens containing various grain size. *Ceramics International*, 28(7), 785-789.
- Thostenson, E. T., & Chou, T. W. (1999). Microwave processing: fundamentals and applications. *Composites Part A* 30, 1055–1071.
- Tong, H., Tanaka, C. B., Kaizer, M. R., & Zhang, Y. (2016). Characterization of three commercial Y-TZP ceramics produced for their High-Translucency, High-Strength and High-Surface Area. *Ceramics International*, 42(1), 1077-1085.
- Toraya, H., Yoshimura, M., & Somiya, S. (1984). Calibration Curve for Quantitative Analysis of the Monoclinic-Tetragonal ZrO<sub>2</sub> System by X-Ray Diffraction. *Journal of the American Ceramic Society*, 67(6), C-119-C-121.
- Tredici, I. G., Sebastiani, M., Massimi, F., Bemporad, E., Resmini, A., Merlati, G., & Anselmi-Tamburini, U. (2016). Low temperature degradation resistant nanostructured yttria-stabilized zirconia for dental applications. *Ceramics International*, 42(7), 8190-8197.
- Trunec, M. (2008). Effect of grain size on mechanical properties of 3Y-TZP ceramics. *Ceram. Silik*, 52(3), 165-171.
- Valefi, M., Pathiraj, B., de Rooij, M., de Vries, E., & Schipper, D. J. (2012). Influence of countersurface materials on dry sliding performance of CuO/Y-TZP composite at 600° C. *Journal of the European Ceramic Society*, 32(16), 4137-4147.

- Vasylykiv, O., Sakka, Y., & Skorokhod, V. V. (2003). Low-Temperature Processing and Mechanical Properties of Zirconia and Zirconia–Alumina Nanoceramics. *Journal of the American Ceramic Society*, 86(2), 299-304.
- Vidotti, H. A., Pereira, J. R., Insaurralde, E., Almeida, A. L. P. F. d., & Valle, A. L. d. (2013). Thermo and mechanical cycling and veneering method do not influence Y-TZP core/veneer interface bond strength. *Journal of Dentistry*, 41(4), 307-312.
- Wang, J., & Gao, L. (2005). Photoluminescence properties of nanocrystalline ZnO ceramics prepared by pressureless sintering and spark plasma sintering. *Journal of American Ceramics Society*, 88, 1637-1639.
- Wang, X.-H., Chen, P.-L., & Chen, I. W. (2006). Two-Step Sintering of Ceramics with Constant Grain-Size, I: Y<sub>2</sub>O<sub>3</sub>. *Journal of the American Ceramic Society*, 89(2), 431-437.
- Wang, X. H., Deng, X. Y., Bai, H.-L., Zhou, H., Qu, W.-G., Li, L. T., & Chen, I. W. (2006). Two-Step Sintering of Ceramics with Constant Grain-Size, II: BaTiO<sub>3</sub> and Ni–Cu–Zn Ferrite. *Journal of the American Ceramic Society*, 89(2), 438-443.
- Wei, C., & Gremillard, L. (2018). Towards the prediction of hydrothermal ageing of 3Y-TZP bioceramics from processing parameters. *Acta Materialia*, 144, 245-256.
- Winnubst, A. (1988). Aging behavior of ultrafine-grained Y-TZP in hot water. *Adv. Ceram.*, 24 App., 39.
- Wu, Z., Li, N., & Wen, Y. (2013). Effect of a small amount of Al<sub>2</sub>O<sub>3</sub> addition on the hydrothermal degradation of 3Y-TZP. *Journal of Materials Science*, 48(3), 1256-1261.
- Wurst, J. C., & Nelson, J. A. (1972). Lineal Intercept Technique for Measuring Grain Size in Two-Phase Polycrystalline Ceramics. *Journal of the American Ceramic Society*, 55(2), 109-109.
- Yadoji, P., Peelamedu, R., Agrawal, D., & Roy, R. (2003). Microwave sintering of Ni–Zn ferrites: comparison with conventional sintering. *Materials Science and Engineering: B*, 98(3), 269-278.
- Yang, C.-L., Hsiang, H.-I., & Chen, C.-C. (2005). Characteristics of yttria stabilized tetragonal zirconia powder used in optical fiber connector ferrule. *Ceramics International*, 31(2), 297-303.

- Yoshimura, M., Noma, T., Kawabata, K., & Sōmiya, S. (1987). Role of H<sub>2</sub>O on the degradation process of Y-TZP. *Journal of Materials Science Letters*, 6(4), 465-467.
- Yu, P. C., Li, Q. F., Fuh, J. Y. H., Li, T., & Lu, L. (2007). Two-stage sintering of nano-sized yttria stabilized zirconia process by powder injection moulding. *Journal of Materials Processing Technology*, 192–193, 312-318.
- Zhang, F., Batuk, M., Hadermann, J., Manfredi, G., Mariën, A., Vanmeensel, K., . . . Vleugels, J. (2016). Effect of cation dopant radius on the hydrothermal stability of tetragonal zirconia: grain boundary segregation and oxygen vacancy annihilation. *Acta Materialia*, 106, 48-58.
- Zhang, F., Inokoshi, M., Vanmeensel, K., Van Meerbeek, B., Naert, I., & Vleugels, J. (2015). Lifetime estimation of zirconia ceramics by linear ageing kinetics, *Acta Mater.* 92, 290-298.
- Zhang, F., Vanmeensel, K., Batuk, M., Hadermann, J., Inokoshi, M., Van Meerbeek, B., . . . Vleugels, J. (2015). Highly-translucent, strong and aging-resistant 3Y-TZP ceramics for dental restoration by grain boundary segregation. *Acta Biomaterialia*, 16, 215-222.
- Zhang, F., Vanmeensel, K., Inokoshi, M., Batuk, M., Hadermann, J., Van Meerbeek, B., . . . Vleugels, J. (2014). 3Y-TZP ceramics with improved hydrothermal degradation resistance and fracture toughness. *Journal of the European Ceramic Society*, 34(10), 2453-2463.
- Zhang, F., Vanmeensel, K., Inokoshi, M., Batuk, M., Hadermann, J., Van Meerbeek, B., . . . Vleugels, J. (2015). Critical influence of alumina content on the low temperature degradation of 2–3mol% yttria-stabilized TZP for dental restorations. *Journal of the European Ceramic Society*, 35(2), 741-750.
- Zhou, H., Li, J., Yi, D., & Xiao, L. (2011). Effect of Manganese Oxide on the Sintered Properties of 8YSZ. *Physics Procedia*, 22, 14-19.

## LIST OF PUBLICATIONS AND PAPERS PRESENTED

1. C.H. Ting, S. Ramesh, N. Lwin, U. Sutharsini. (2016). Sintering properties and low-temperature degradation behaviour of Y-TZP ceramics. *Journal of Ceramic Processing Research*, Vol. 17, No. 12, 1265-1269. (ISI-Cited Publication)
2. C.H. Ting, S. Ramesh, C. Y. Tan, N. Z. Abidin, W. D. Teng, I. Urriés, & L. T. Bang. (2017). Low-temperature sintering and prolonged holding time on the densification and properties of zirconia ceramic. *Journal of Ceramic Processing Research*, Vol. 18, No. 8, 569-574. (ISI-Cited Publication)